

# Non-Gamma-ray Applications of TeV Telescopes

**Michael Daniel**

[<michael.daniel@cfa.harvard.edu>](mailto:michael.daniel@cfa.harvard.edu)

36th ICRC 25th July, 2019



# Outline

- How is a TeV telescope useful for non-TeV science?
- Eclipses/Occultations/Transits
- Intensity Interferometry
- Optical Communications



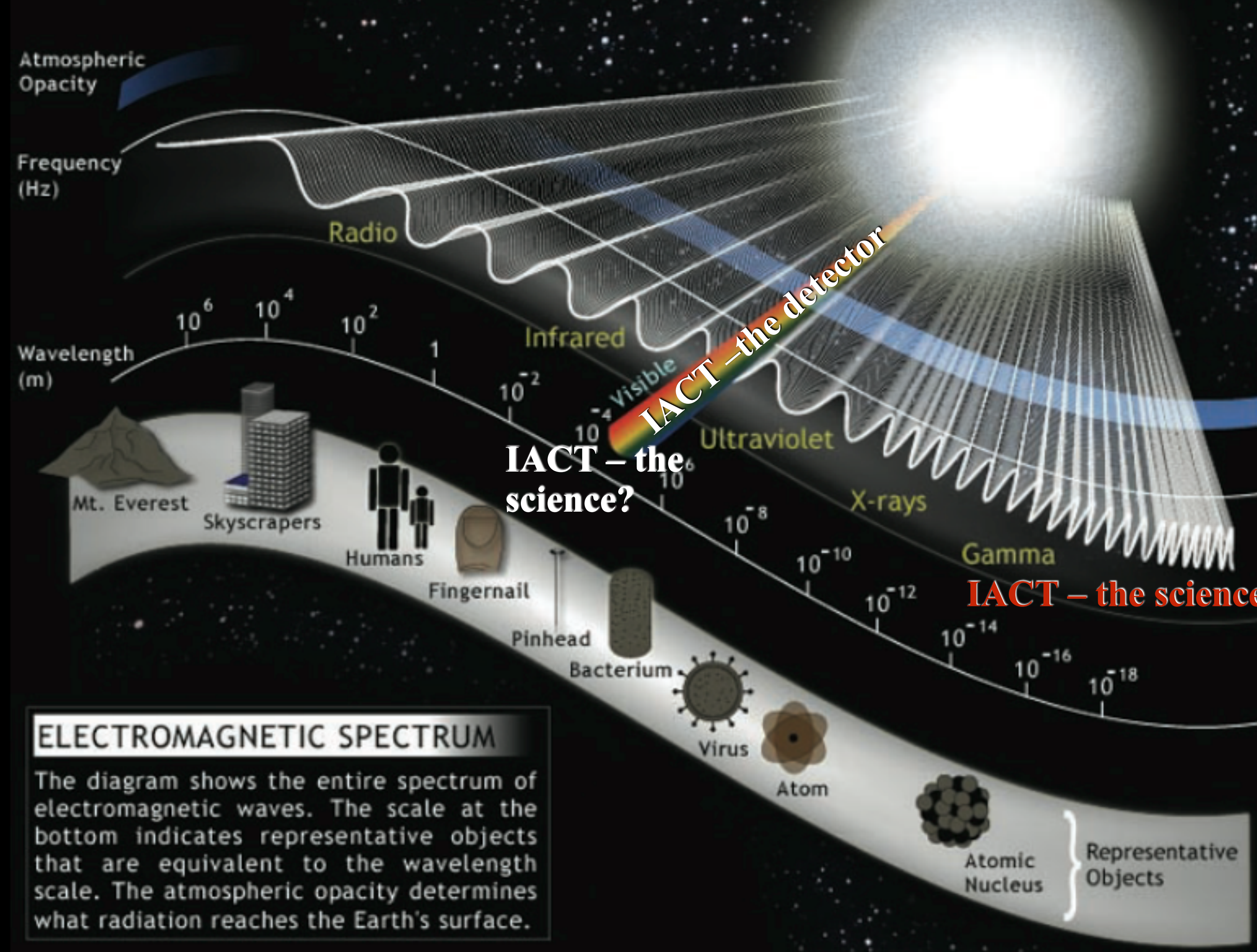
# Outline

- How is a TeV telescope useful for non-TeV science?
- Eclipses/Occultations/Transits
- Intensity Interferometry
- Optical Communications





- eclipses (binaries)
- occultations (asteroids/KBOs/
- transits (exoplanets)
- intensity interferometry
- OSETI
- FRB counterparts
- ...



- SNR
- Pulsars/PWN
- Binaries
- AGN
- DM/LIV
- ...



Noise sources in optical astronomy

$$\sigma^2 \simeq \sigma_{\text{flicker}}^2 + \sigma_{\text{scintillation}}^2 + \sigma_{\text{shot}}^2$$

Source

Atmosphere

Detector

The diagram illustrates three noise sources in optical astronomy. At the top, a bright orange sun-like sphere is labeled 'Flicker'. Four vertical dashed yellow lines with arrowheads point downwards from the sun. In the middle, three wavy blue lines are labeled 'Scintillation'. The four dashed lines pass through these wavy lines. At the bottom, a silver metal bucket is labeled 'Shot'. The four dashed lines end with arrowheads pointing into the bucket.

CENTER FOR

ASTROPHYSICS

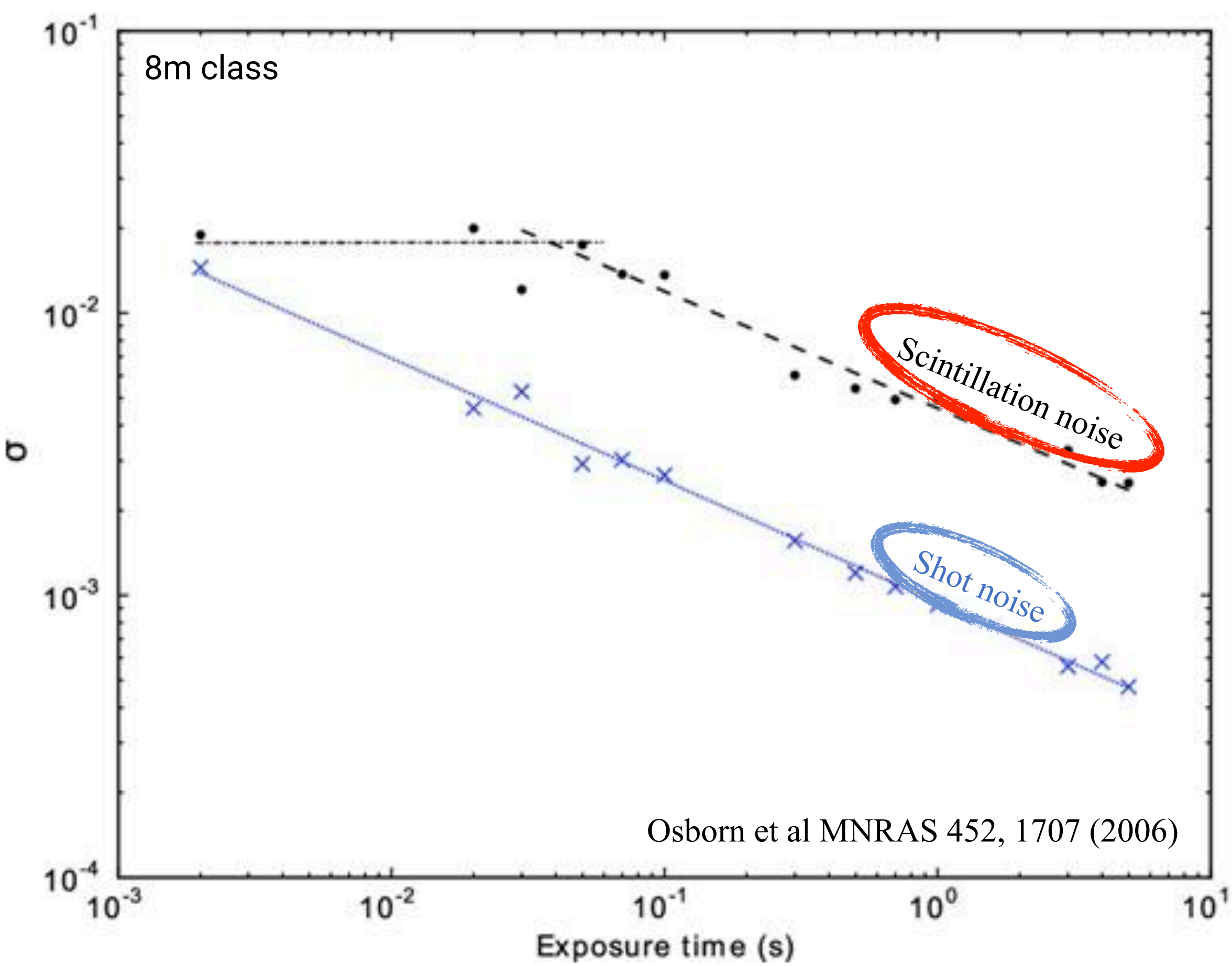
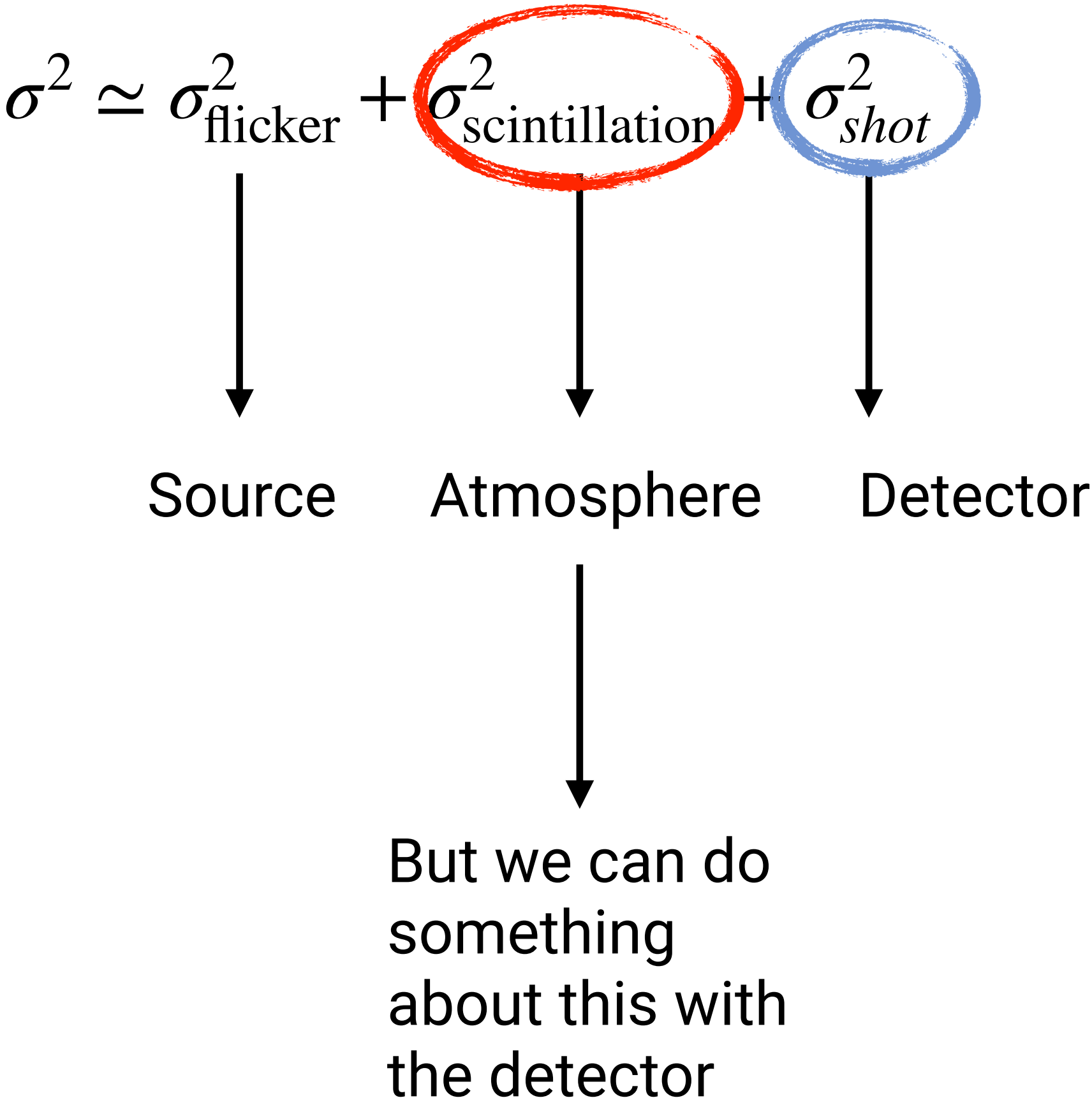
HARVARD & SMITHSONIAN

36th ICRC - Madison 2019

5

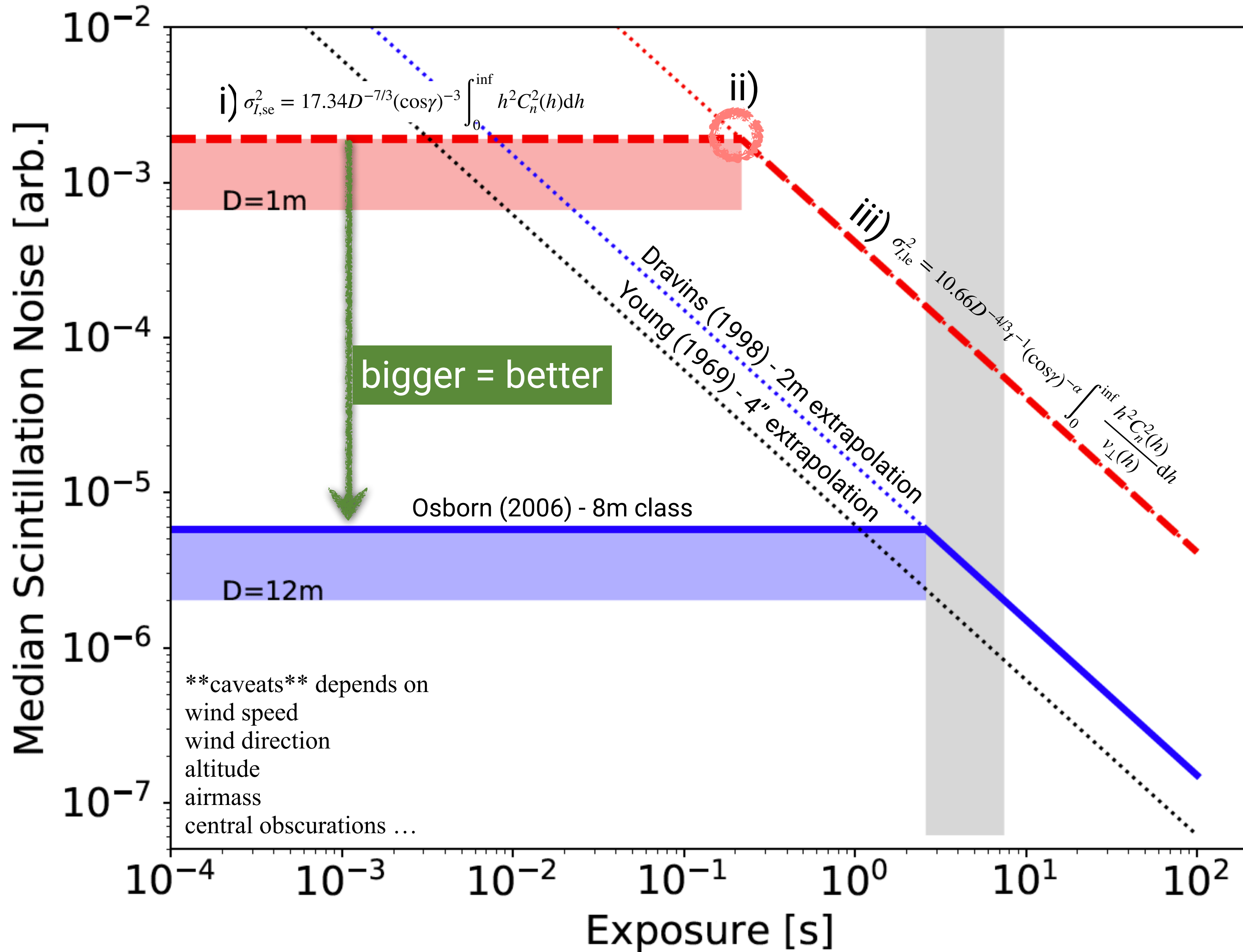


# Noise sources in optical astronomy





# Temporal Power Spectrum of Scintillation

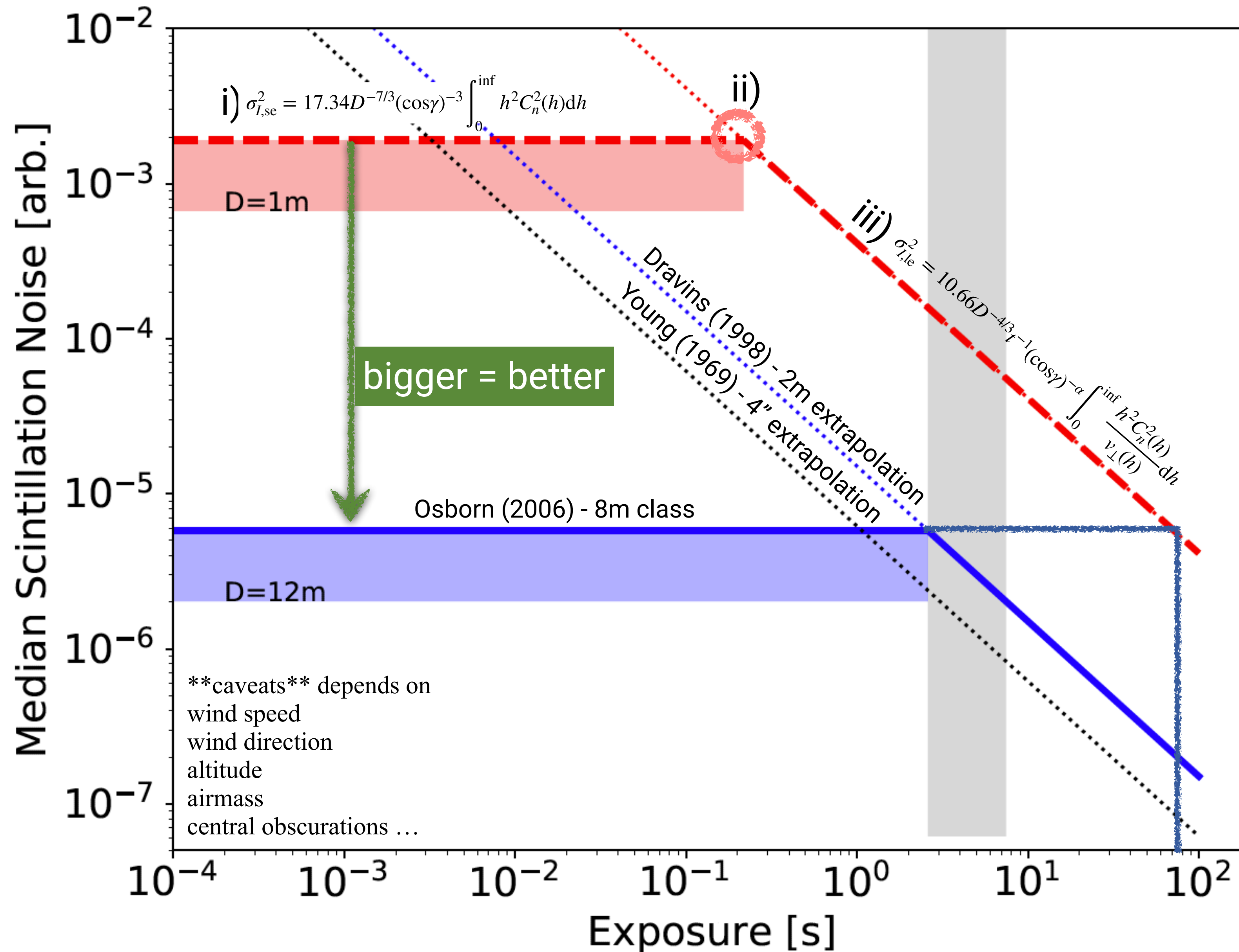


## Scintillation is complex process

- i) short exposure regime
  - speckles appear frozen
  - no temporal averaging
- ii)  $\sim$ size of speckles
  - significant wavelength dependence
- iii) long exposure regime
  - speckles traverse pupil
  - noise reduced by temporal averaging



# Temporal Power Spectrum of Scintillation

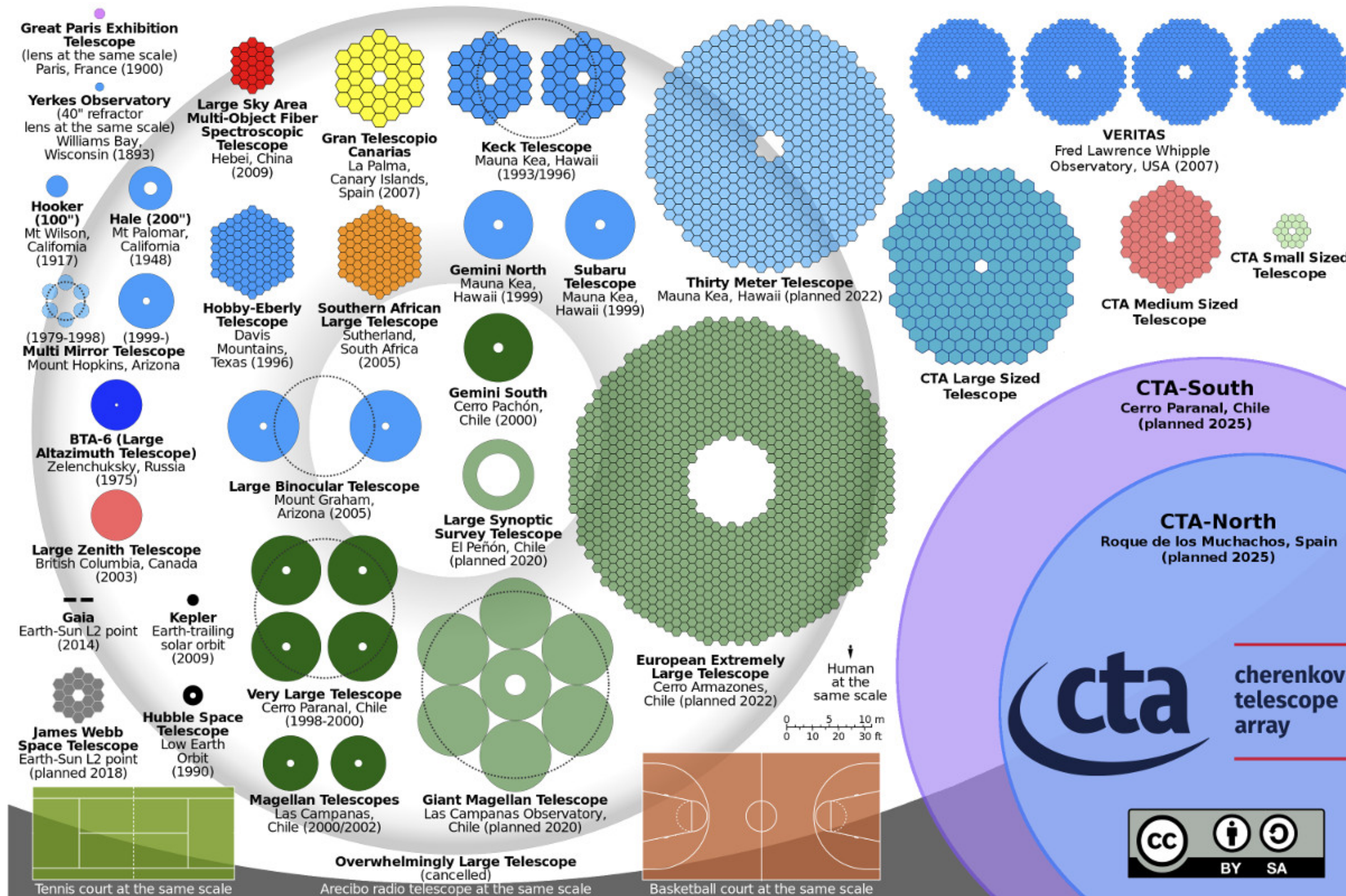


Scintillation is complex process

- i) short exposure regime
  - speckles appear frozen
  - no temporal averaging
- ii) ~size of speckles
  - significant wavelength dependence
- iii) long exposure regime
  - speckles traverse pupil
  - noise reduced by temporal averaging



If bigger = better



Then Cherenkov telescopes should rank among the best (in terms photometric capability)

CMG Lee / T. Hassan



**So what sort of optical things have  
been done with IACTs?**



# Whipple 10m first to measure meteors down to 12<sup>th</sup> magnitude

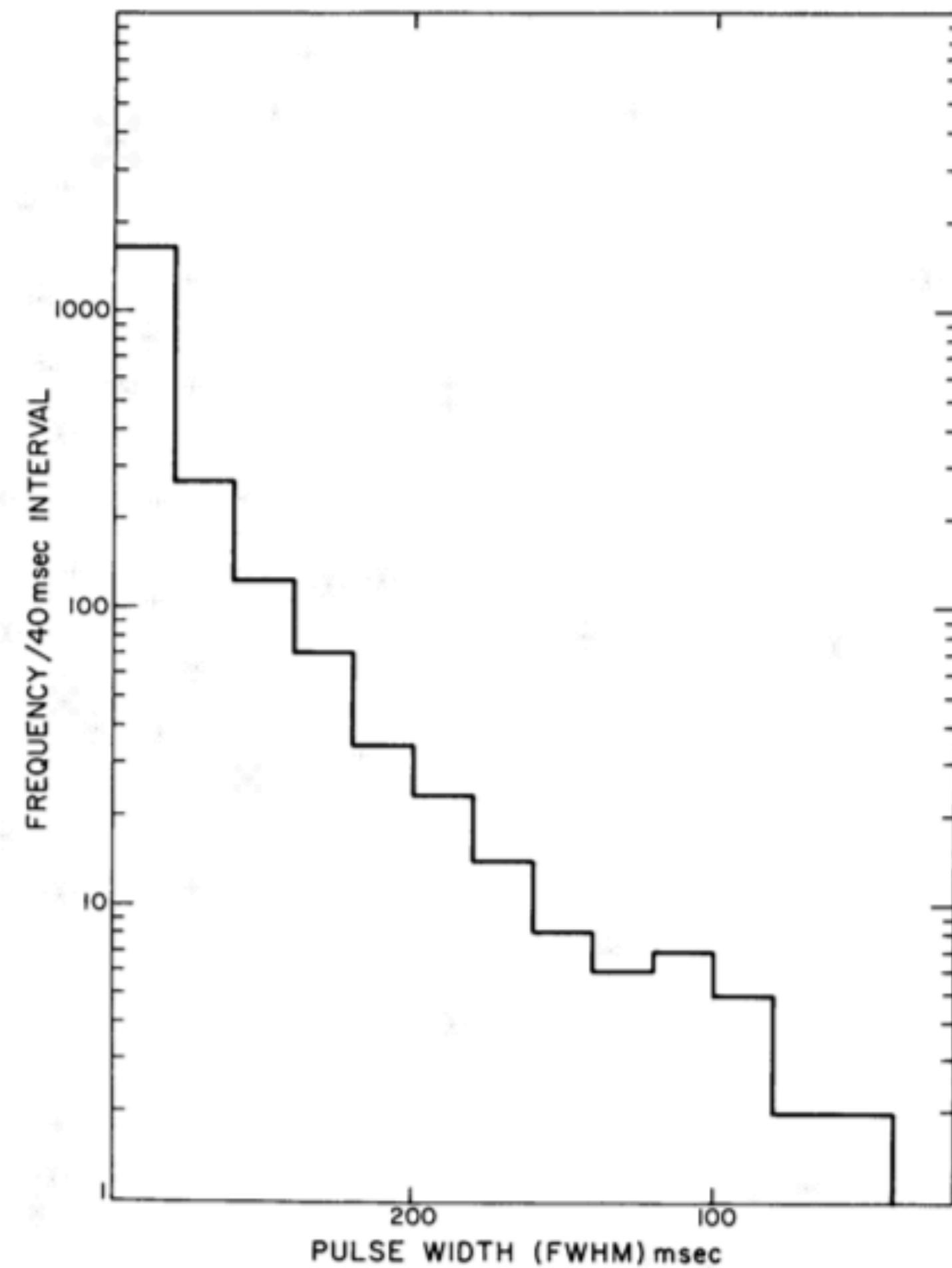


**Figure 4.** The distribution of pulse widths with time (FWHM).

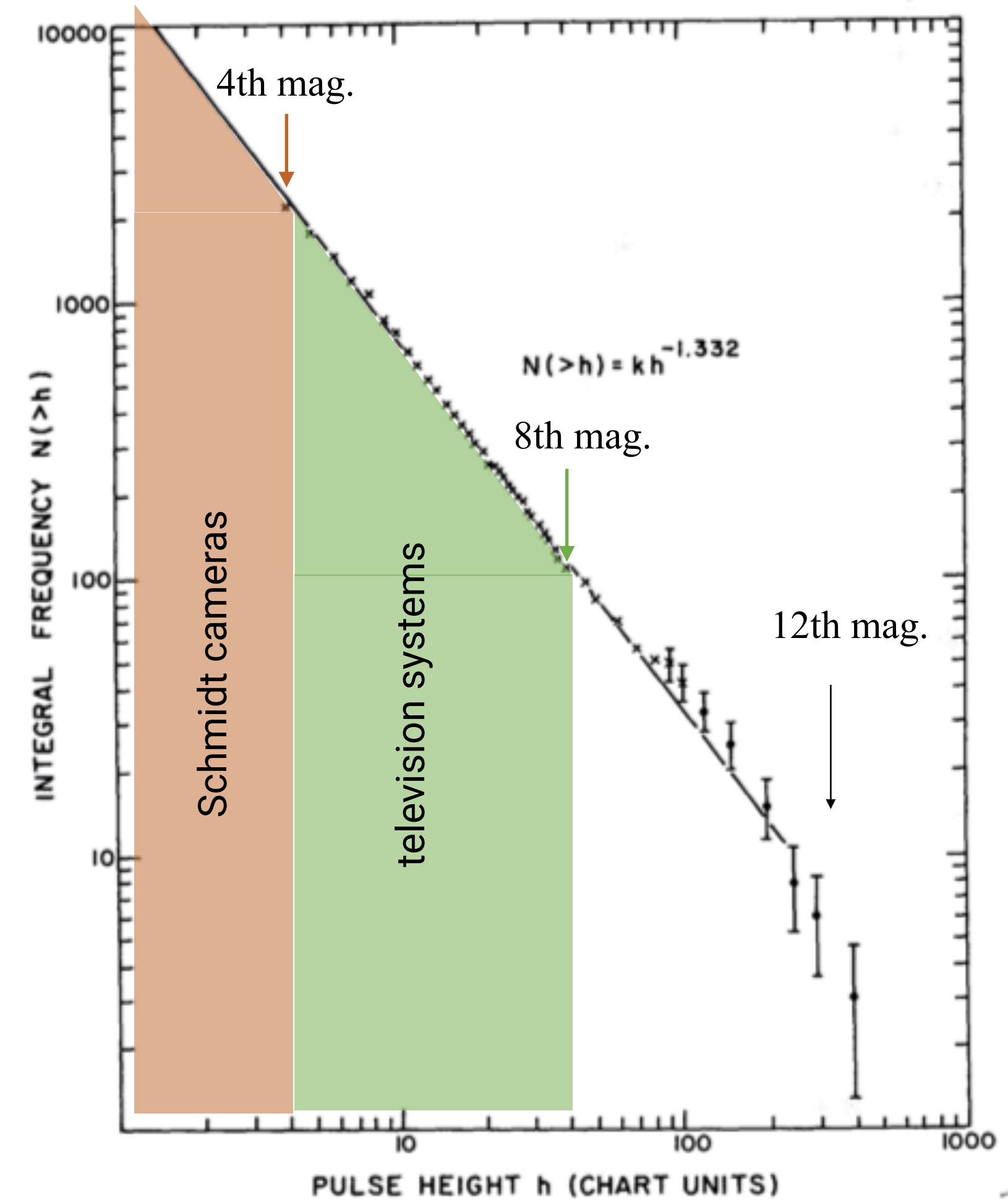


**Figure 5.** Integral pulse height distribution of all the recorded meteors in the detector channel A.

Cook et al. MNRAS 193, 645 (1980).



# Optical observations setting limits on DM candidates

## LETTERS TO NATURE

### Nuclearites—a novel form of cosmic radiation

A. De Rújula\* & S. L. Glashow†‡

\* Theory Division, CERN, CH-1211 Geneva 23, Switzerland

† Department of Physics, Boston University, Boston, Massachusetts 02215, USA

E. Witten (personal communication) has raised the intriguing possibility that nuclear matter consisting of aggregates of up, down and strange quarks in roughly equal proportions may be less massive than ordinary nuclear matter of the same quark number consisting of protons and neutrons (triplets of non-strange quarks). These nuggets of strange quark matter may be stable for almost any baryon number ( $A$ ), including values intermediate between those of ordinary nuclei ( $A \lesssim 263$ ) and neutron stars ( $A \sim 10^{57}$ ). We use the term 'nuclearite' to describe such strange quark nuggets in collision with Earth and suggest experiments to detect these encounters.

Ordinary nuclear matter has an energy density of  $\sim 938$  MeV per nucleon. Ordinary quark matter—a purely hypothetical form of matter in which the constituent up and down quarks and gluons are not confined within individual nucleons—evidently has a higher energy density, for otherwise nuclei would decay into quark matter. Strange quark matter (consisting of equal numbers of up, down and strange quarks) differs energetically from ordinary quark matter in two ways: strange quarks are considerably heavier than ordinary quarks, which is why strange baryons are some 200 MeV heavier than nucleons. On the other hand, the Pauli exclusion principle acts so as to make strange quark matter more stable than ordinary quark matter. In a degenerate gas of massless quarks at zero temperature, the energy per quark depends on the number of quark species, and in a three-flavour system (strange quark matter) it is estimated by Witten to be  $\sim 90\%$  of what it is in a two-flavour system.

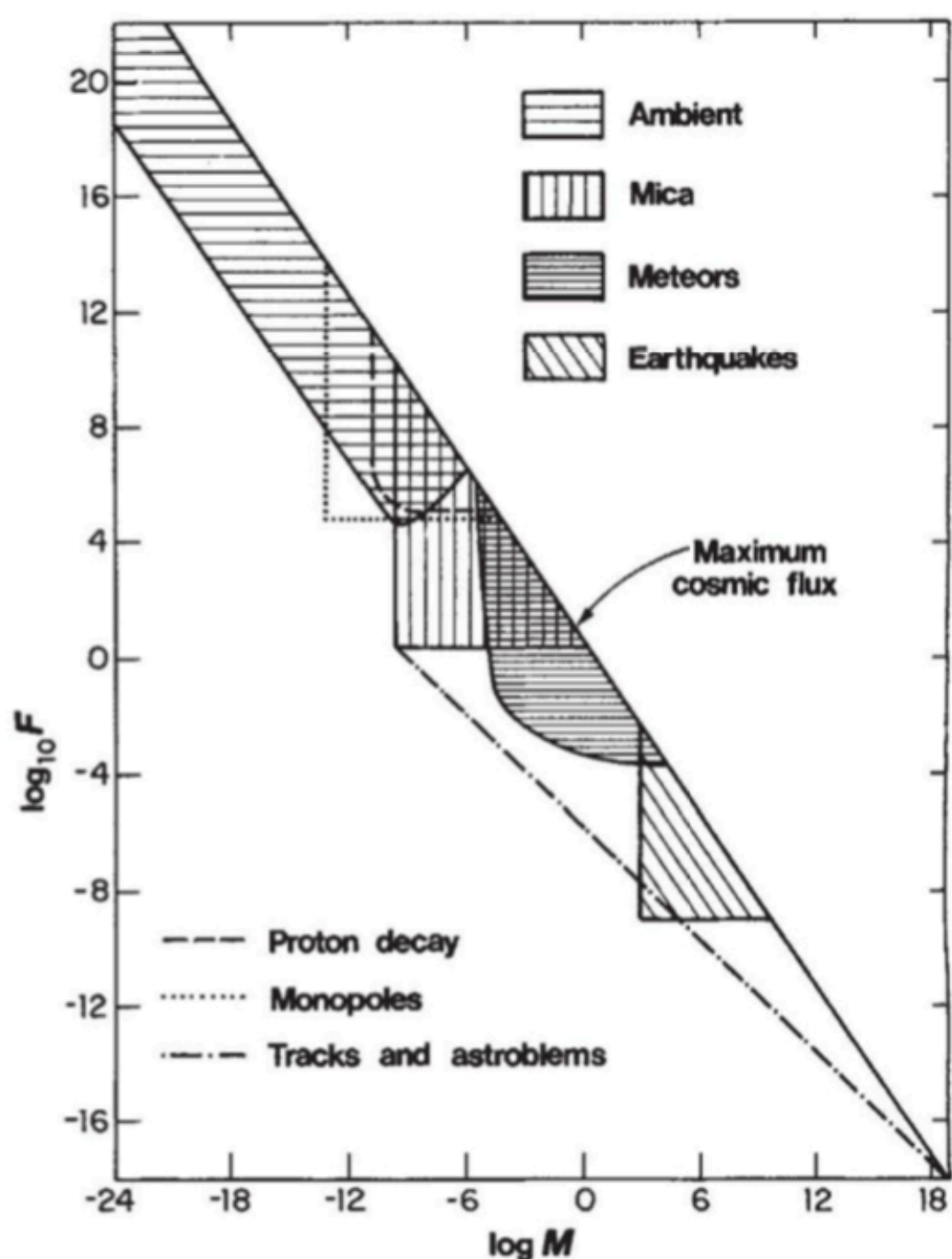


Fig. 1 The maximum possible cosmic flux of nuclearites  $F$  ( $\text{km}^{-2} \text{yr}^{-1} (2\pi \text{sr})^{-1}$ ) as a function of mass. Also shown are regions that would be excluded by the several experiments discussed in the text. (Of these, only the 'mica' limit corresponds to an experiment actually performed.)

De Rújula & Glashow (1984)

- Aggregates of up, down, strange quarks formed at early epoch  
➡Dark Matter candidate
- Surrounded by electron 'shield'  
➡  $\therefore$  electrically neutral
- passage through atmosphere causes light much like a meteorite
- but travelling at galactic velocities ( $\sim 270 \text{ km/s}$ , c.f. meteorites 12-72 km/s)



# Optical observations setting limits on DM candidates

## LETTERS TO NATURE

### Nuclearites—a novel form of cosmic radiation

A. De Rújula\* & S. L. Glashow†‡

\* Theory Division, CERN, CH-1211 Geneva 23, Switzerland  
† Department of Physics, Boston University, Boston, Massachusetts 02215, USA

E. Witten (personal communication) has raised the intriguing possibility that nuclear matter consisting of aggregates of up, down and strange quarks in roughly equal proportions may be less massive than ordinary nuclear matter of the same quark number consisting of protons and neutrons (triplets of non-strange quarks). These nuggets of strange quark matter may be stable for almost any baryon number ( $A$ ), including values intermediate between those of ordinary nuclei ( $A \leq 263$ ) and neutron stars ( $A \sim 10^{57}$ ). We use the term 'nuclearite' to describe such strange quark nuggets in collision with Earth and suggest experiments to detect these encounters.

Ordinary nuclear matter has an energy density of  $\sim 938$  MeV per nucleon. Ordinary quark matter—a purely hypothetical form of matter in which the constituent up and down quarks and gluons are not confined within individual nucleons—evidently has a higher energy density, for otherwise nuclei would decay into quark matter. Strange quark matter (consisting of equal numbers of up, down and strange quarks) differs energetically from ordinary quark matter in two ways: strange quarks are considerably heavier than ordinary quarks, which is why strange baryons are some 200 MeV heavier than nucleons. On the other hand, the Pauli exclusion principle acts so as to make strange quark matter more stable than ordinary quark matter. In a degenerate gas of massless quarks at zero temperature, the energy per quark depends on the number of quark species, and in a three-flavour system (strange quark matter) it is estimated by Witten to be  $\sim 90\%$  of what it is in a two-flavour system.

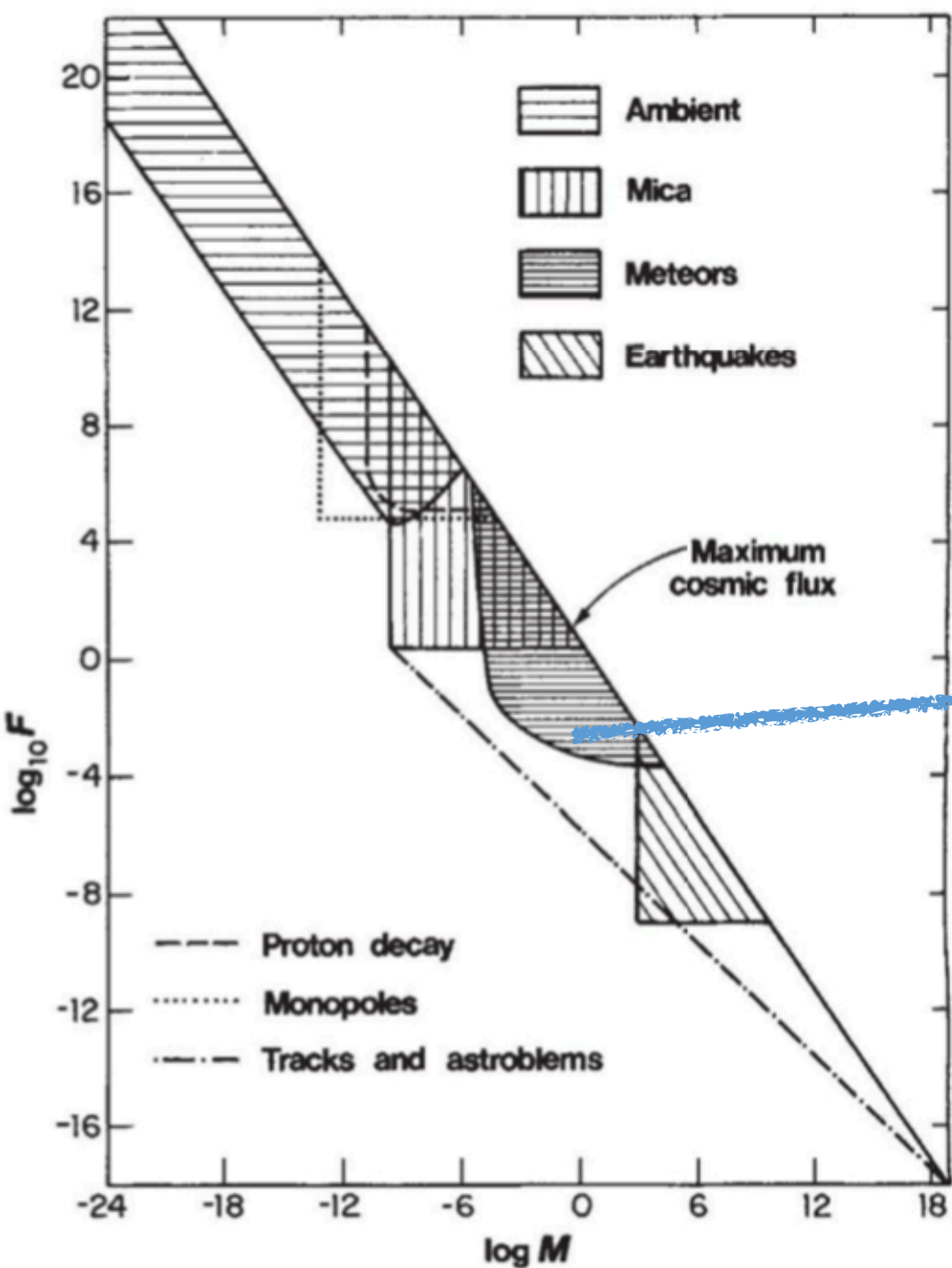


Fig. 1 The maximum possible cosmic flux of nuclearites  $F$  ( $\text{km}^{-2} \text{yr}^{-1} (2\pi \text{sr})^{-1}$ ) as a function of mass. Also shown are regions that would be excluded by the several experiments discussed in the text. (Of these, only the 'mica' limit corresponds to an experiment actually performed.)

De Rújula & Glashow (1984)

NATURE VOL. 316 4 JULY 1985

LETTERS TO NATURE

### A search for evidence of nuclearites in astrophysical pulse experiments

N. A. Porter\*, D. J. Fegan\*, G. C. MacNeill\* & T. C. Weekes†

\* Physics Department, University College, Dublin 4, Ireland  
† Harvard-Smithsonian Center for Astrophysics, Whipple Observatory, Arizona 85645-0097, USA

De Rújula and Glashow<sup>1</sup> have suggested that nuclearites, aggregates of up, down and strange quarks in roughly equal proportions, may form a component of the material reaching the Earth from the Galaxy. On traversing the atmosphere they will look something like meteors, but will travel faster. The masses of these aggregates may vary over a wide range and their velocities will be typically  $250 \text{ km s}^{-1}$ , corresponding to the Sun's galactic rotation. If all the dark matter in the Galaxy is assumed to be in the form of nuclearites, a limit can be set to the incoming flux. We report here upper limits derived from four experiments, originally carried out to detect cosmic  $\gamma$  rays, as well as some derived by other authors, which would be sensitive to pulses of light from nuclearites in the lower atmosphere. Our upper limits are compatible with the suggested maximum flux and competitive with a search for tracks etched in mica<sup>2</sup>, which could also be caused by nuclearites.

De Rújula and Glashow show that the visual magnitude of an atmospheric nuclearite:

$$M = 10.8 - 1.67 \log_{10} (m/10^{-6}) + 5 \log_{10} (h/10 \text{ km}) \quad (1)$$

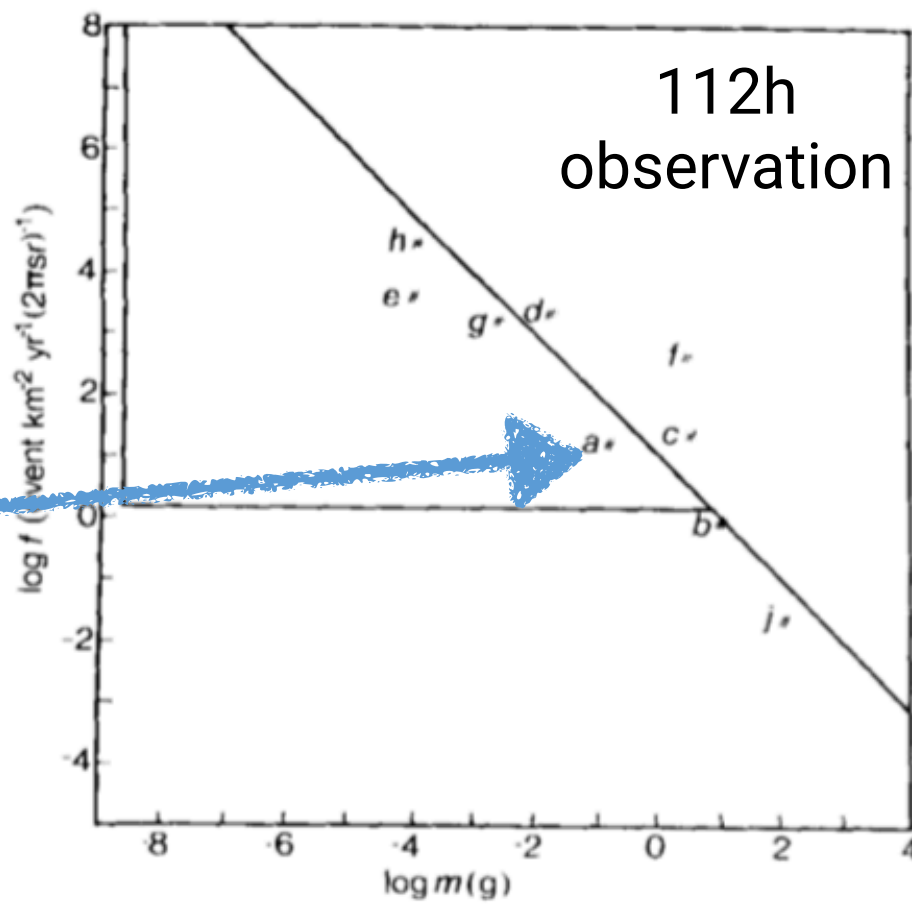


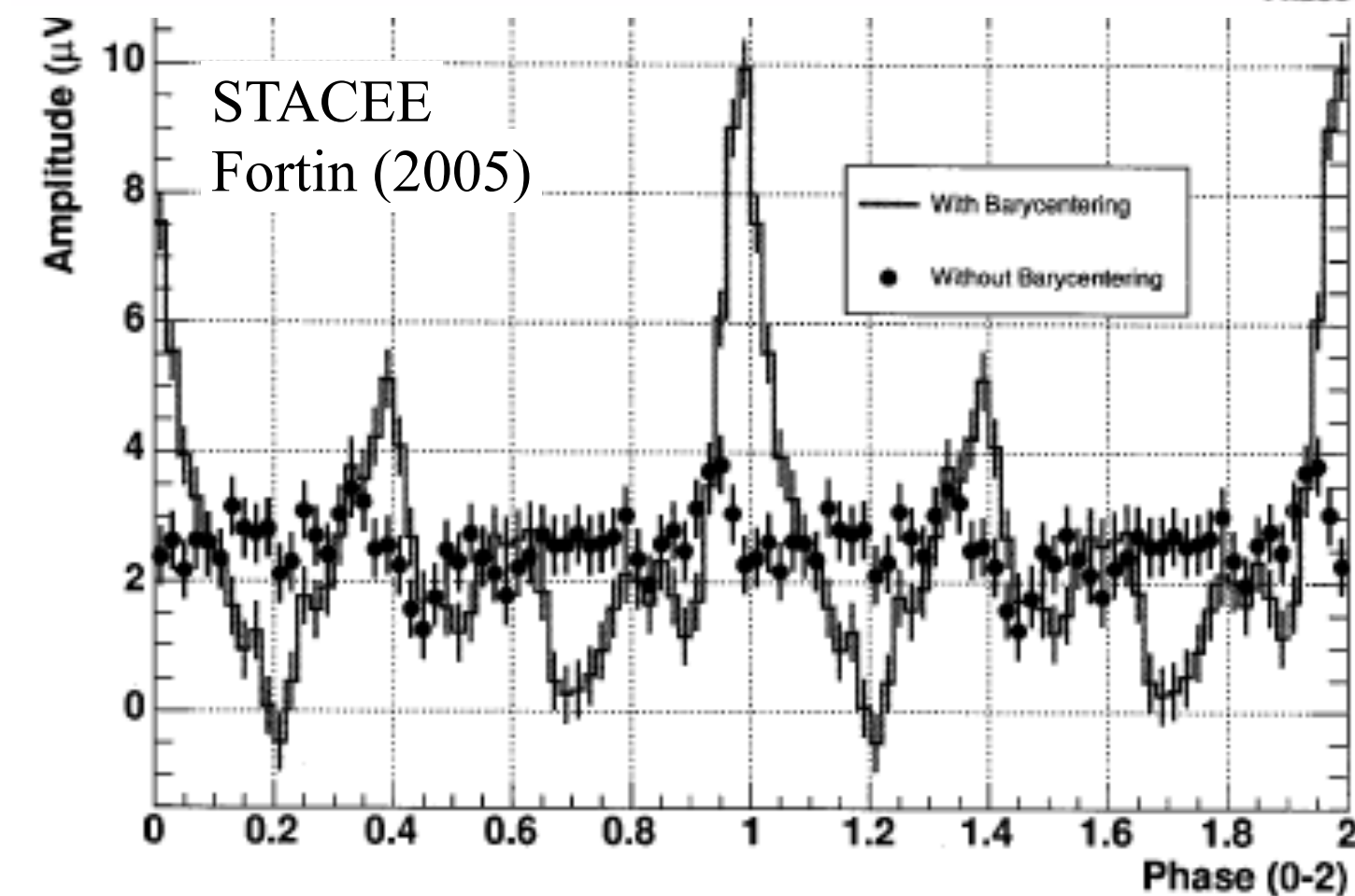
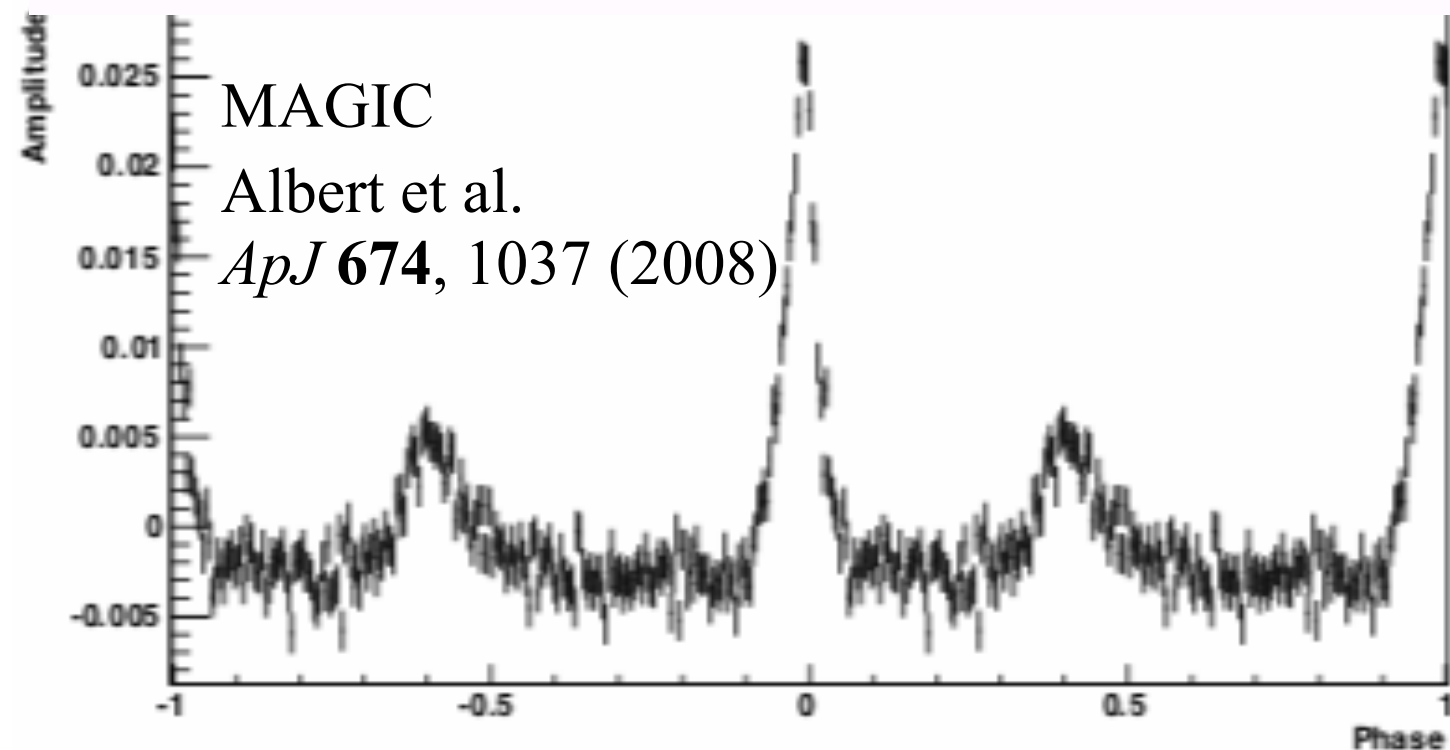
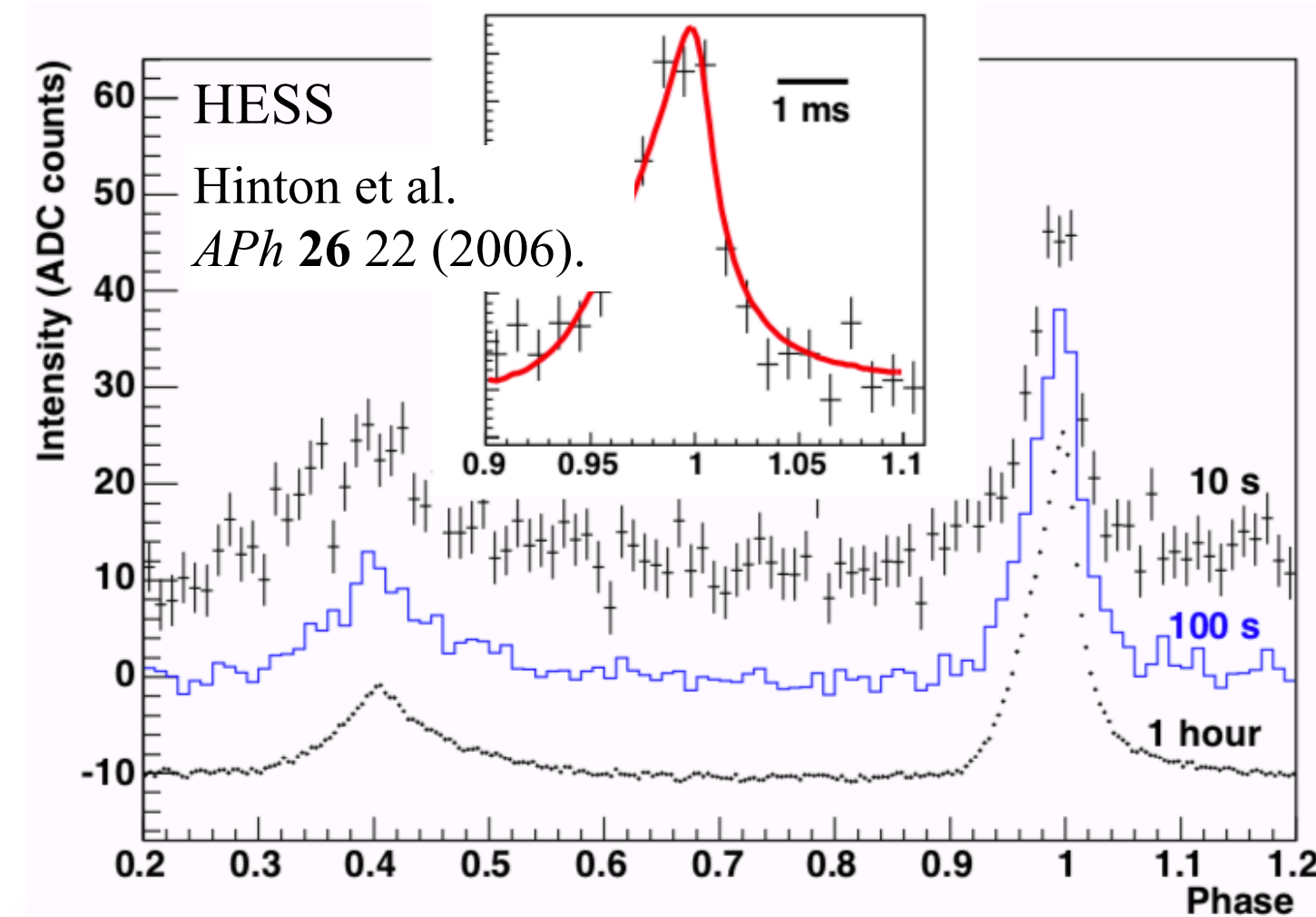
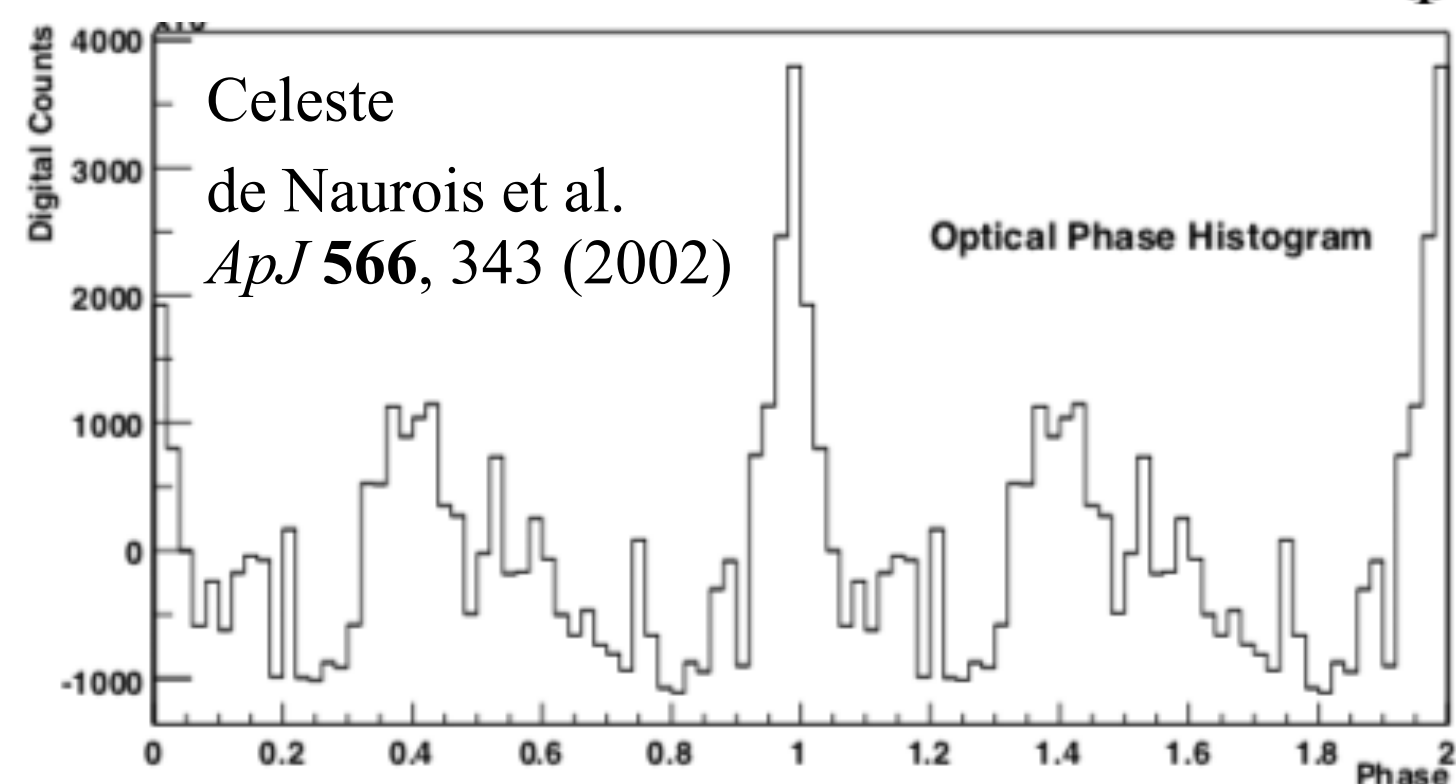
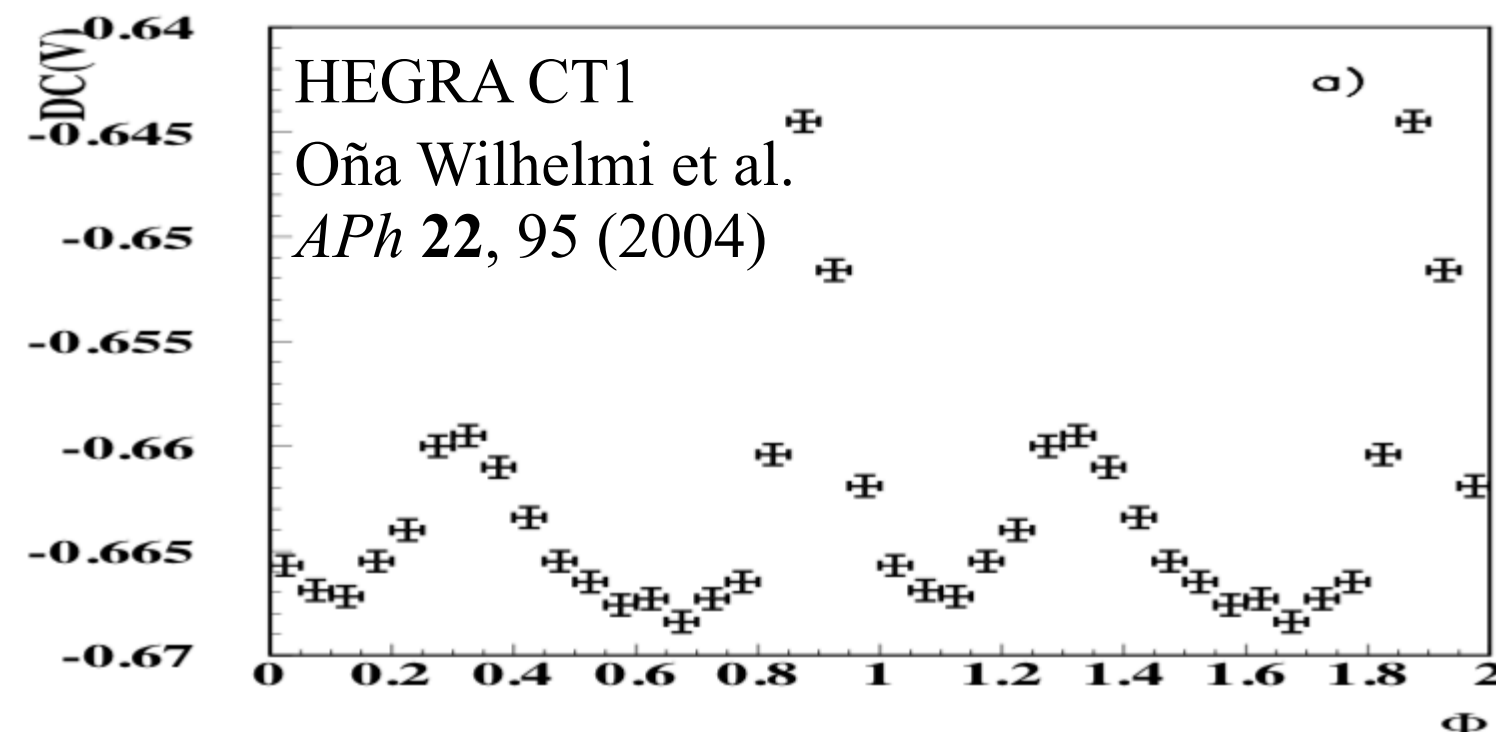
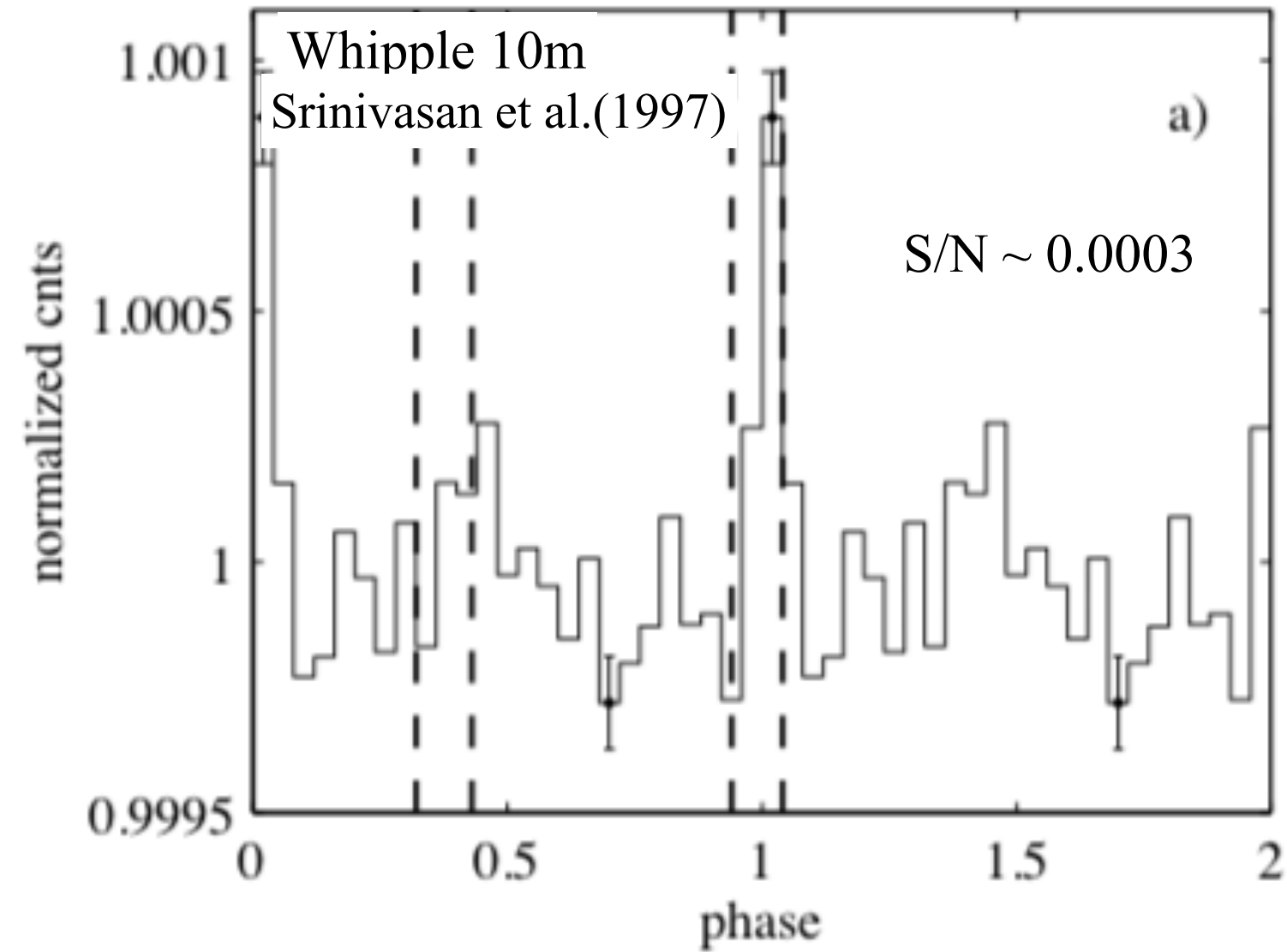
Fig. 1 Mass of the nuclearites plotted against incoming flux. The sources are detailed in Table 1.

plier, we obtain a photon number of 823 photons in  $10^{-8}$  s average illumination over the  $10^{-2}$  s transit time. The area of the reflector was effectively  $60 \text{ m}^2$ , leading to a flux of  $1.37 \times 10^{-3}$  photons  $\text{cm}^{-2}$  in  $10^{-8}$  s, or  $1.37 \times 10^5$  photons  $\text{cm}^{-2} \text{s}^{-1}$ . Converting this to  $\text{erg cm}^{-2} \text{s}^{-1}$  to obtain the visual magnitude<sup>6</sup> and taking  $0 \text{ mag} = 8.5 \times 10^{-6} \text{ erg cm}^{-2} \text{s}^{-1}$ , we obtain a limiting mag-

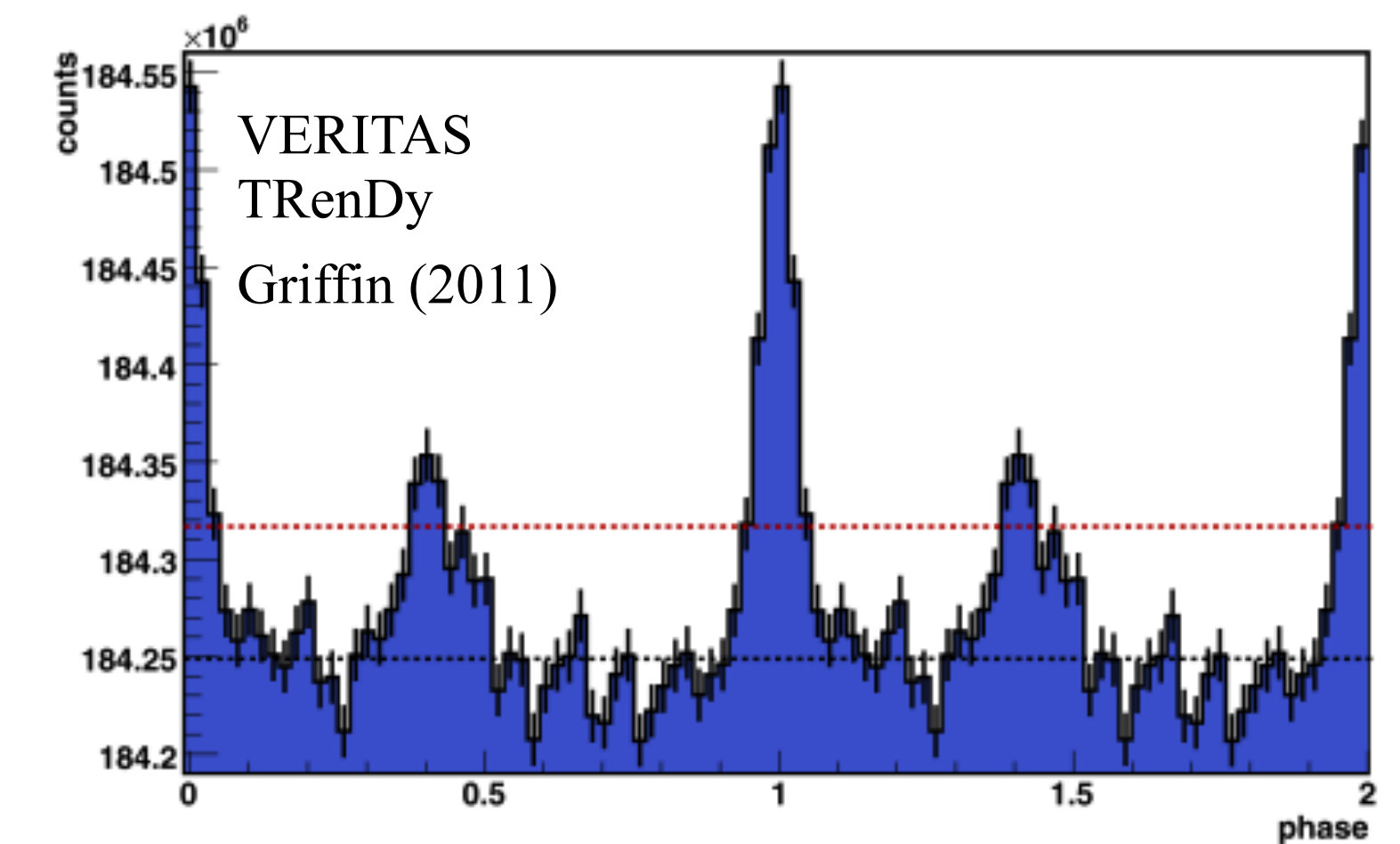
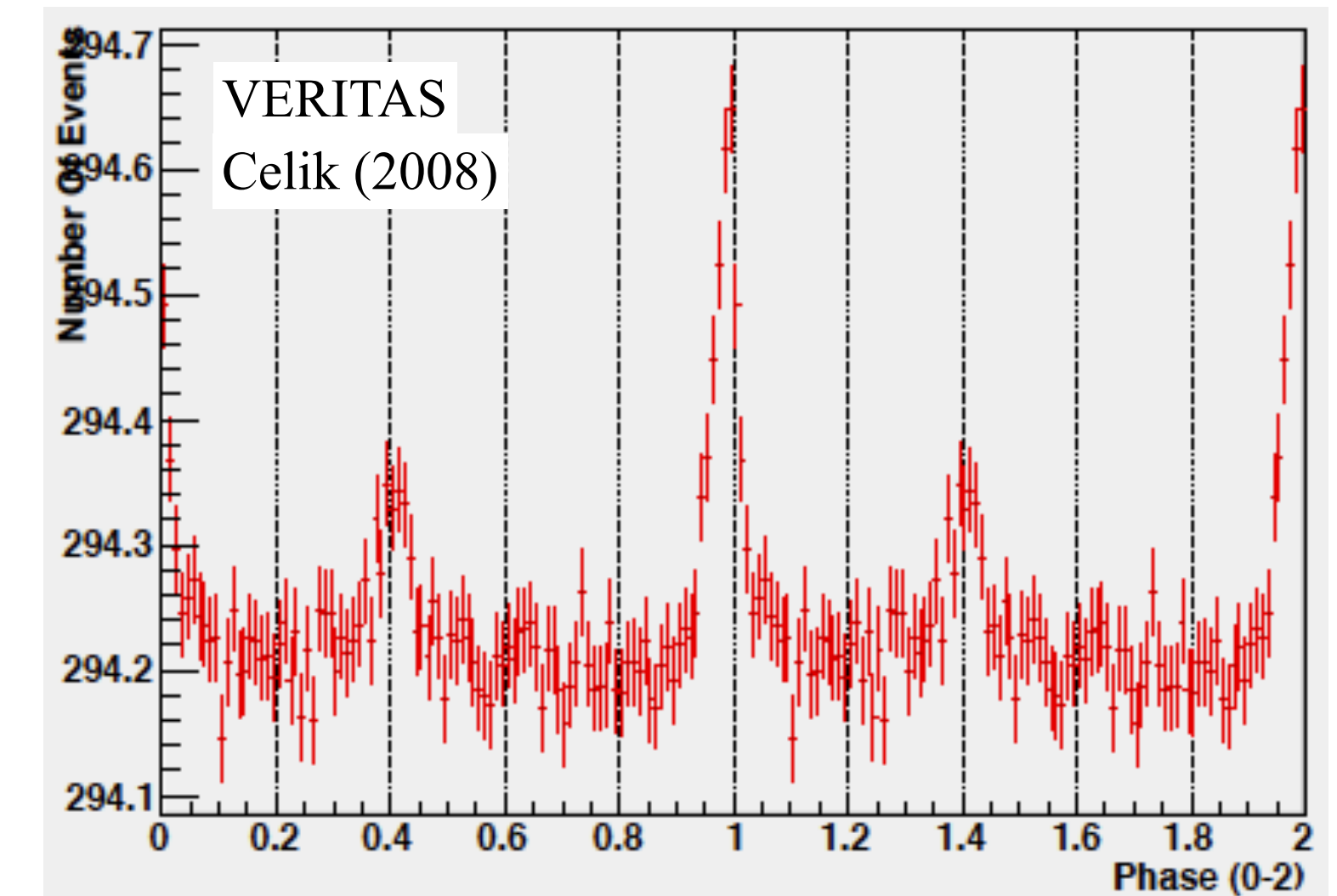
Porter et al.(1985)

Signature is like a meteor, but travels at galactic velocities ( $\sim 270 \text{ km/s}$ ) instead of solar system ( $12\text{-}72 \text{ km/s}$ )





Periodically IACTs measure the Crab optical pulsar to verify their timing analyses...





# High Time Resolution Optical Photometry

Whipple 10m (1974)

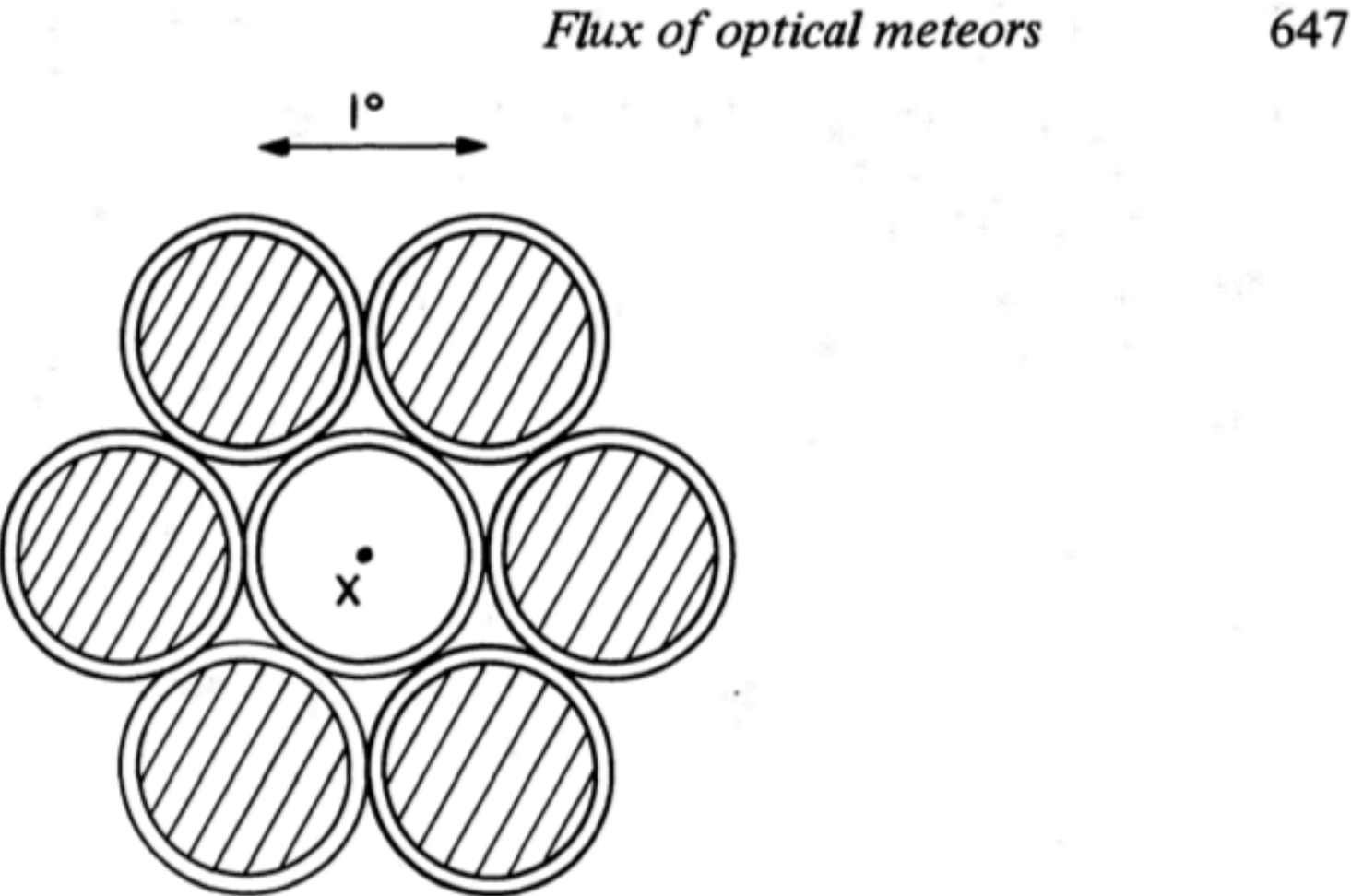


Figure 1. Phototube configuration at focal point of the 10-m reflector. X = detector. Separation between tube centres is 1°.2. Cross-hatched areas are covered by guard ring.

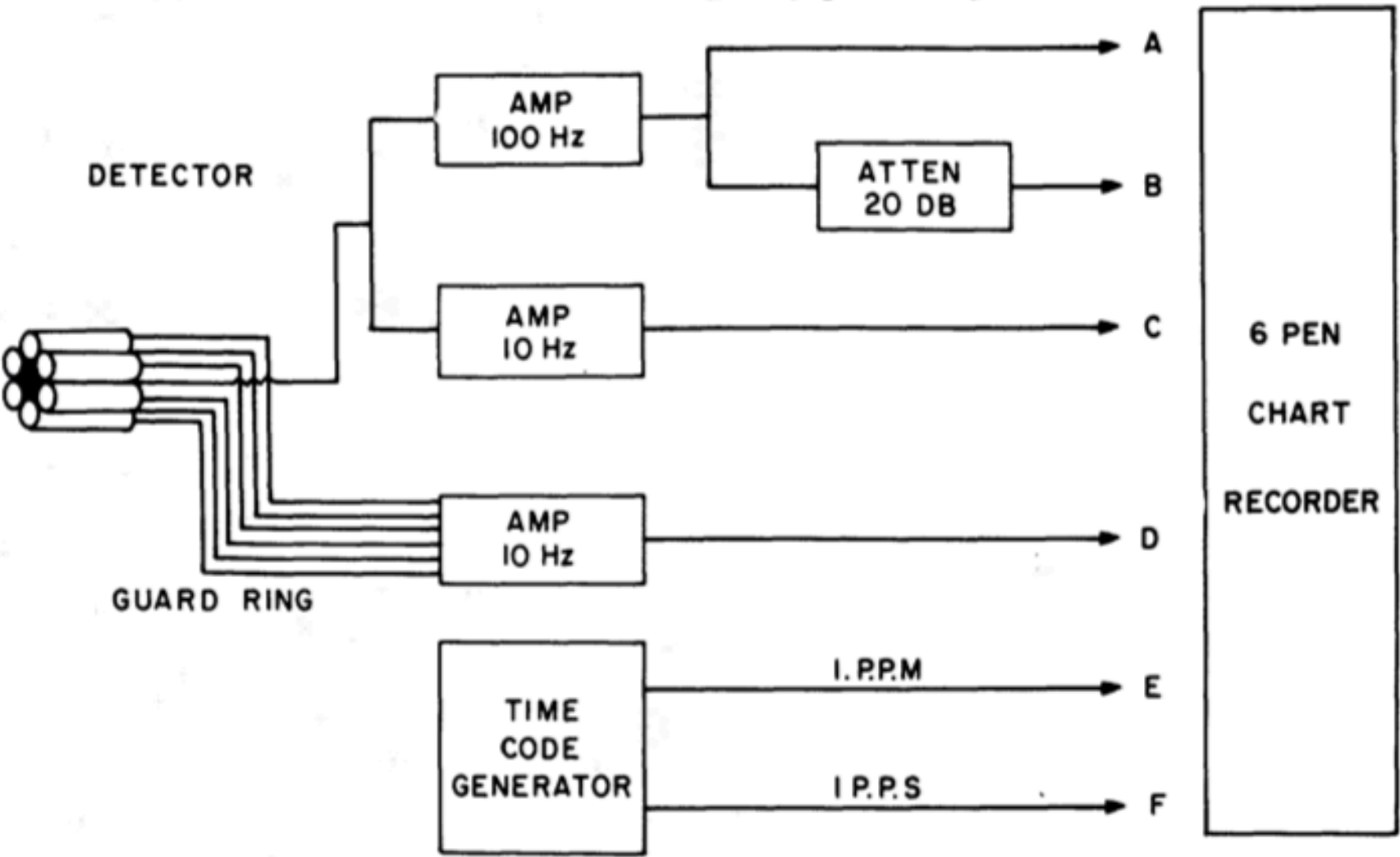


Figure 2. Block diagram of recording system.

Cook et al. *MNRAS* **193**, 645 (1980).

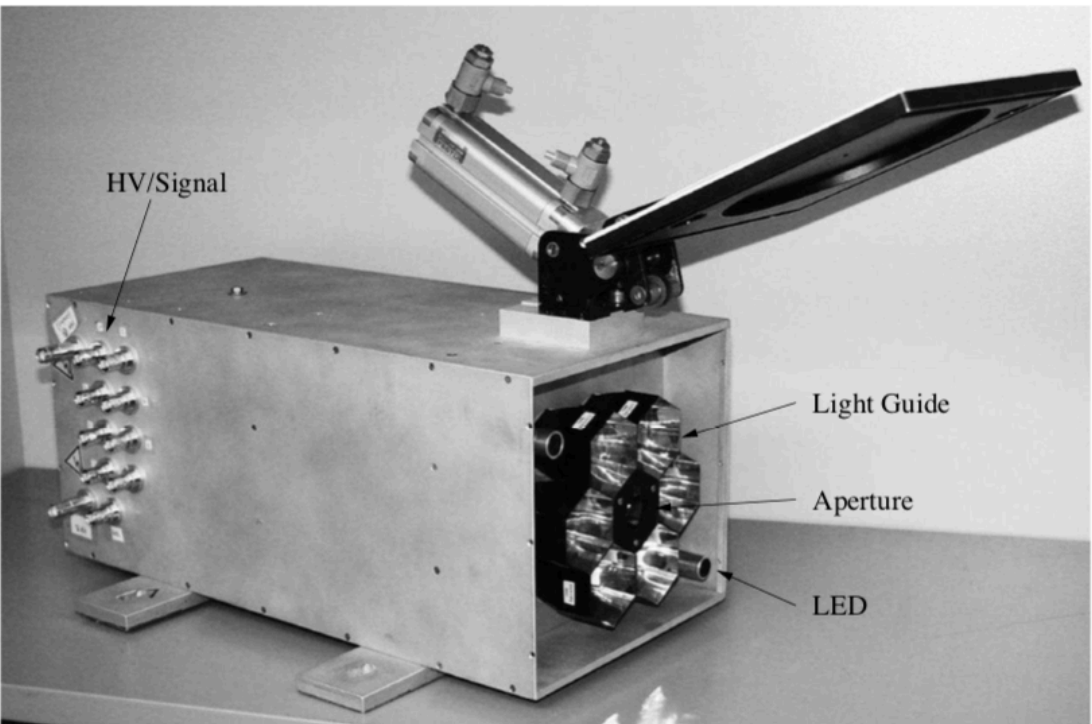
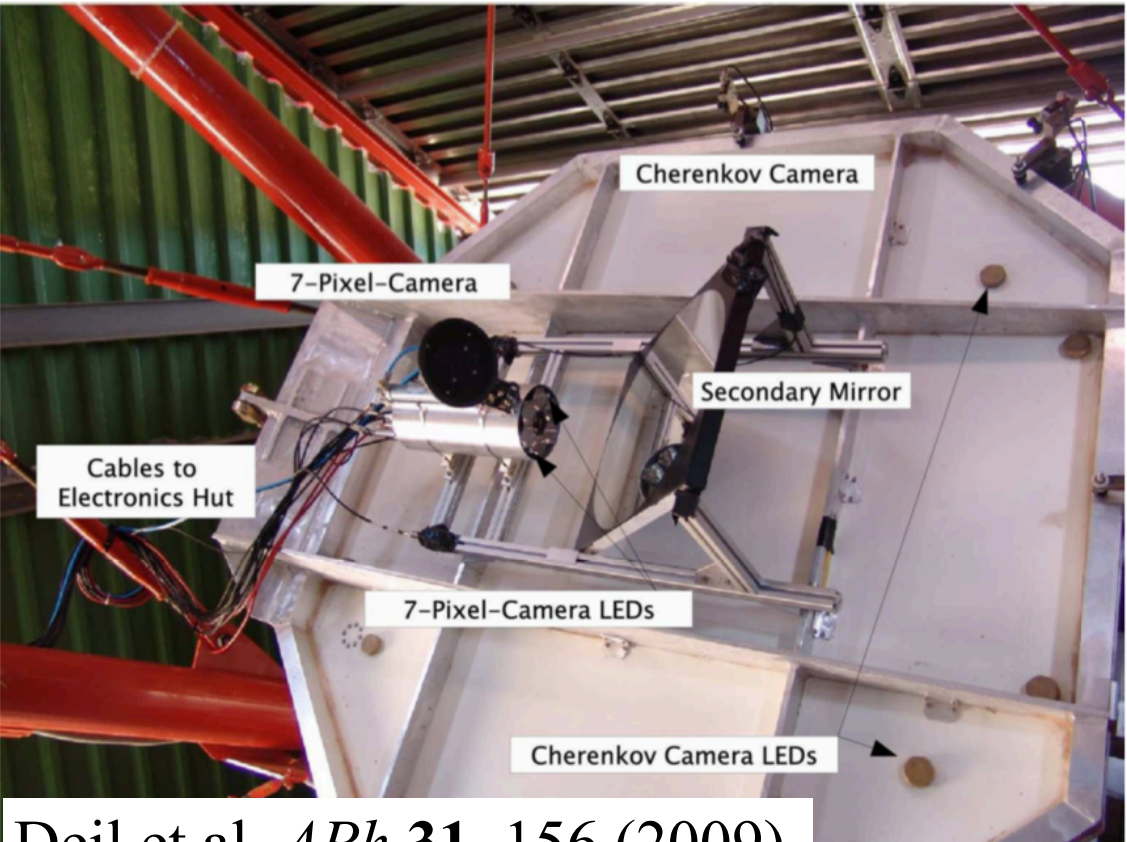
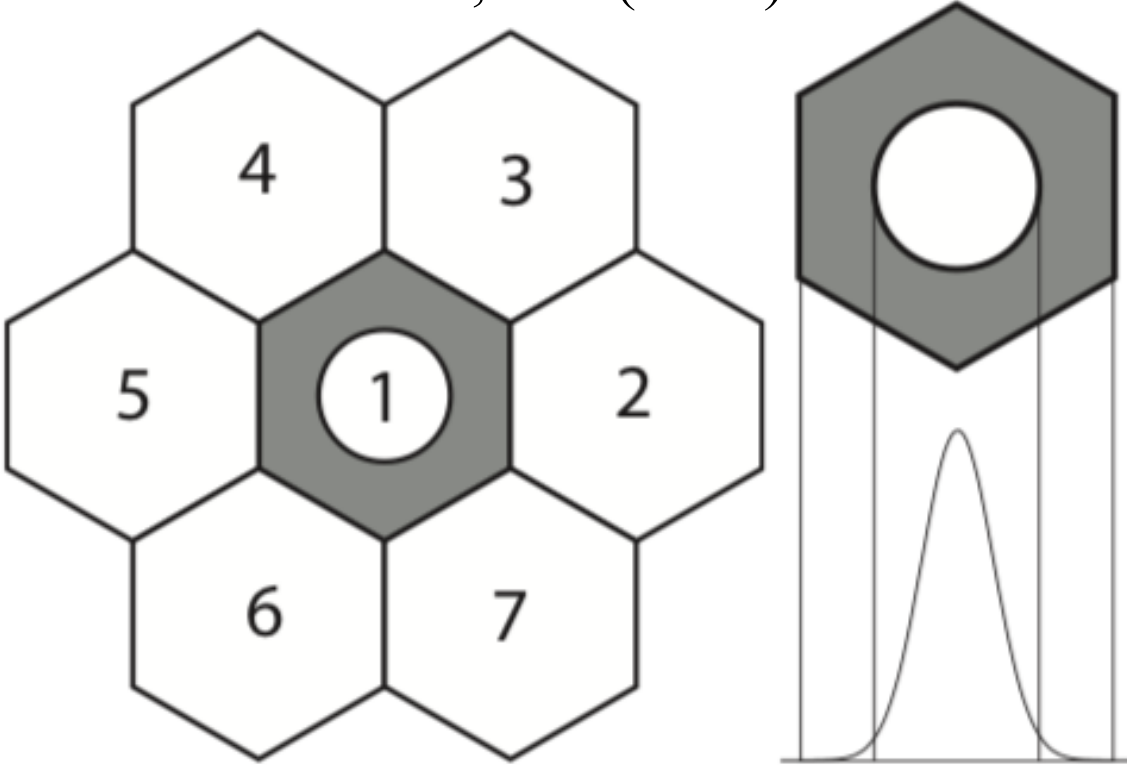


Fig. 1. Photograph showing the principle mechanical components of the optical pulsar camera: the central pixel aperture, the “veto” pixel light guides, the positioning LEDs and the HV inputs/signal outputs for the photomultipliers mounted within the casing.  
Hinton et al. *Aph* **26**, 22 (2006).



Deil et al. *Aph* **31**, 156 (2009).



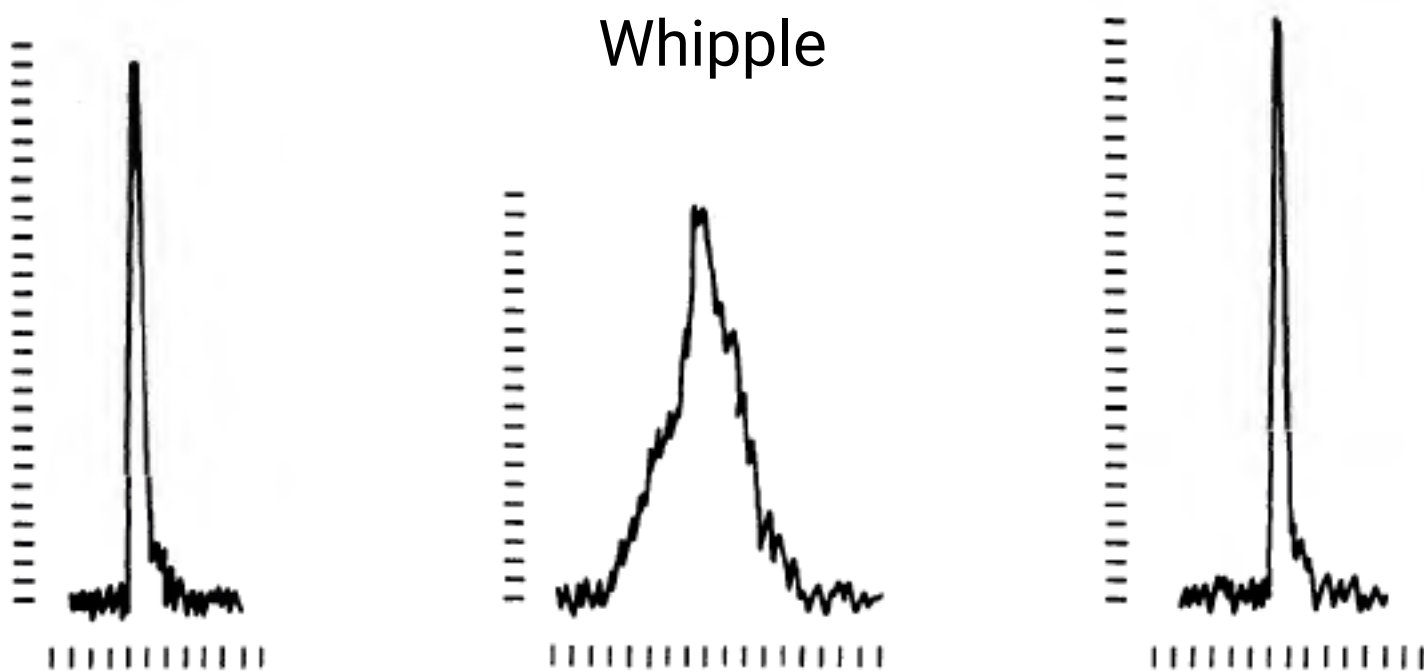
It is a matter of preference as to whether the photodetector is internal or external to the Cherenkov camera, the technology is largely the same, it is just the integration time that varies based on the science case



But mostly it may have felt like meteors are what is mostly (only) seen...

Flux of optical meteors down to  $M_{PG} = +12$

Cook et al. *MNRAS* **193**, 645 (1980).



Capability of Cherenkov Telescopes to Observe Ultra-fast Optical Flares

Deil et al. *Aph* **31**, 156 (2009).

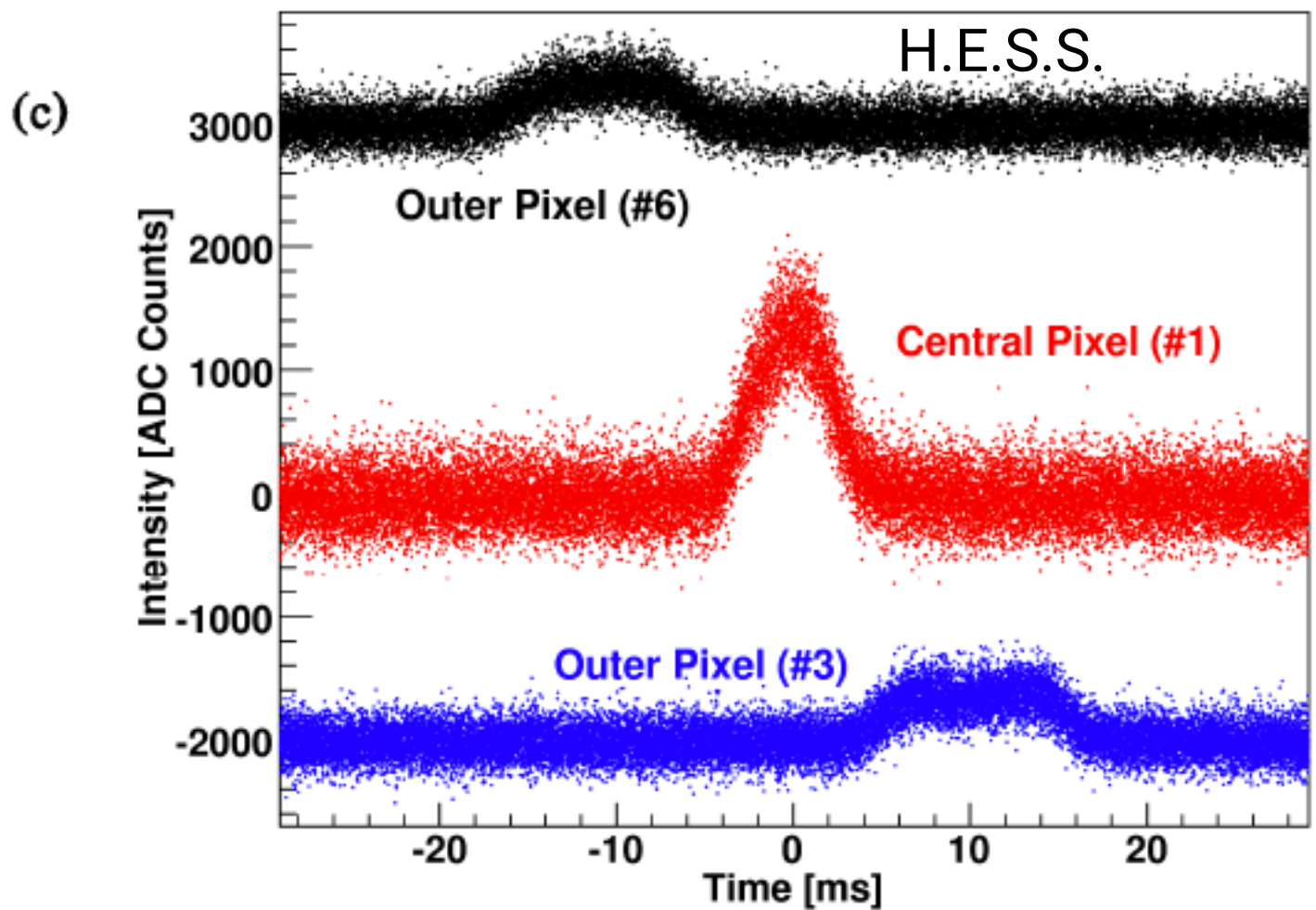
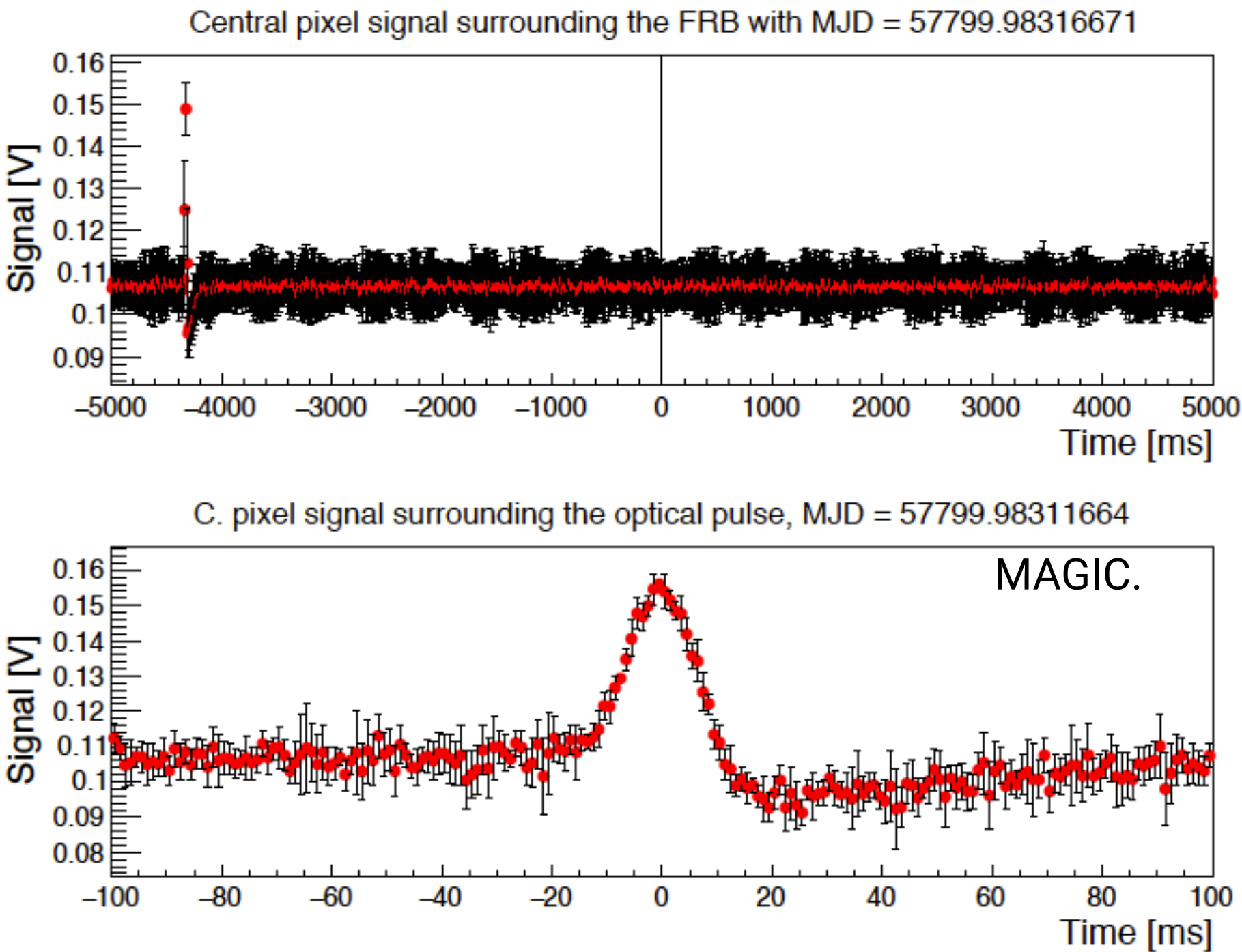


Fig. 5. Example **background events** very likely caused by a shooting star (*top*) and lightning (*bottom*). The intensities were arbitrarily offset such that the light curves from different channels do not overlap.

Constraining very-high-energy and optical emission from FRB 121102 with the MAGIC telescopes

Acciari et al. *MNRAS* **481**, 2479 (2018).

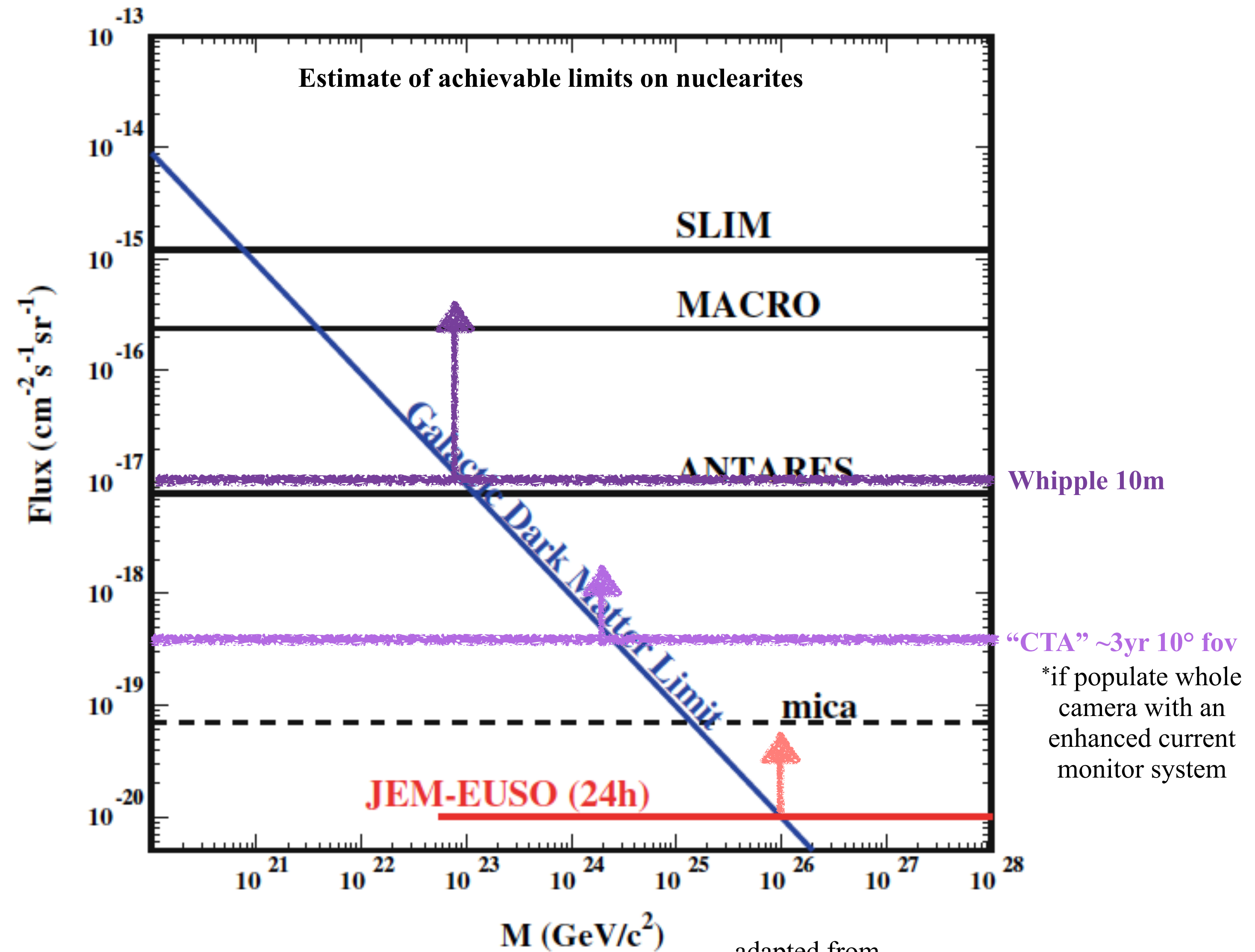


**Figure 3.** *Top:* Optical light curve covering 10 s around the first FRB in our sample, for an integration window of 10 ms. A clear optical pulse is detected 4.3 s before the FRB. *Bottom:* Optical light curve covering 200 ms around the detected optical pulse, for an integration window of 1 ms. The pulse is consistent with a **background event**. Note that the undershoot after the optical flash is caused by the central pixel readout electronics.



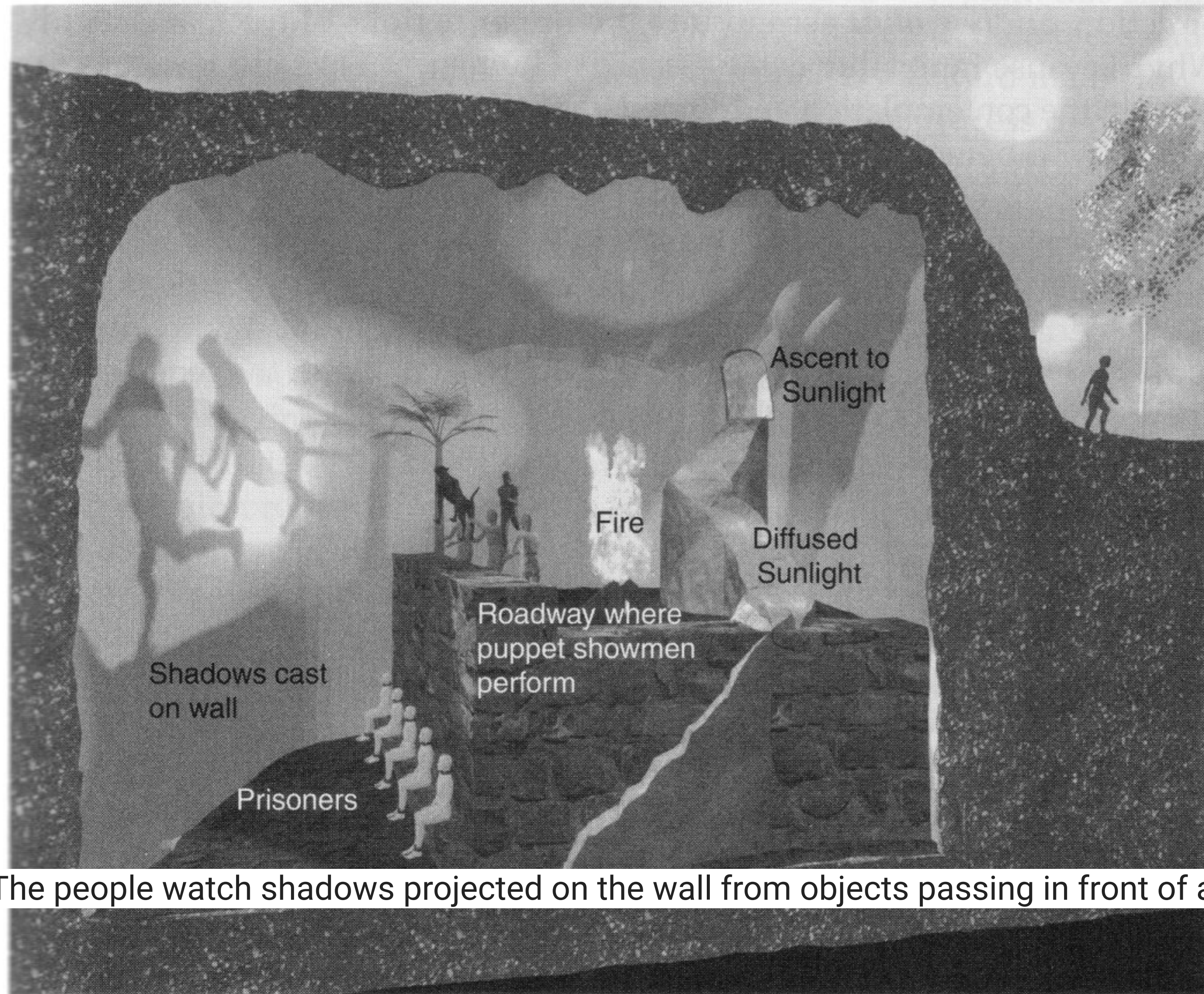
## An aside on FoV

BTW, the more of the field of view you populate, the more you can do.

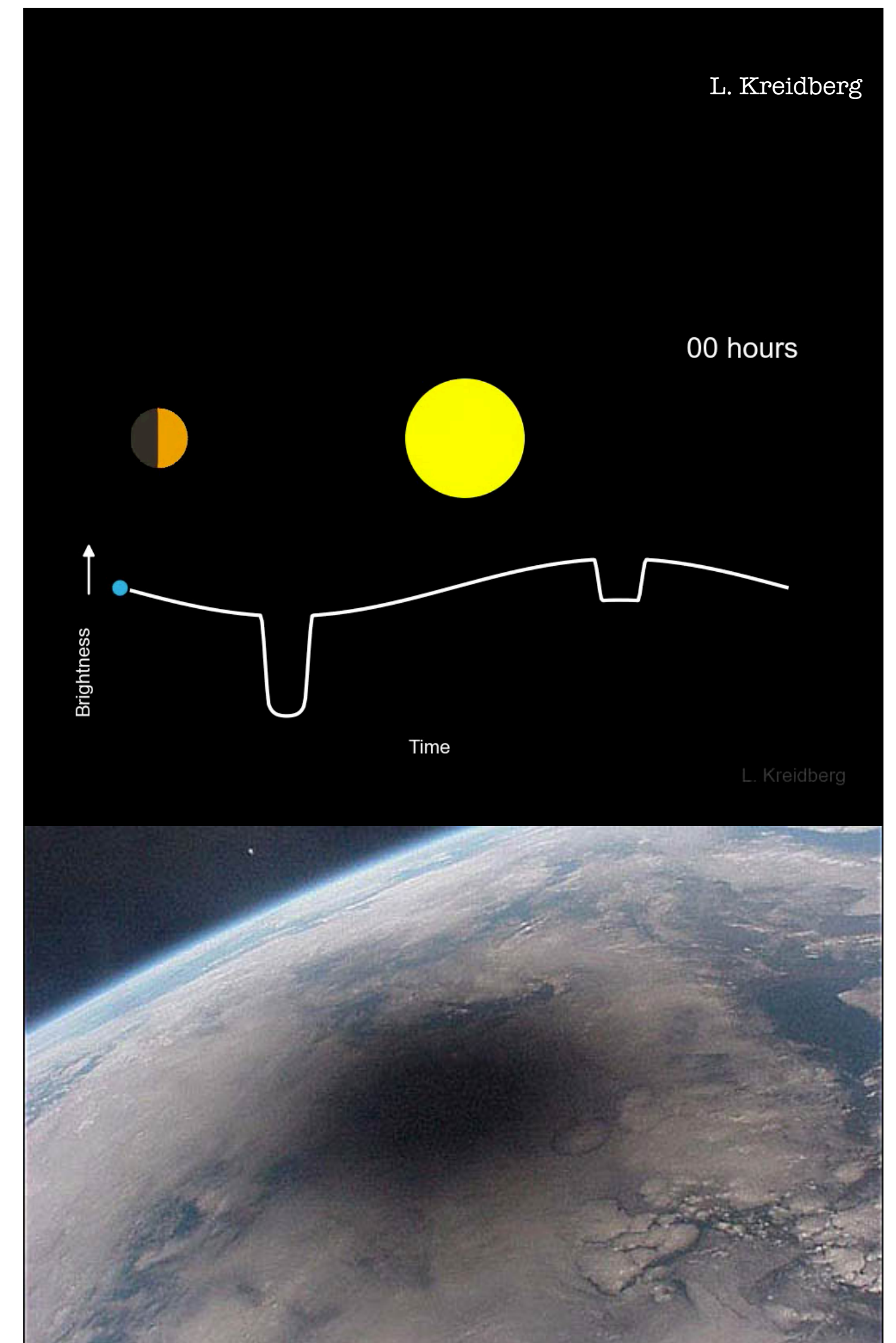




# PLATO'S ALLEGORY OF THE CAVE

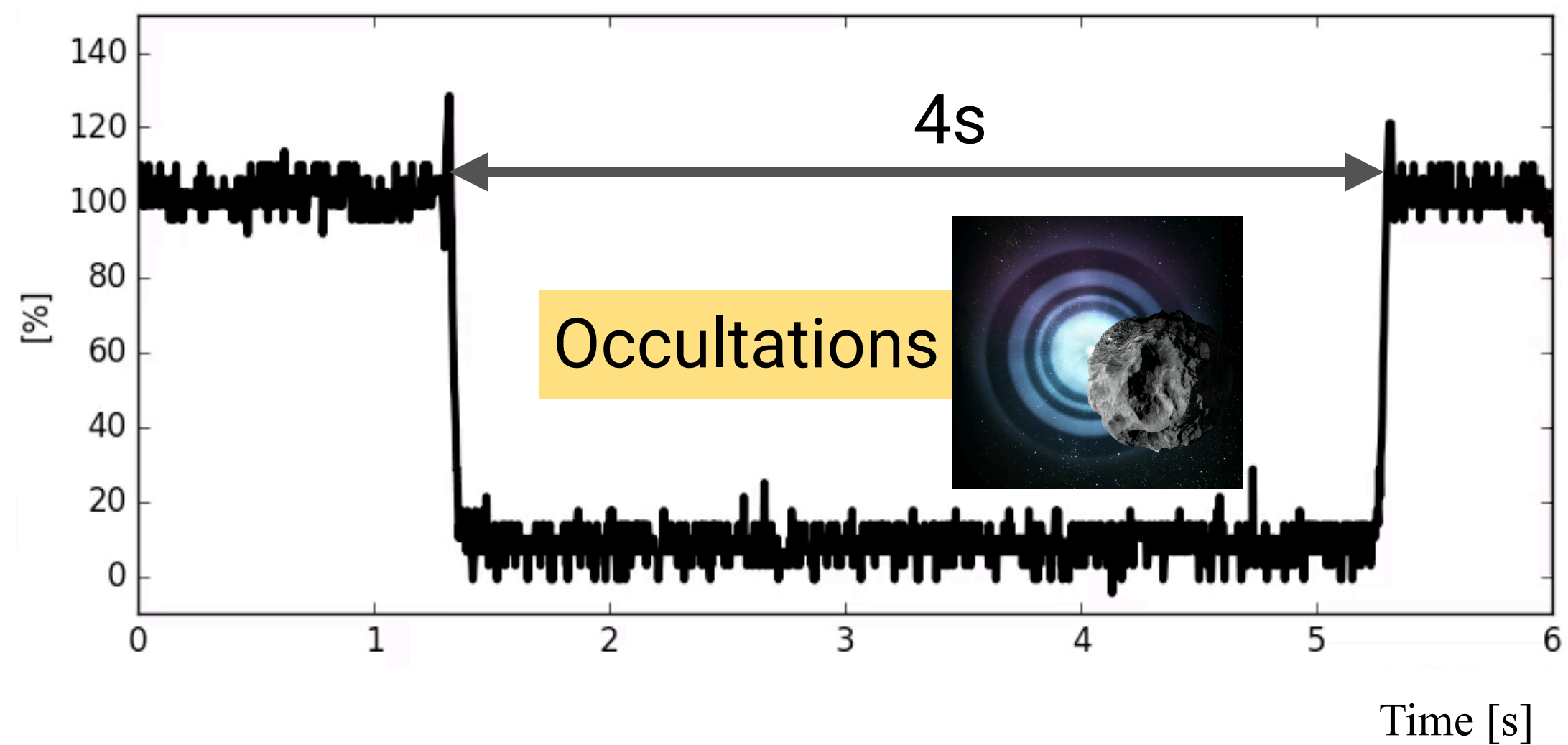
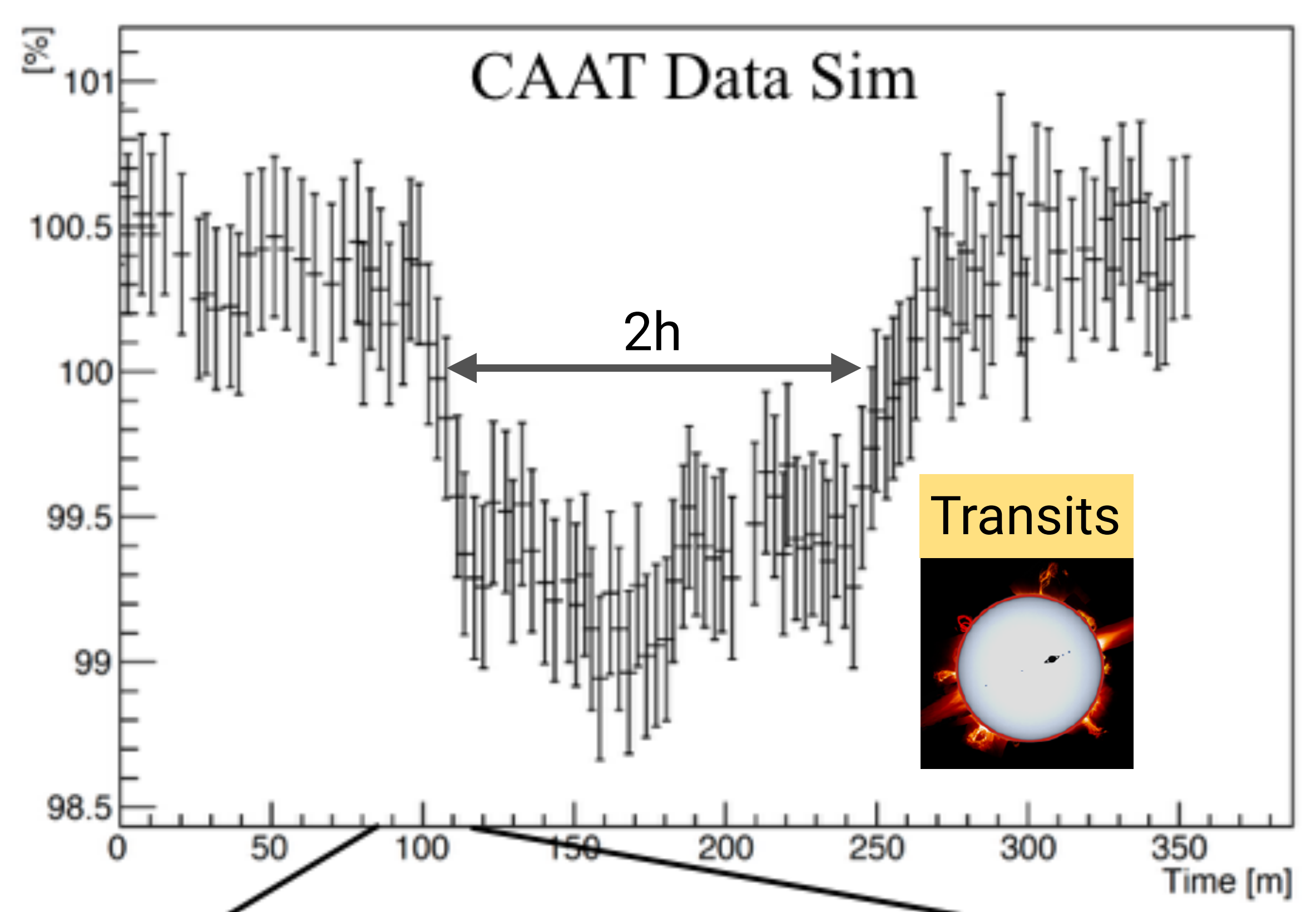
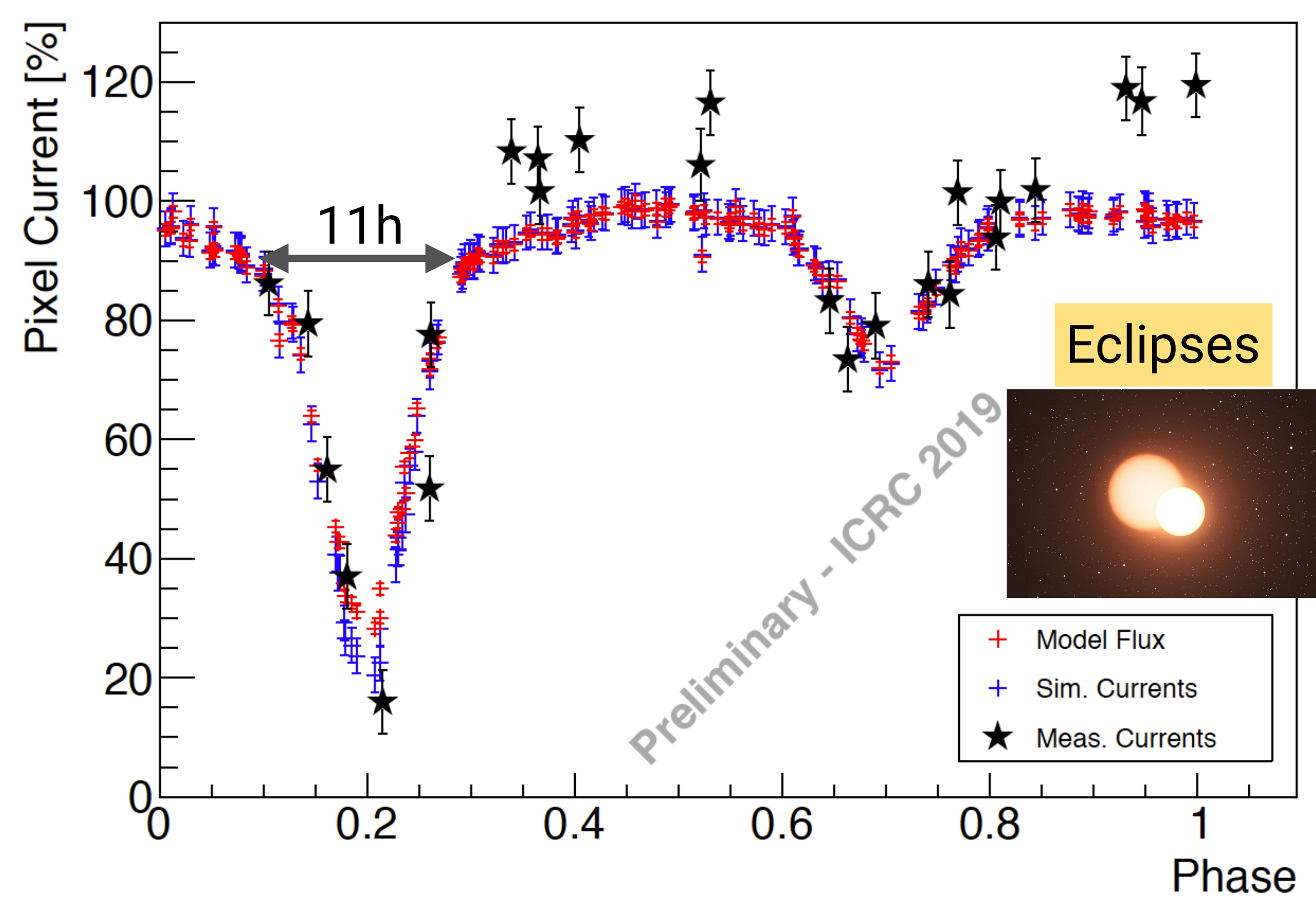


The people watch shadows projected on the wall from objects passing in front of a fire



and give names to these shadows





When it comes to predictable, testable outcomes its hard to beat passing something in front of a star.



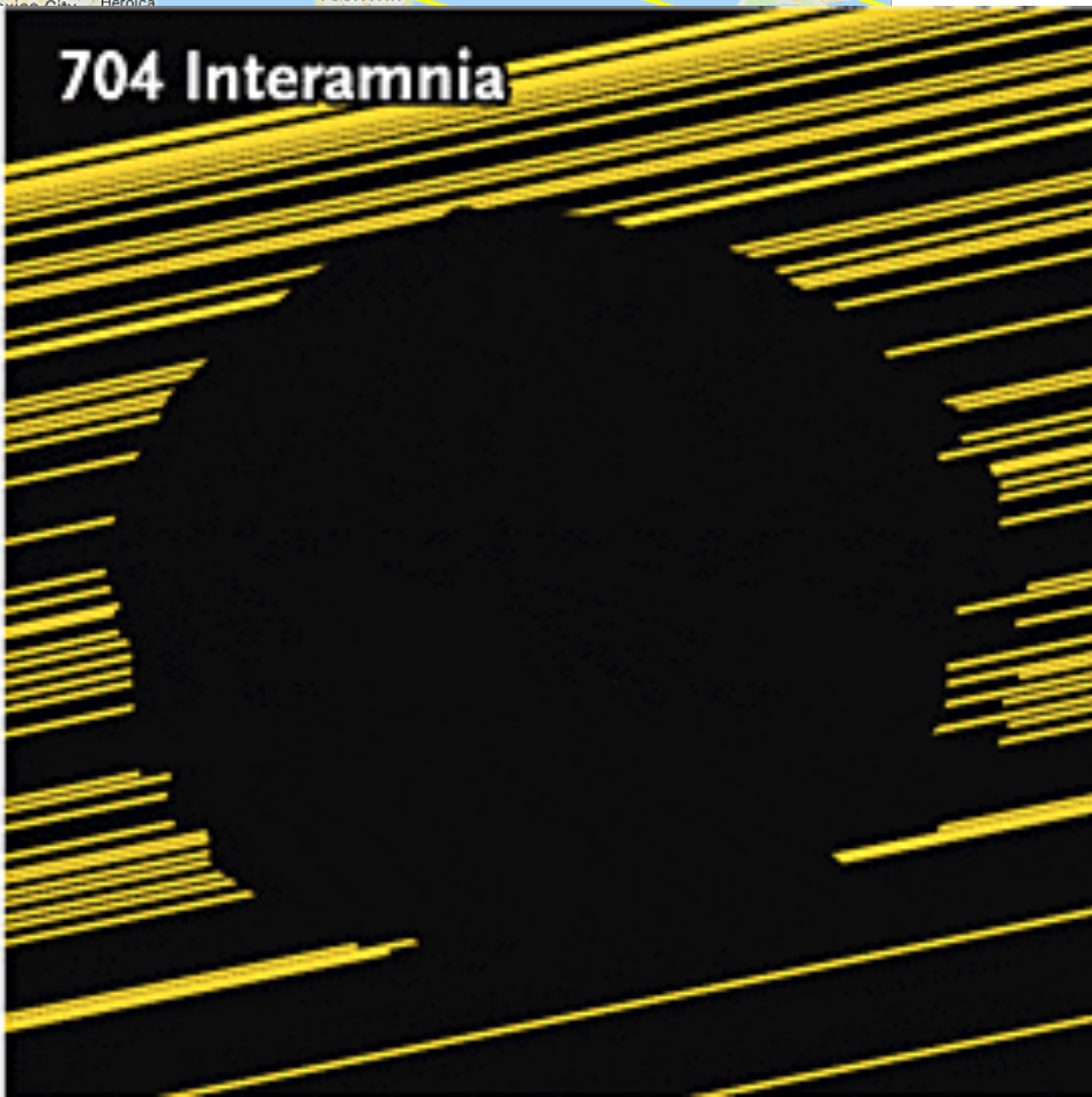
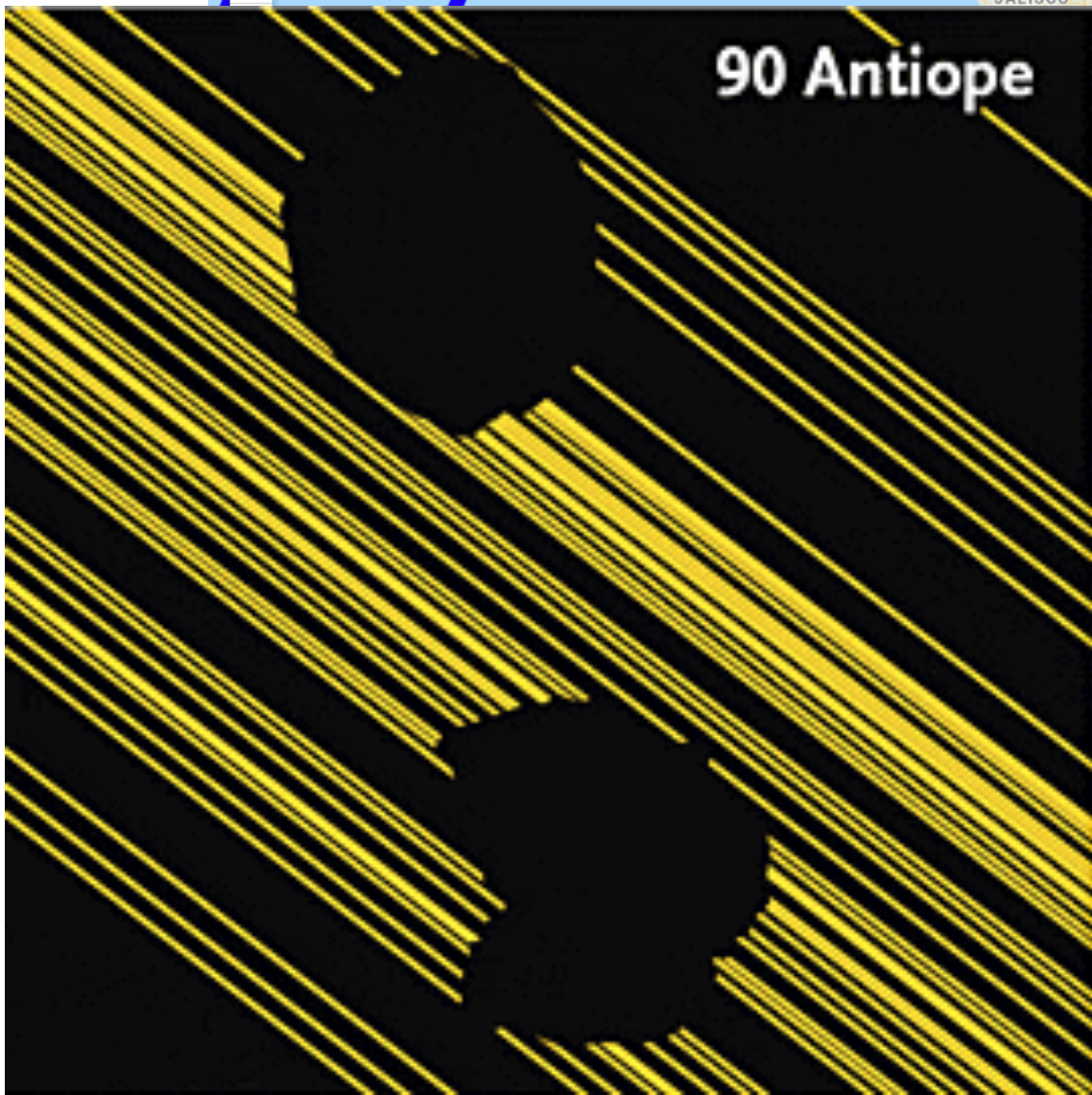
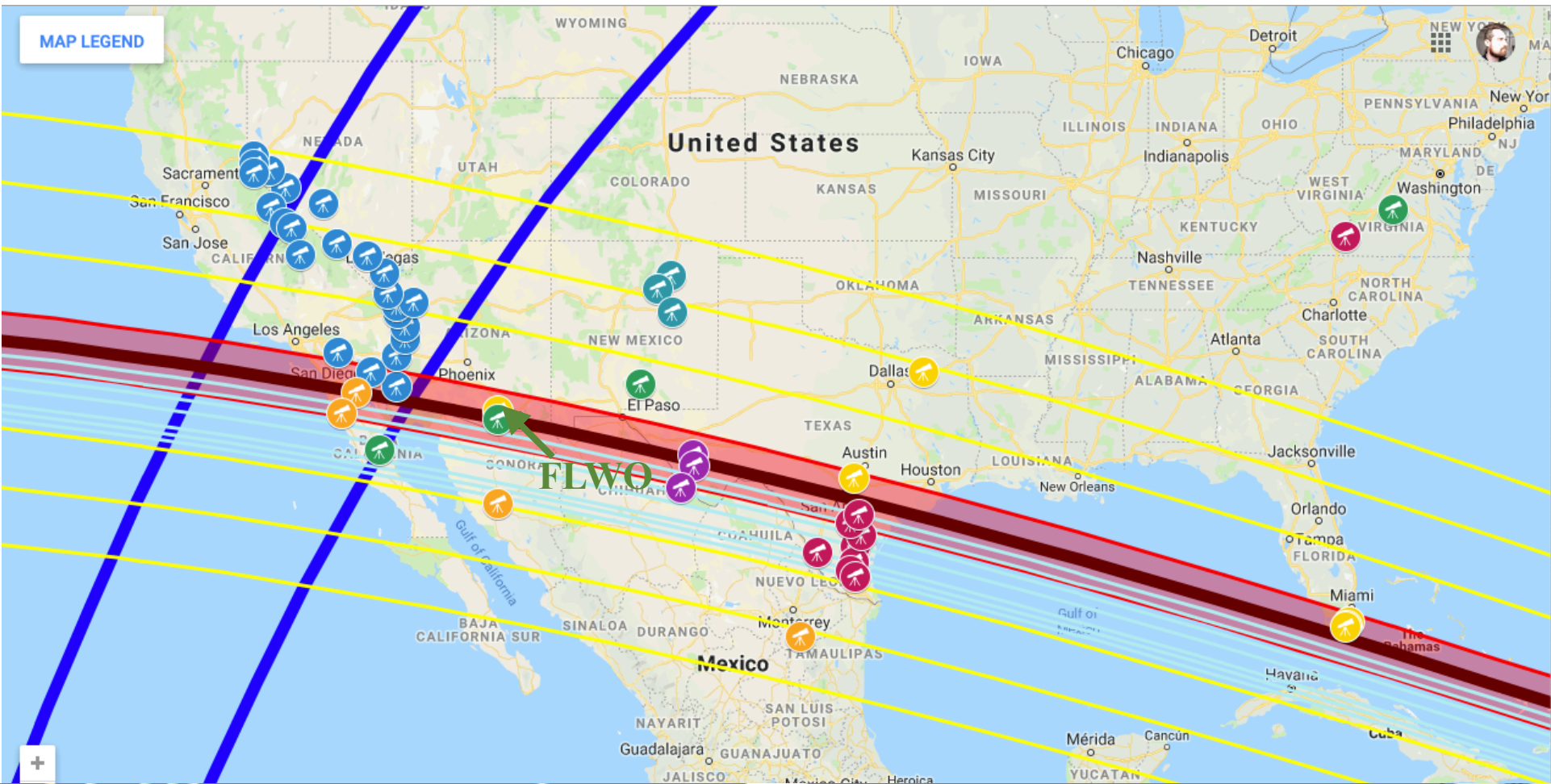
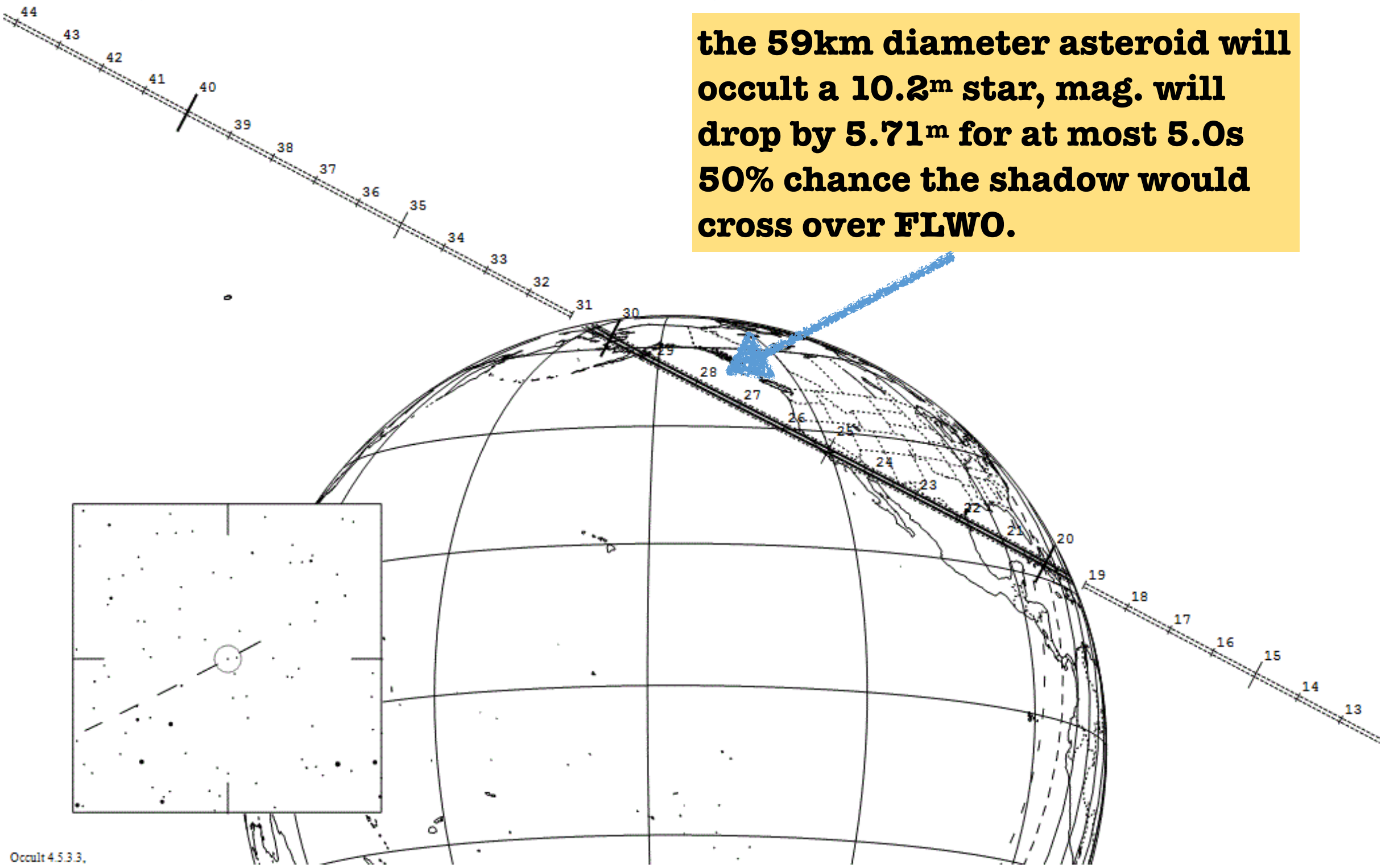


# (1165) Imprinetta / TYC 5517-227-1 occultation

1165 Imprinetta\*\* occults TYC 5517-00227-1 on 2018 Feb 22 from 11h 19m to 11h 31m UT

Star:	Max Duration = 5.0 secs	Asteroid:
Mv = 10.2	Mag Drop = 5.7	Mag = 15.9
RA = 11 46 47.6027 (J2000)	Sun : Dist = 152 deg	Dia = 59km, 0.032"
Dec = - 8 27 14.404	Moon: Dist = 126 deg	Parallax = 3.470"
[of Date: 11 47 44, - 8 33 19]	: illum = 40 %	Hourly dRA = -1.383s
Prediction of 2018 Jan 17.0	E 0.027"x 0.013" in PA 78	dDec = 10.80"

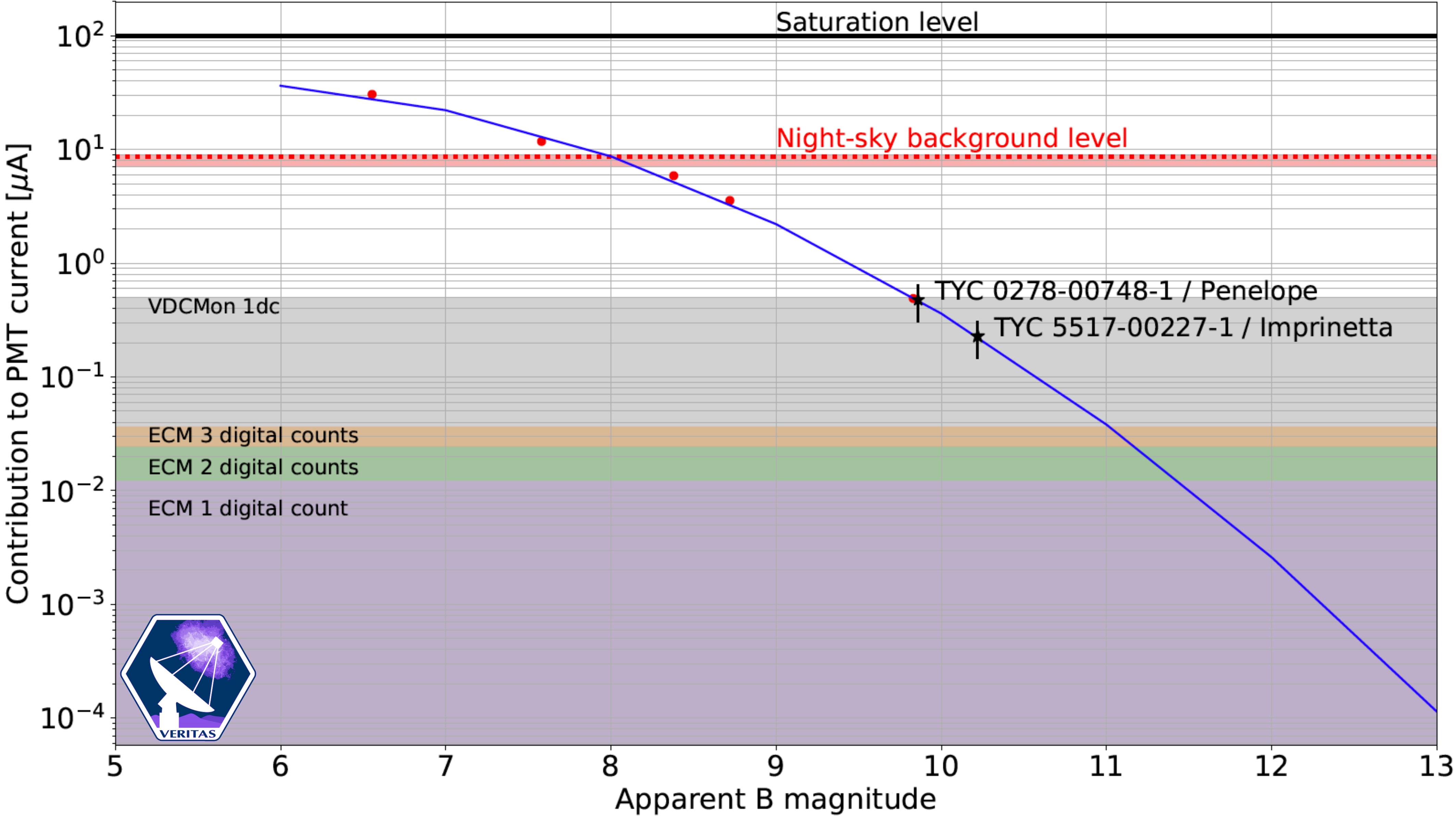
<http://www.asteroidoccultation.com/>



The nice thing is that even a non-detection of the shadow tells something about the size/shape of the asteroid

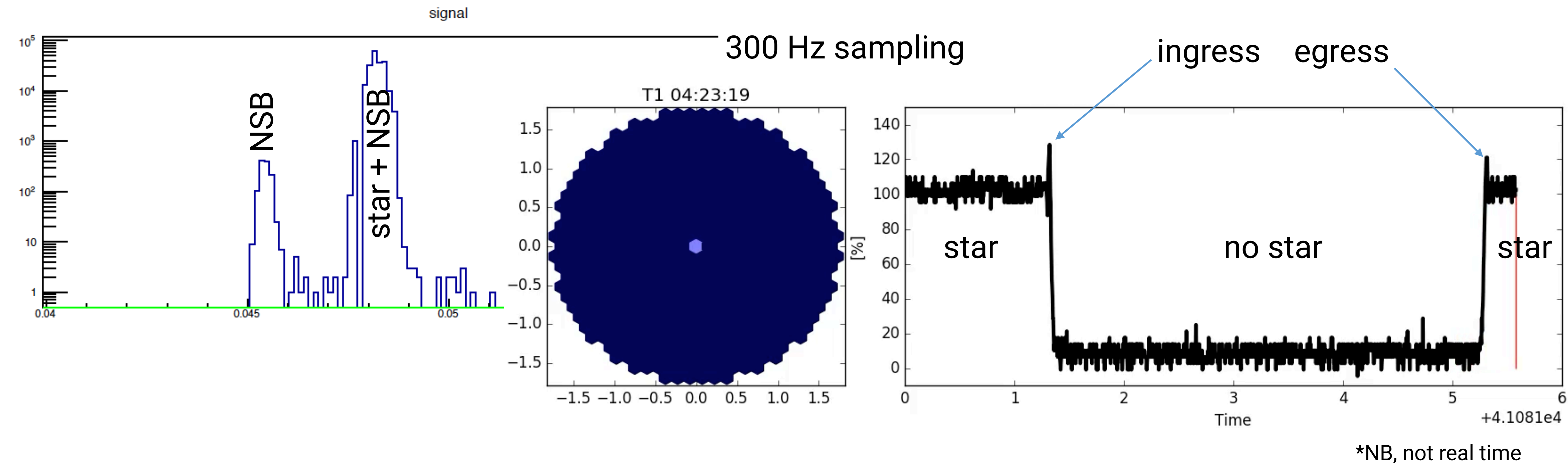


To resolve a star so faint required an upgrade to the pixel current monitor



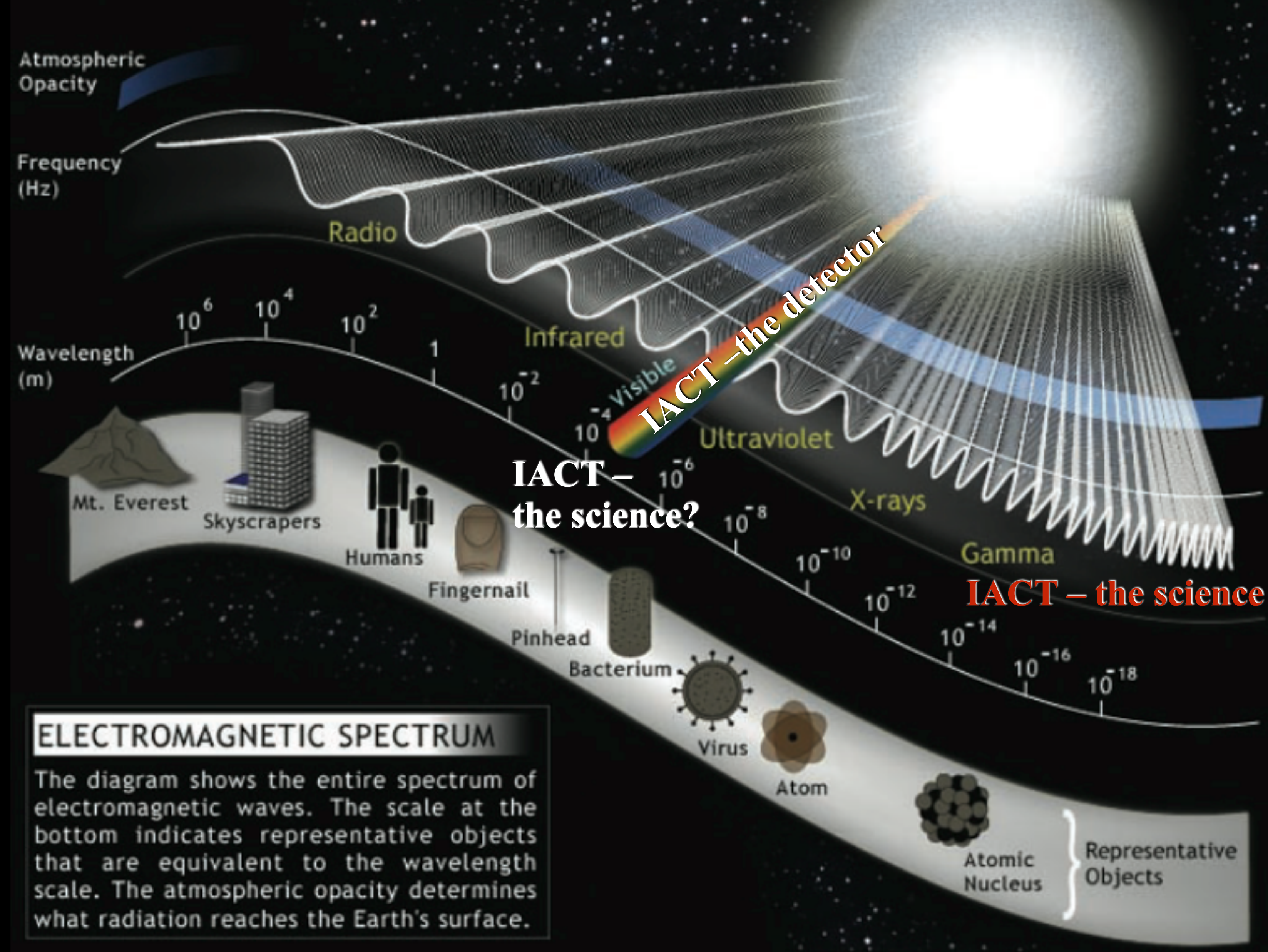


(1165) Imprinetta / TYC 5517-227-1 occultation





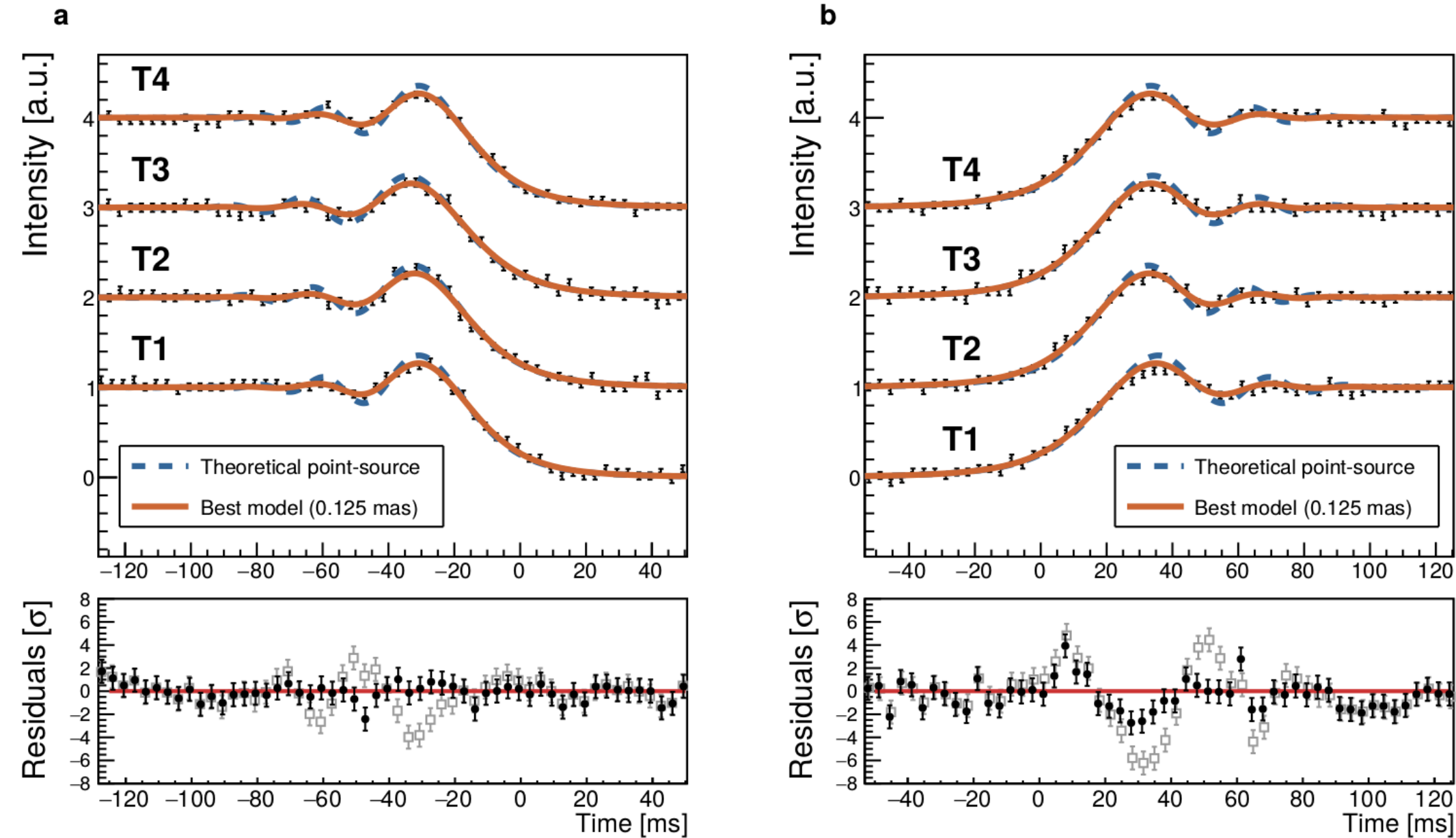
# Wave



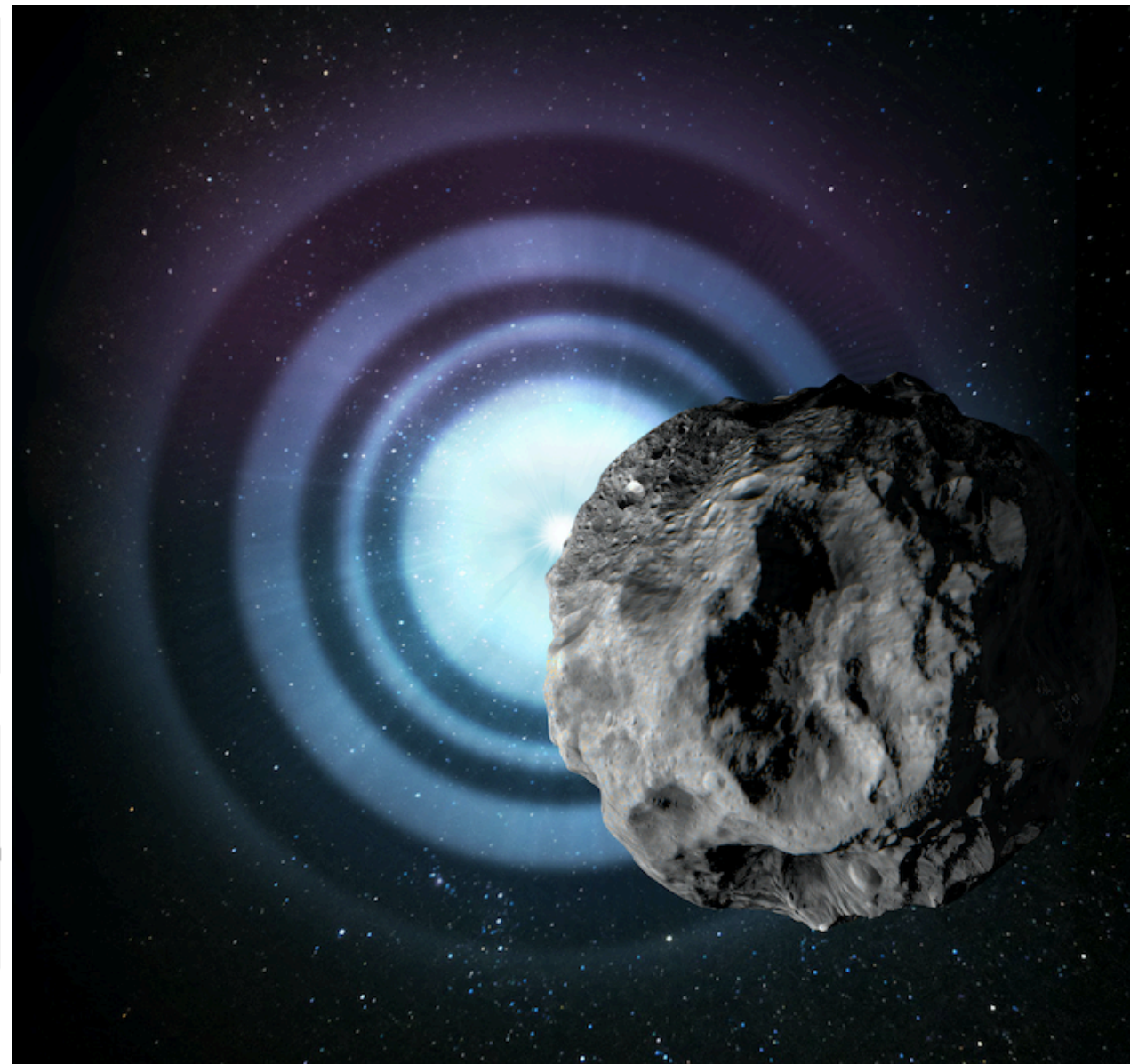
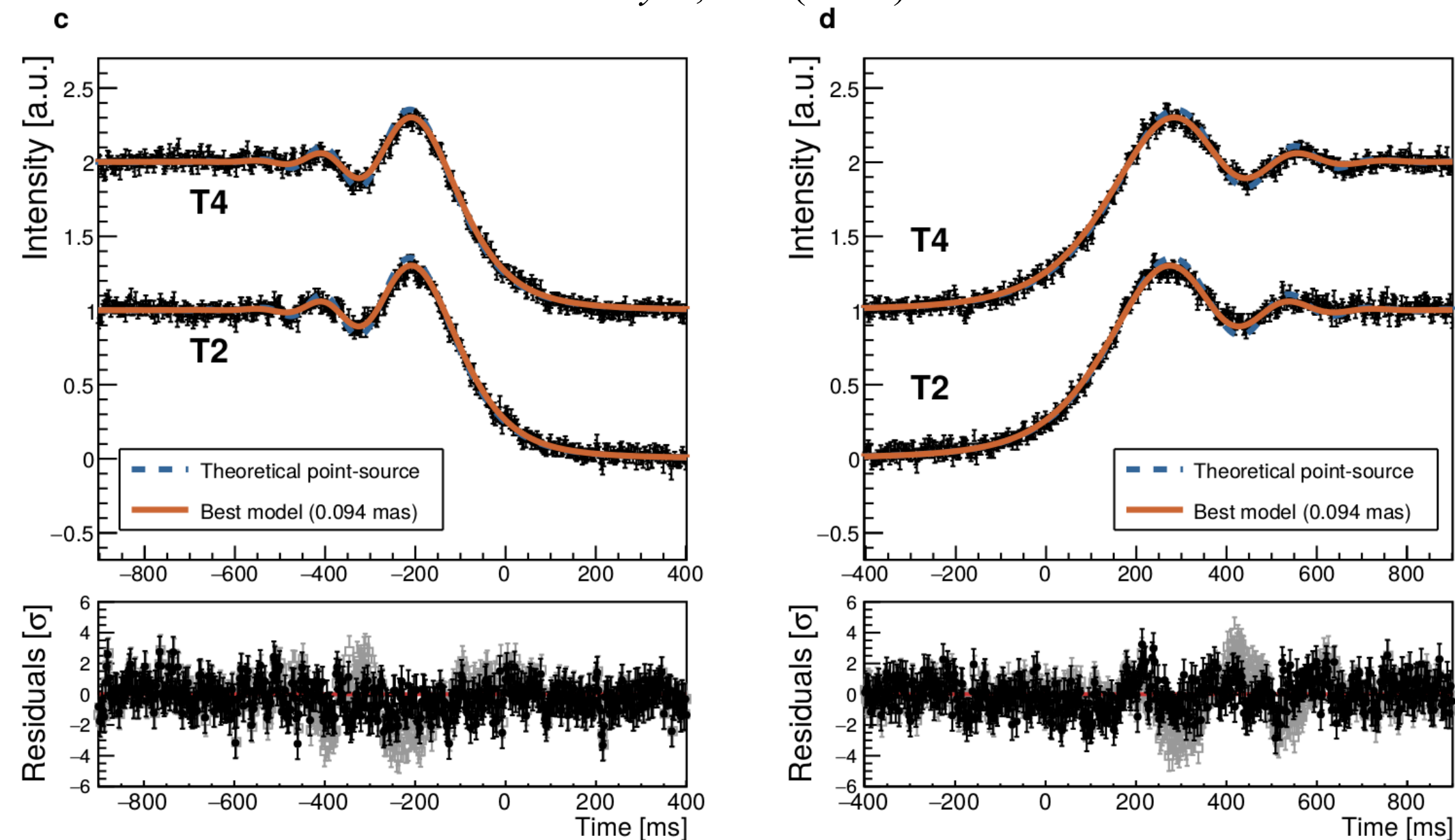
# Particle



# The fringe benefits of asteroid occultations



Benbow et al. *Nature Astronomy* **3**, 511 (2019).



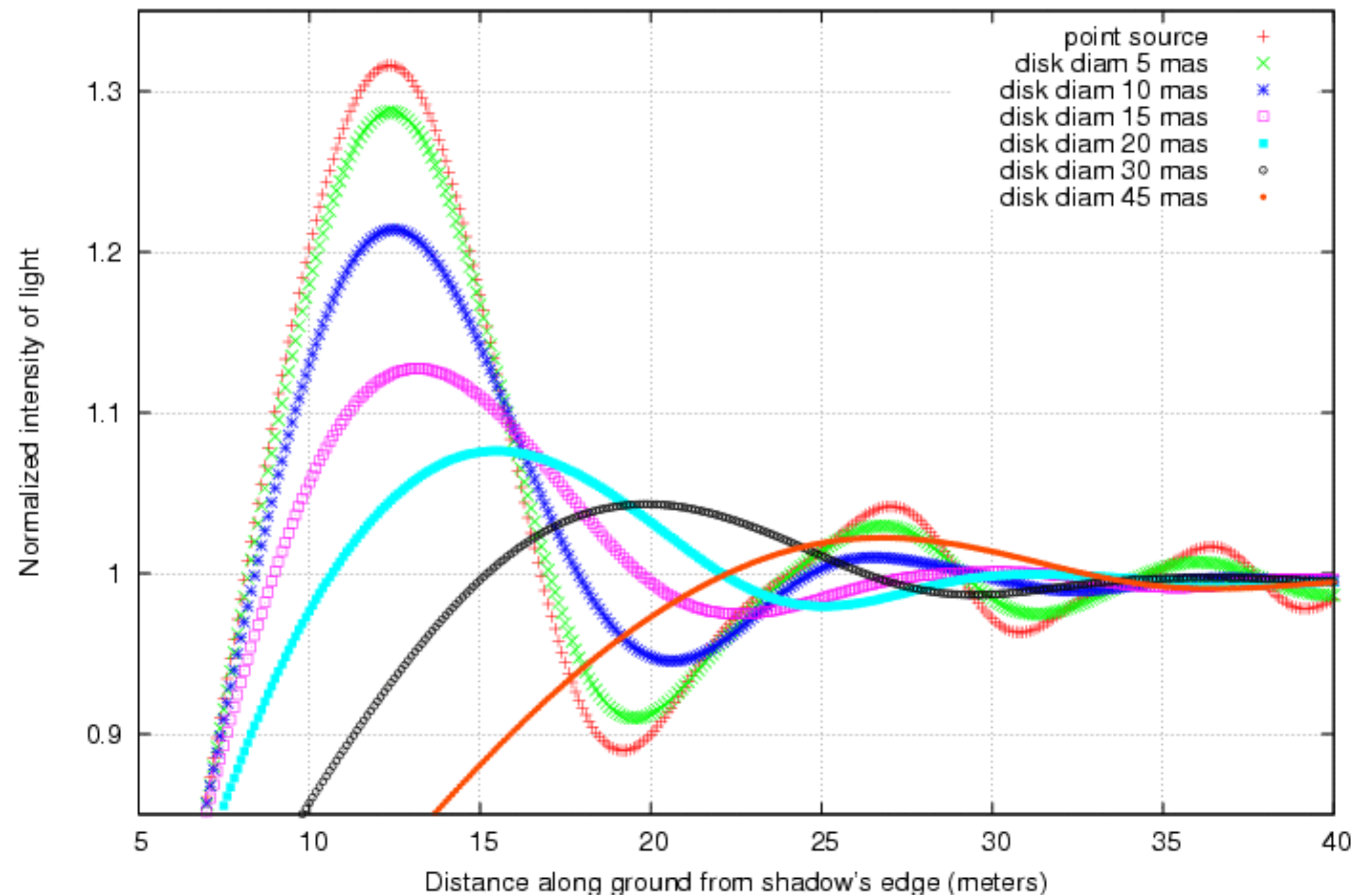
Telescope PSF  $\rightarrow$  point-like source  
 But, not actually a point source:  
 from the diffraction pattern in the shadow  
 we get the angular size of the star!





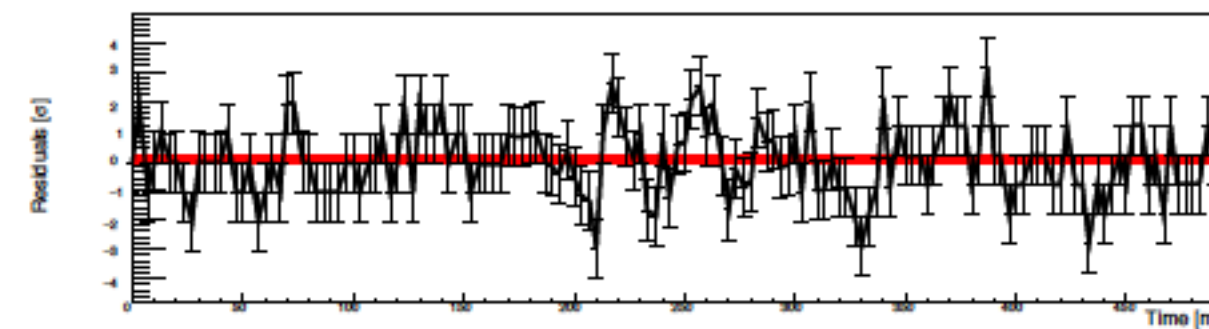
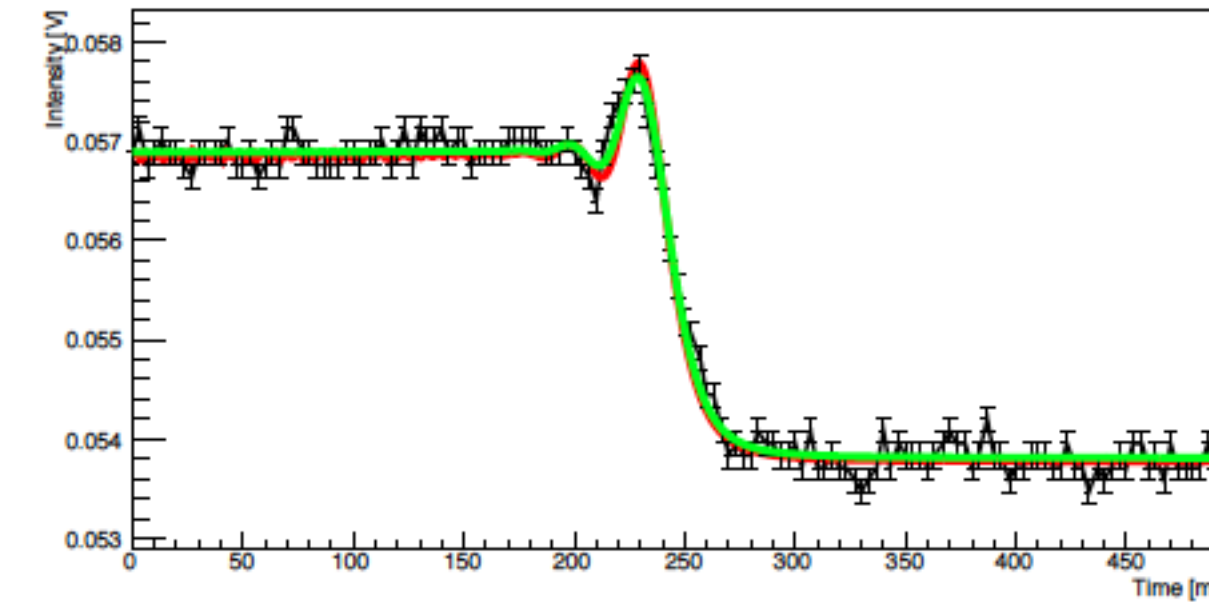
# The extent of the light source reduces the fringe

Effect of a uniform circular disk on fringe pattern

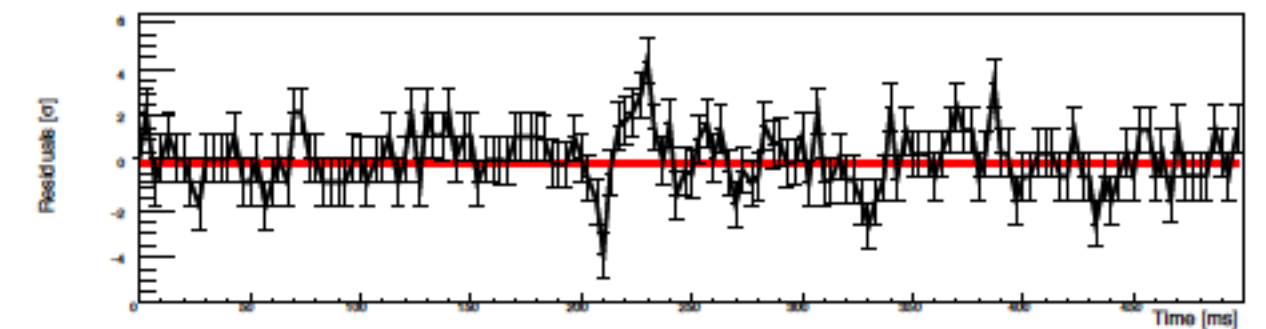
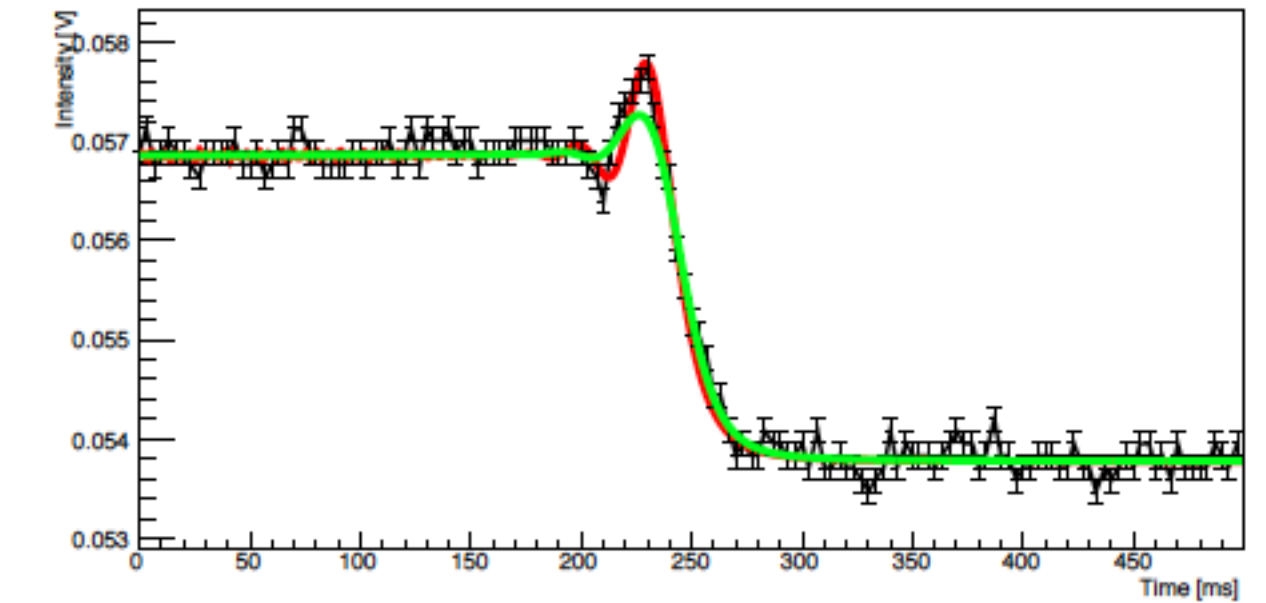


<http://spiff.rit.edu/richmond/occult/bessel/bessel.html>

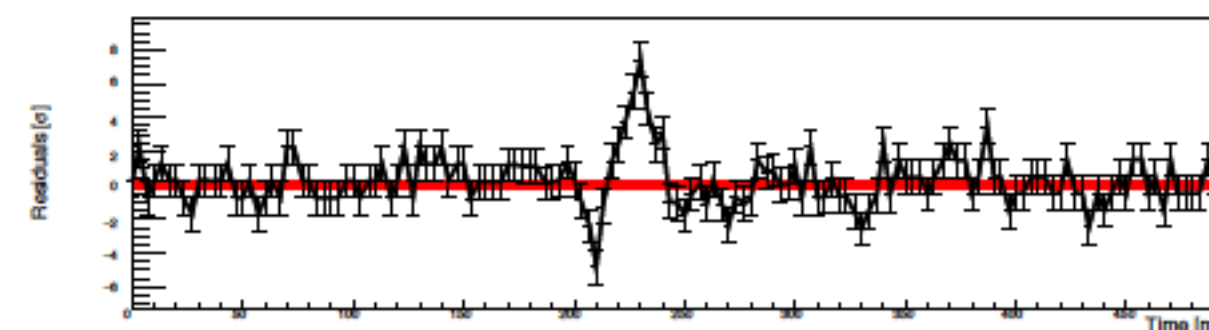
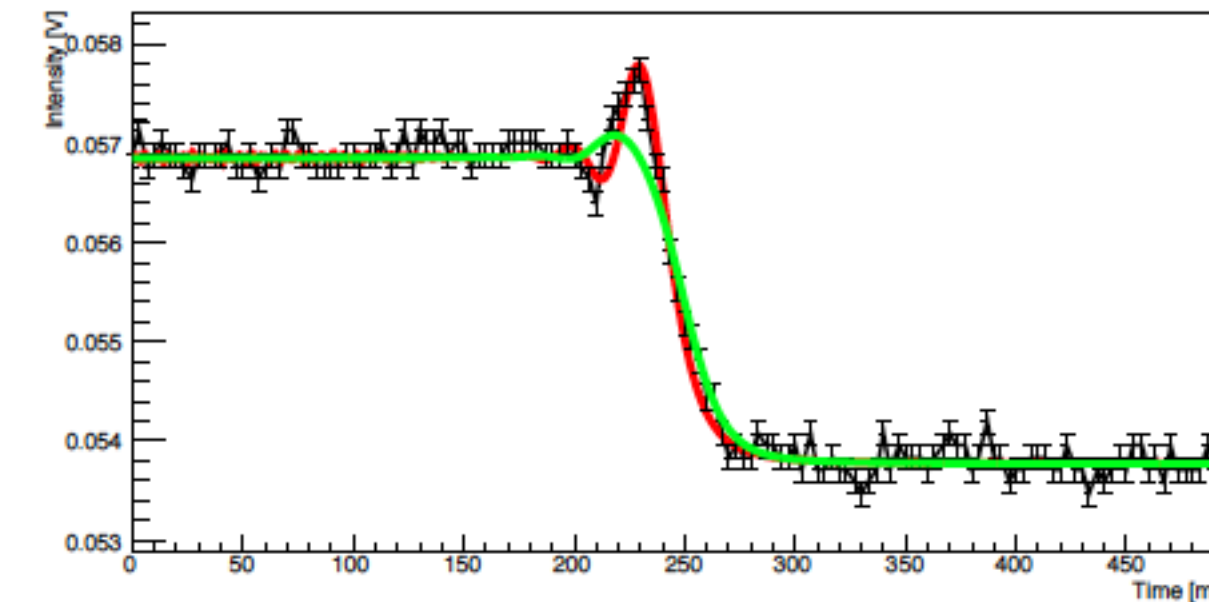
Central pixel of T1, star size of 0.10 mas



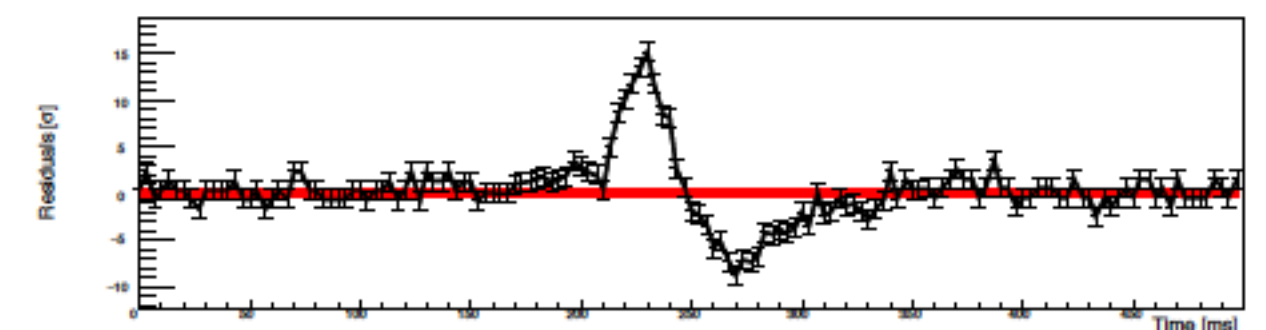
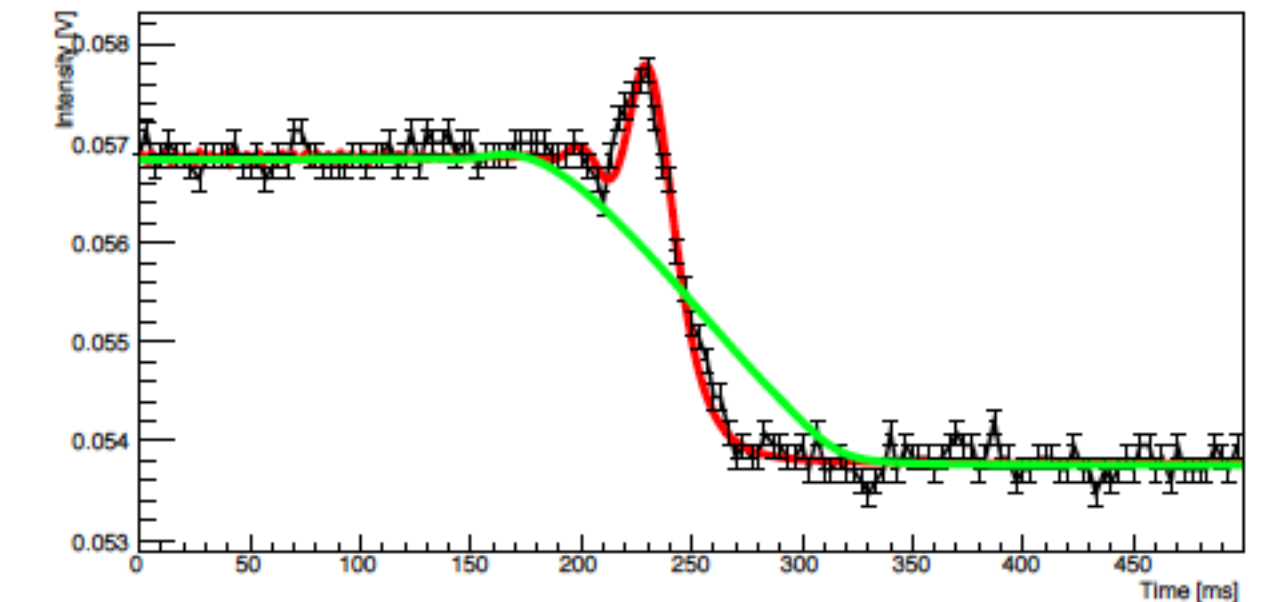
Central pixel of T1, star size of 0.20 mas



Central pixel of T1, star size of 0.30 mas



Central pixel of T1, star size of 1.00 mas





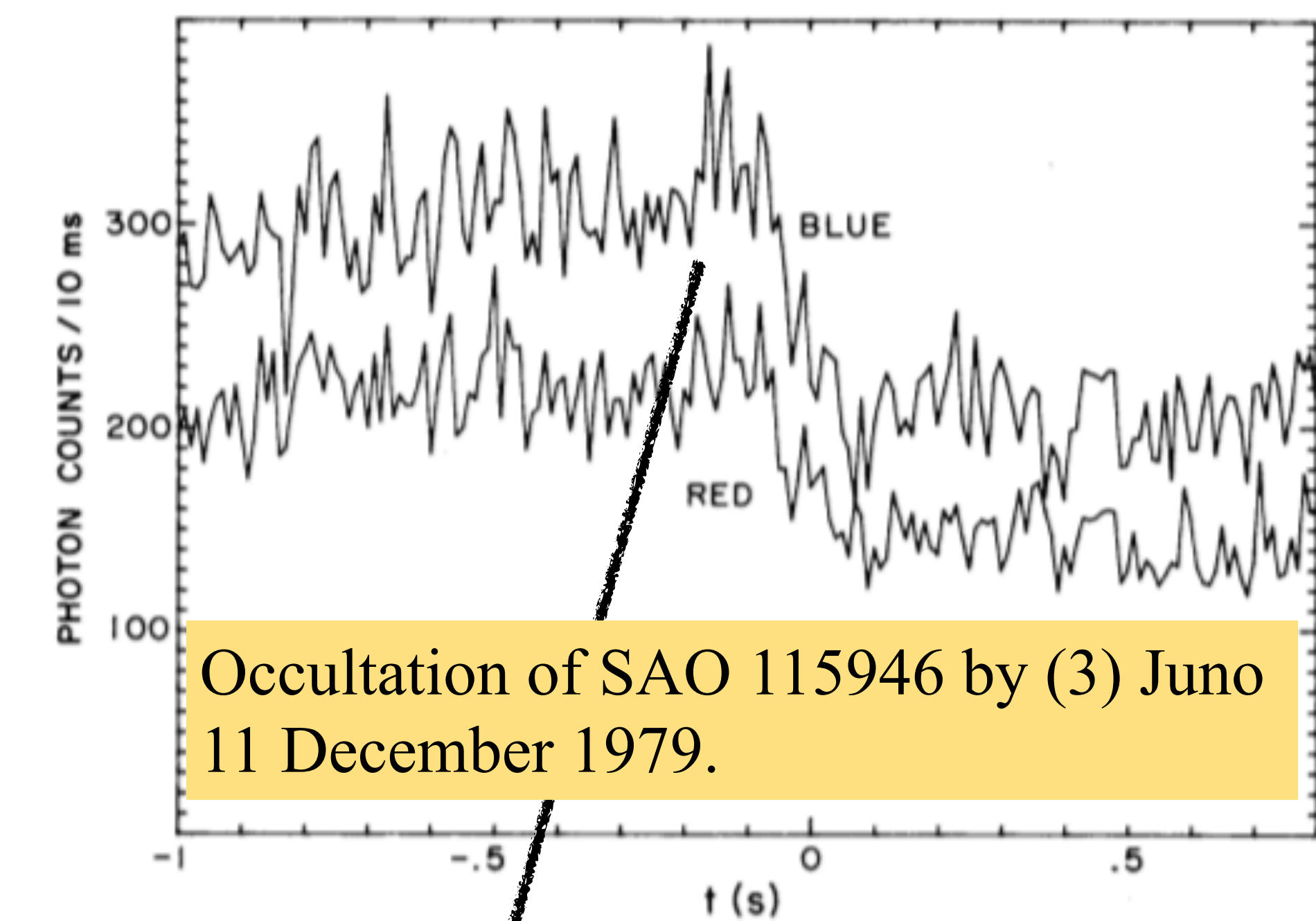


FIG. 2. Ludlow immersion. Each 10-ms data point in the red and blue channels is shown. Note the correlation between red and blue signals (especially at 0<sup>s</sup>.45) caused by scintillation.

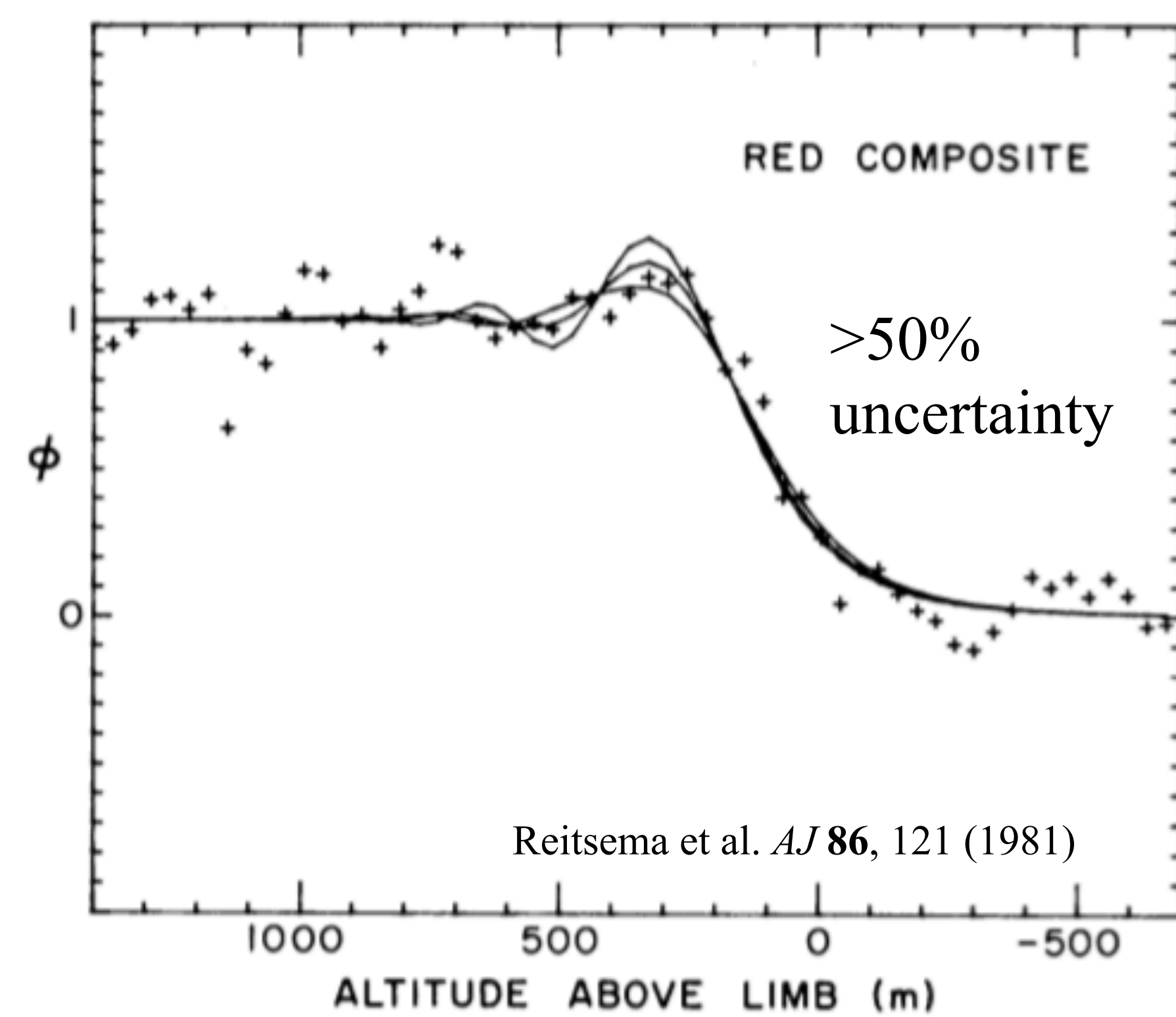
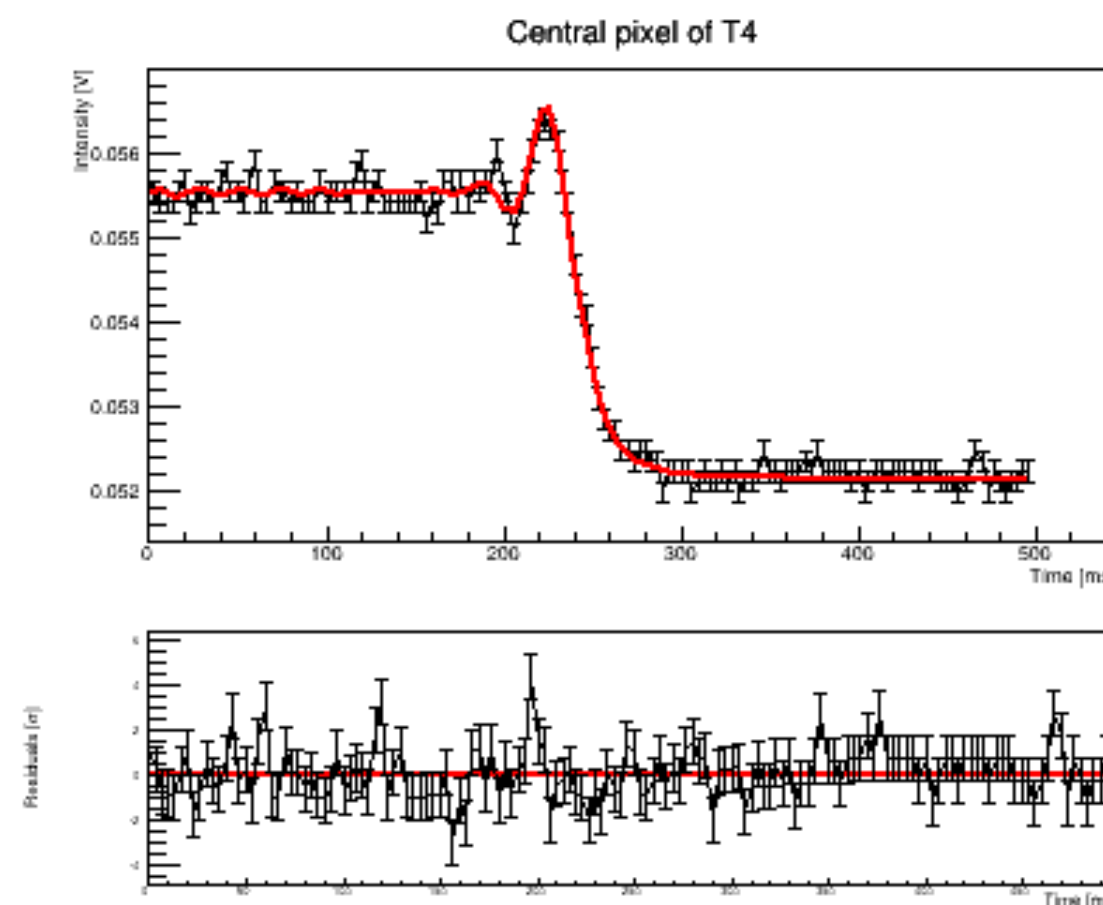
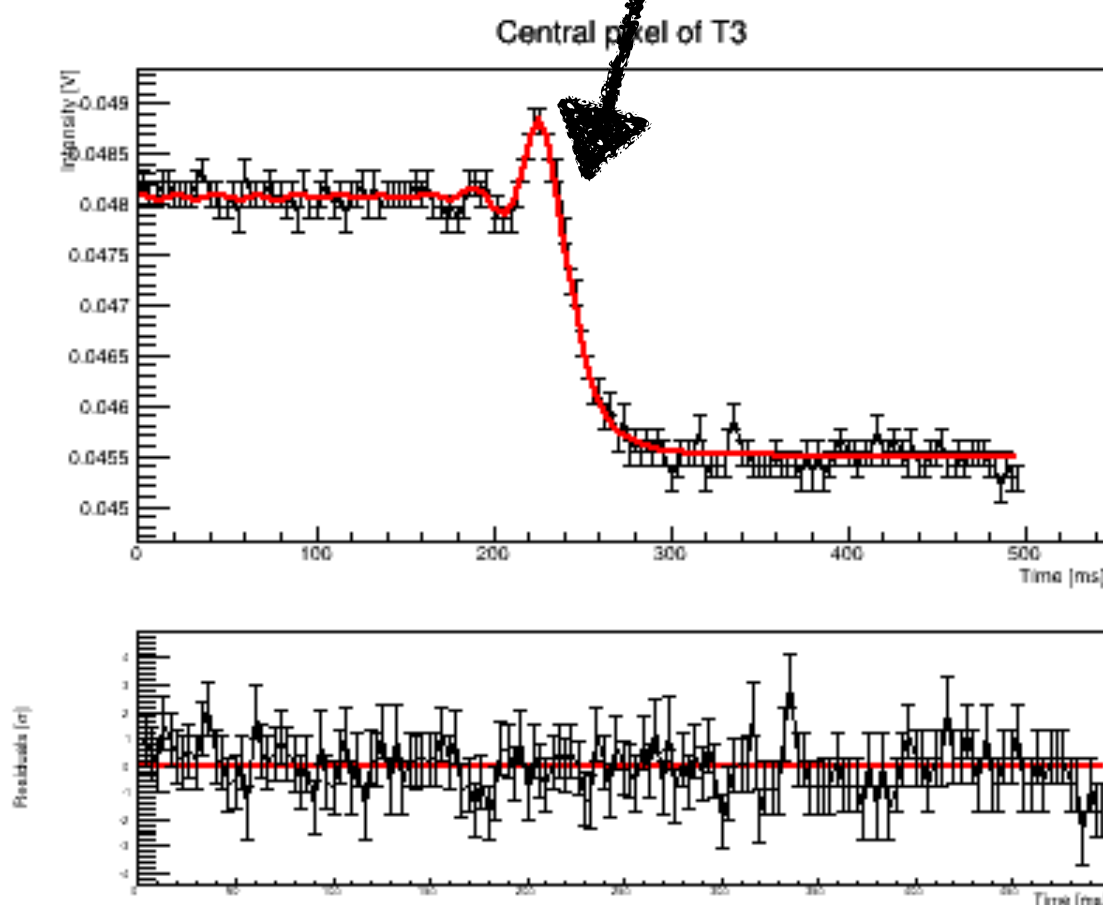


FIG. 4. Same as Fig. 3, but for the red averages.

Reitsema et al. *AJ* **86**, 121 (1981)

2x 36cm Celestrons

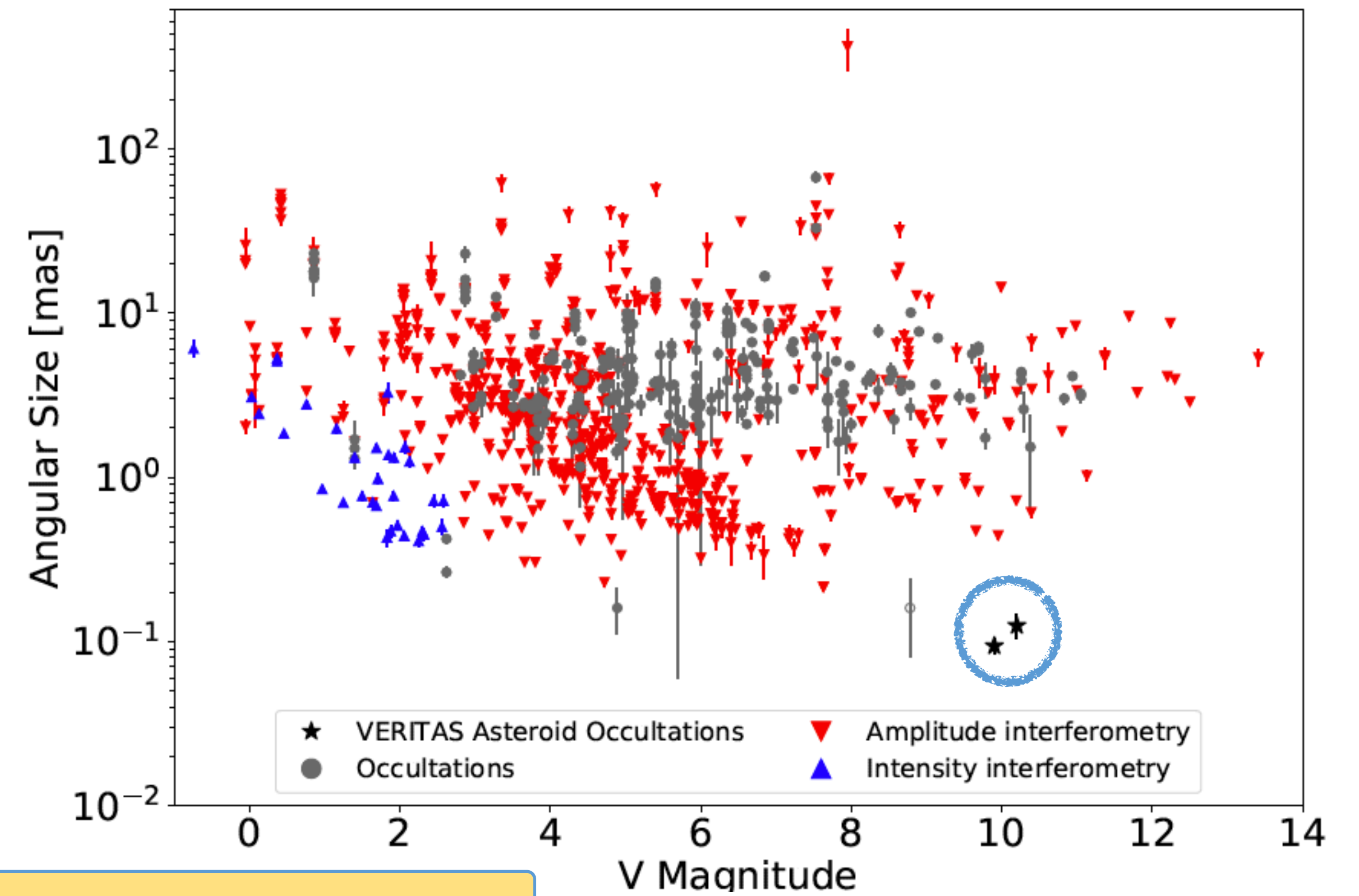
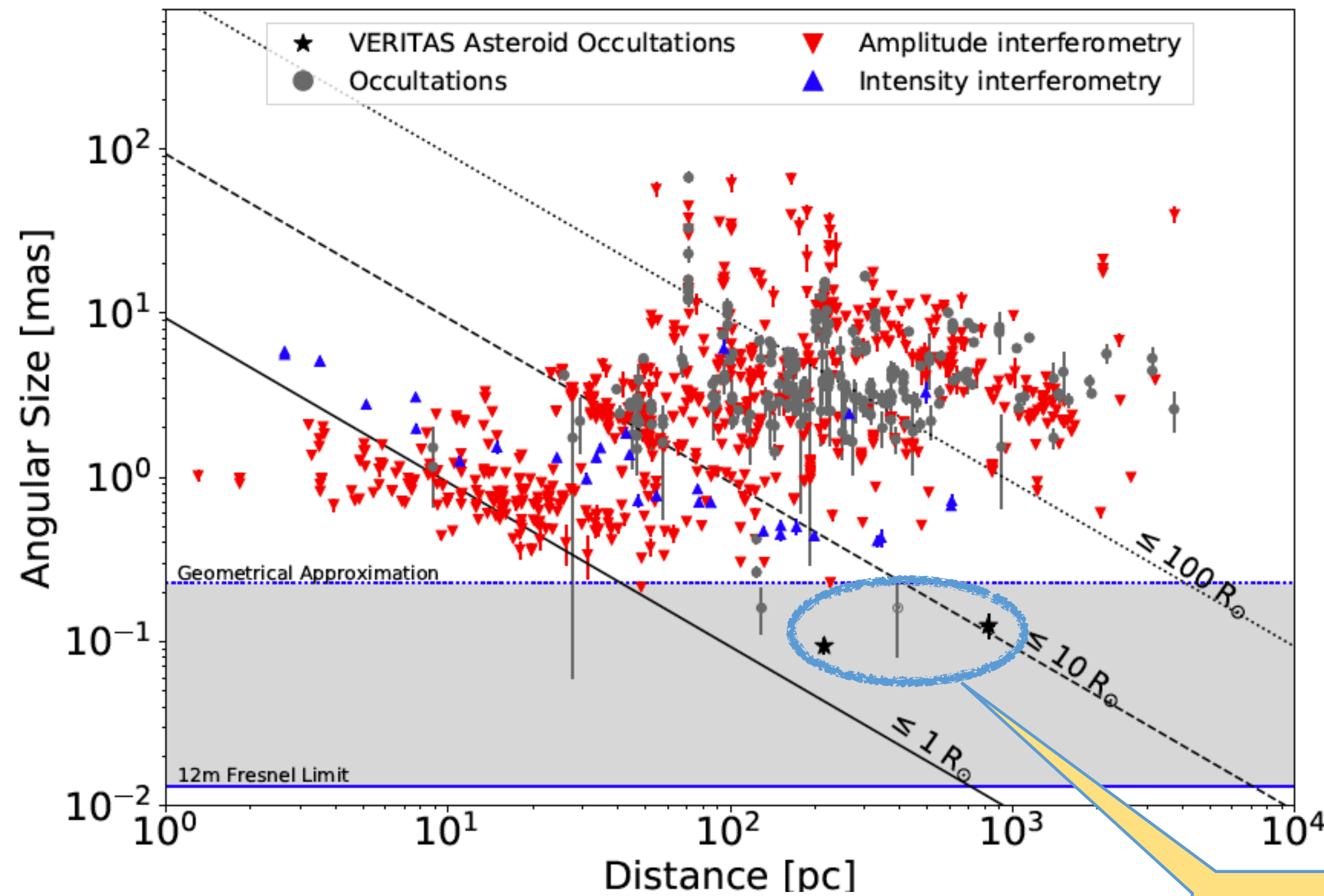
4x 12m “light buckets”

Occultation of TYC 5517-227-1 by (1165) Imprinetta 22 February 2018.

Benbow et al. *Nature Astronomy* **3**, 511 (2019)



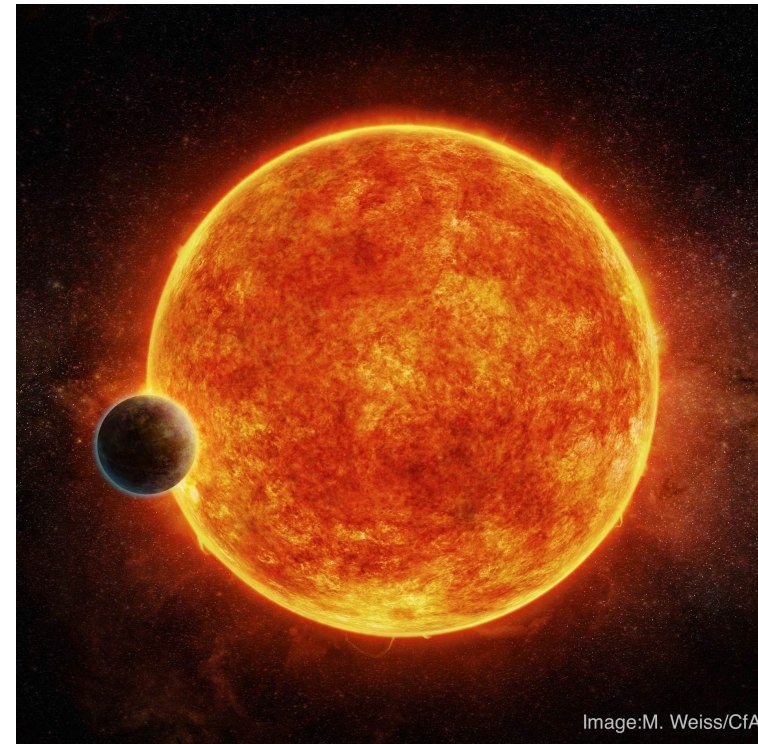
An IACT is optimal for a population of small/faint stars



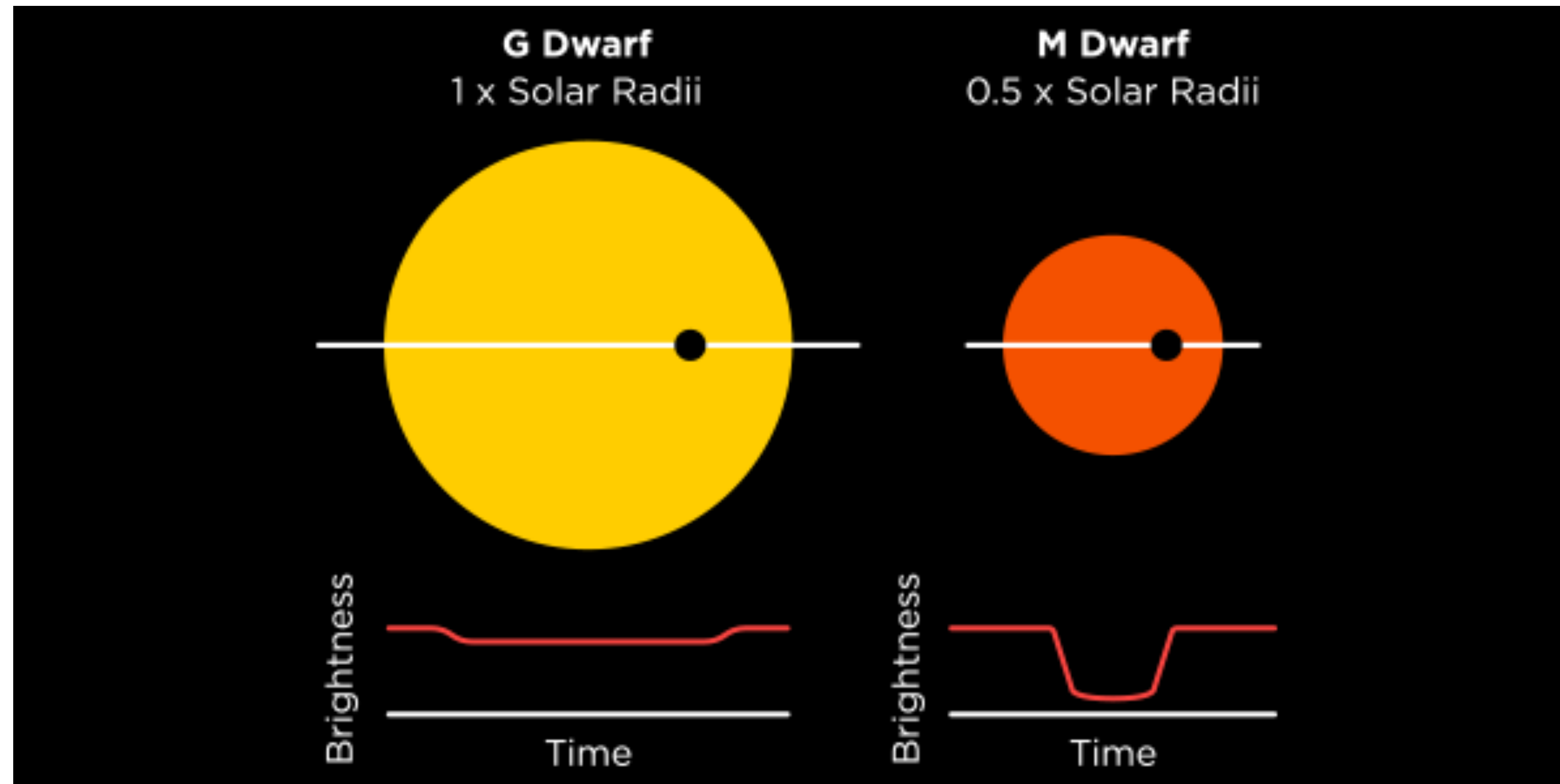
See poster PS1-66 (session 1)



Why are we interested in the radius of small, faint stars?

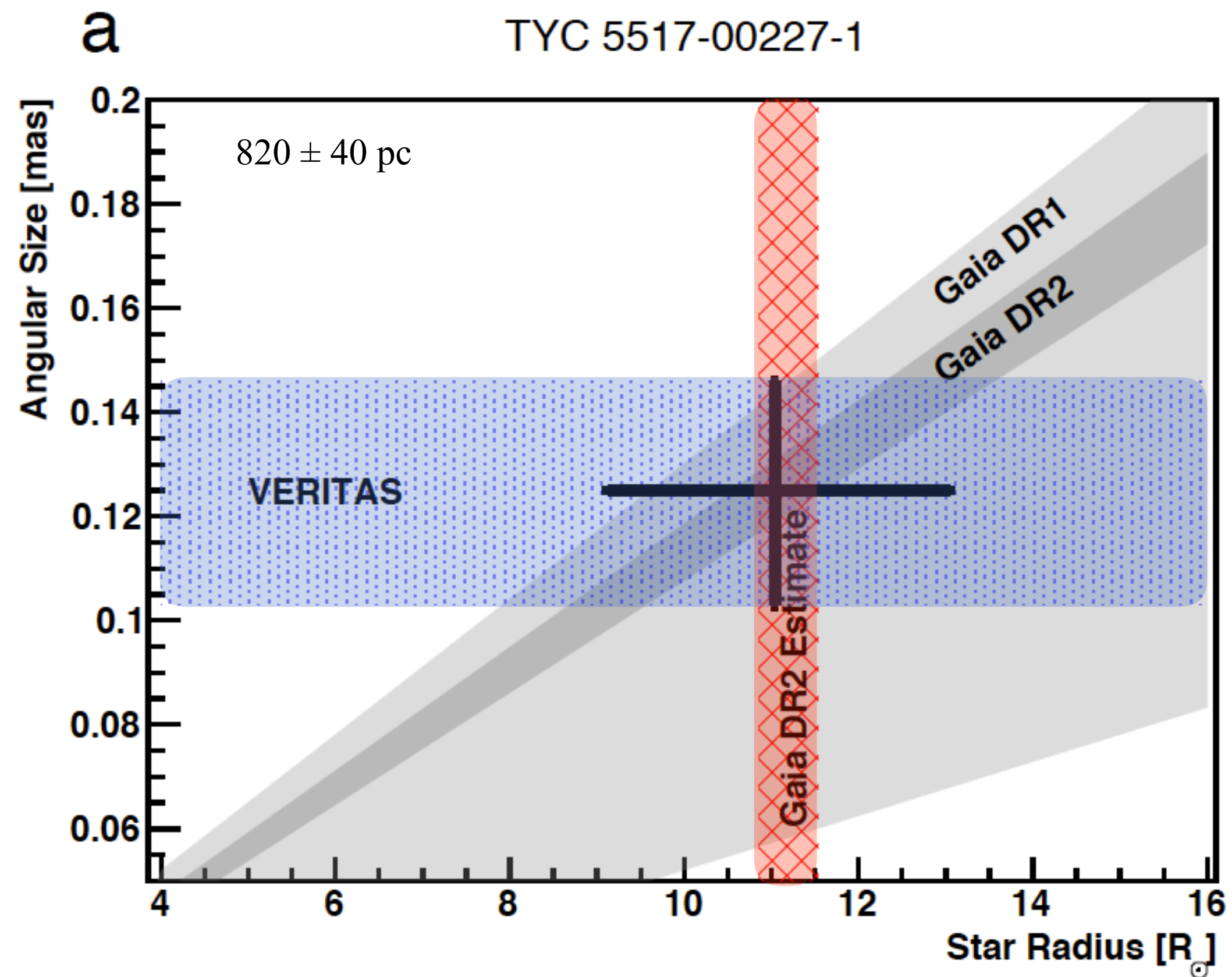


$$\text{Transit Depth} = \left( \frac{R_p}{R_*} \right)^2$$

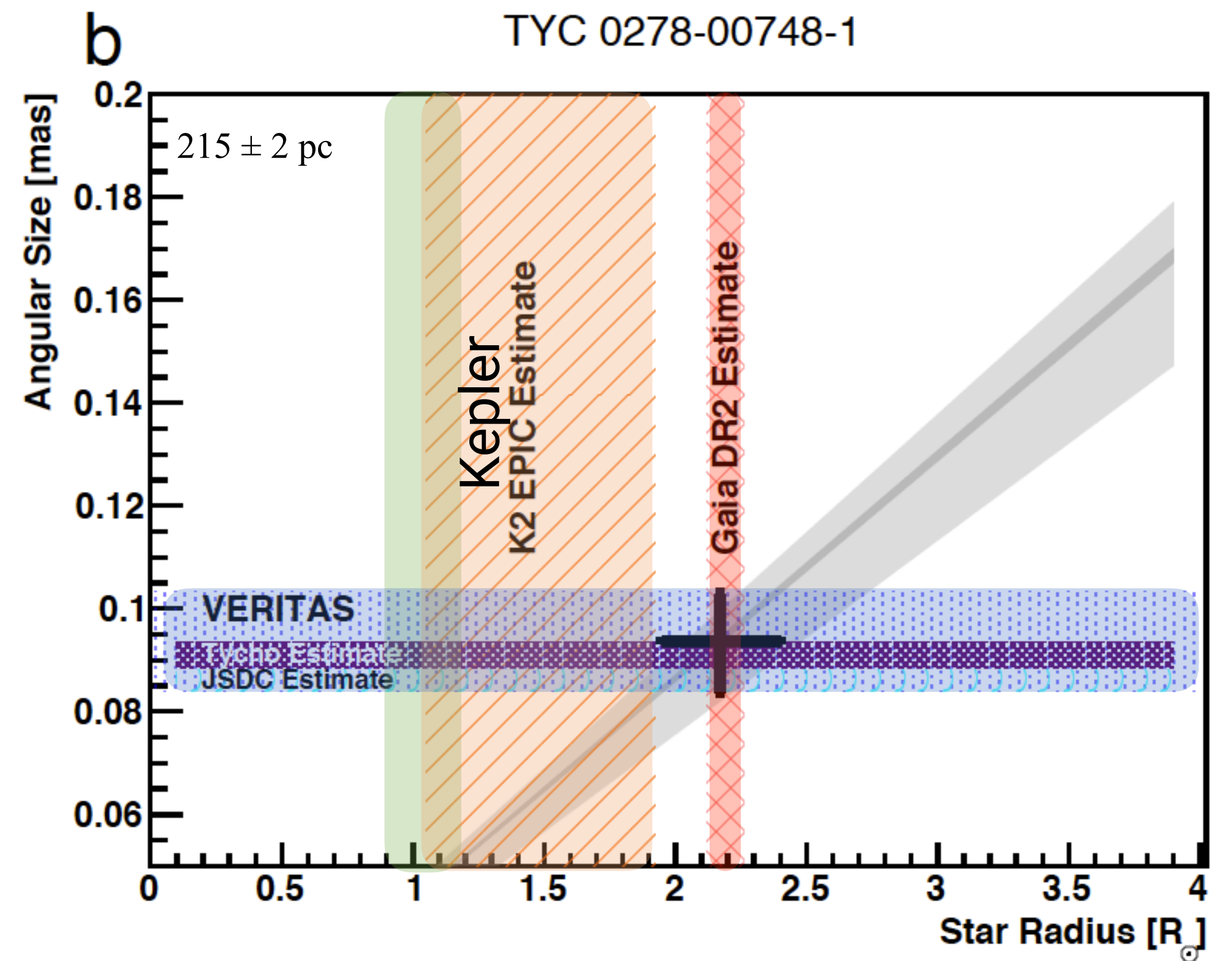


<https://www.cfa.harvard.edu/~avanderb/tutorial/tutorial.html>





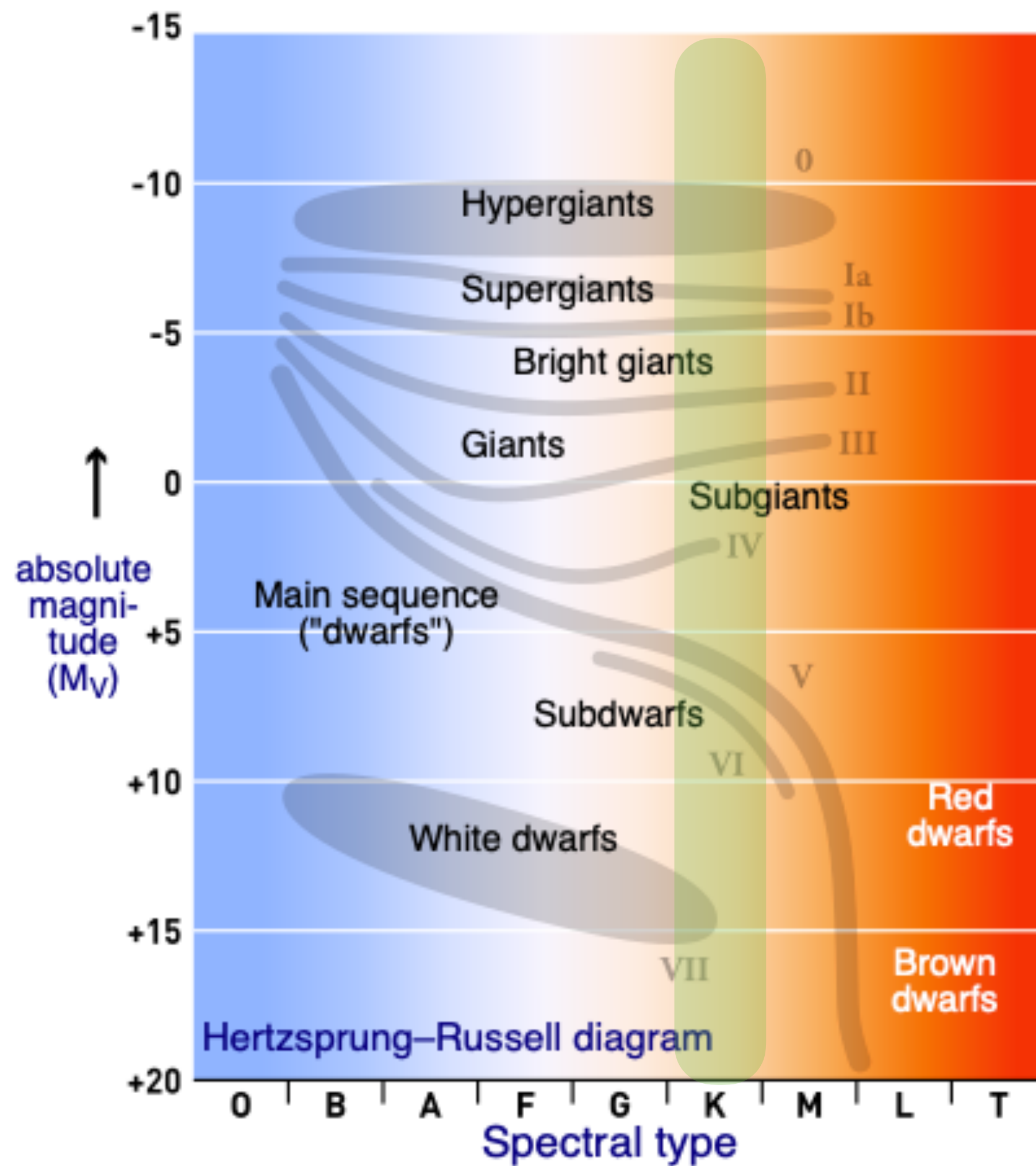
Direct measurement resolves star to be  
supergiant (KIII)



Direct measurement resolves star to be  
sub-giant (GIV) and not main sequence (GV)

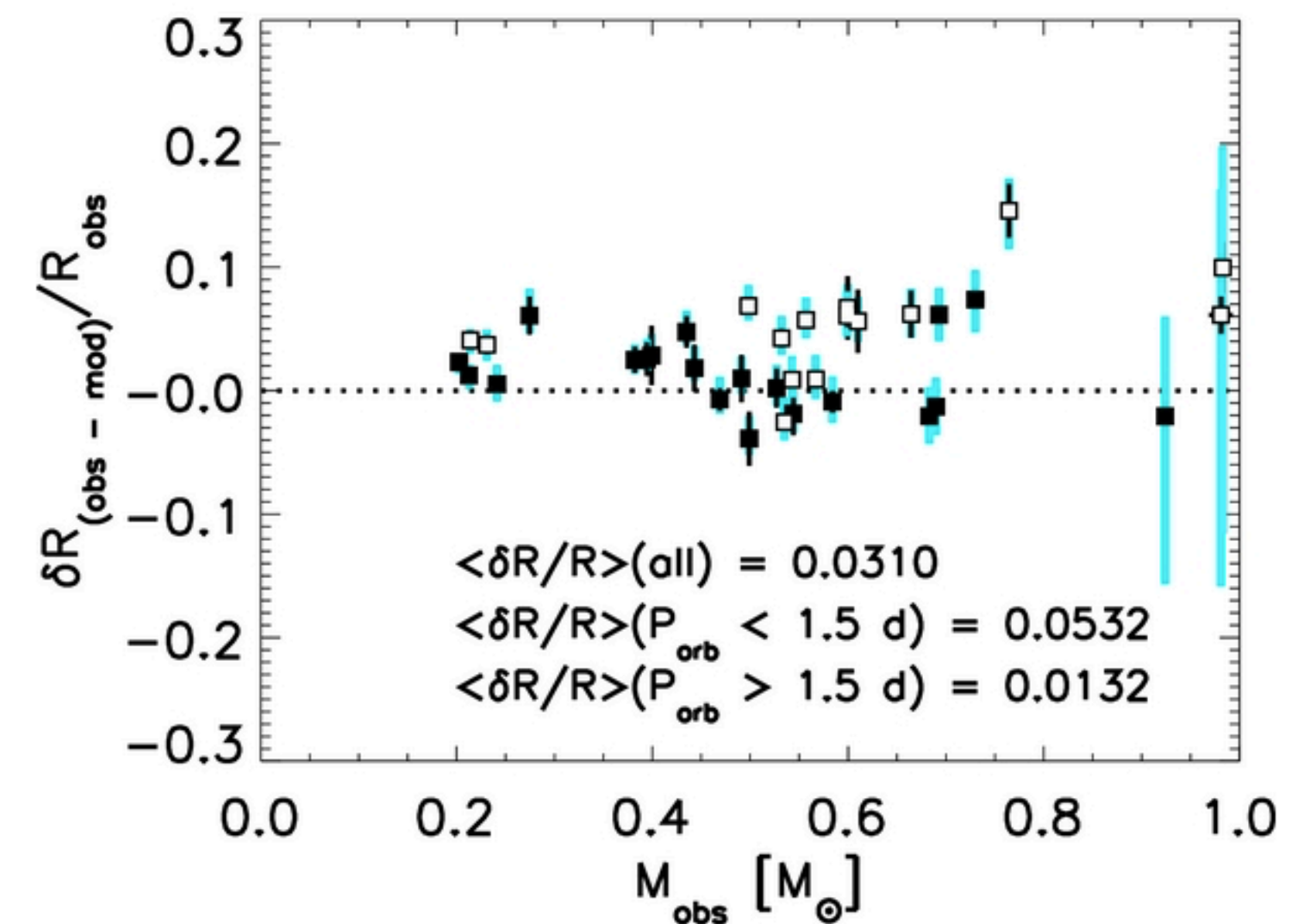


## Why are we interested in small, faint stars?



There's a particular interest in K star radii, since there is growing evidence of a discrepancy between models and reality at the  $\sim 5\%$  level

Spada et al. *ApJ* 776, 87 (2013)



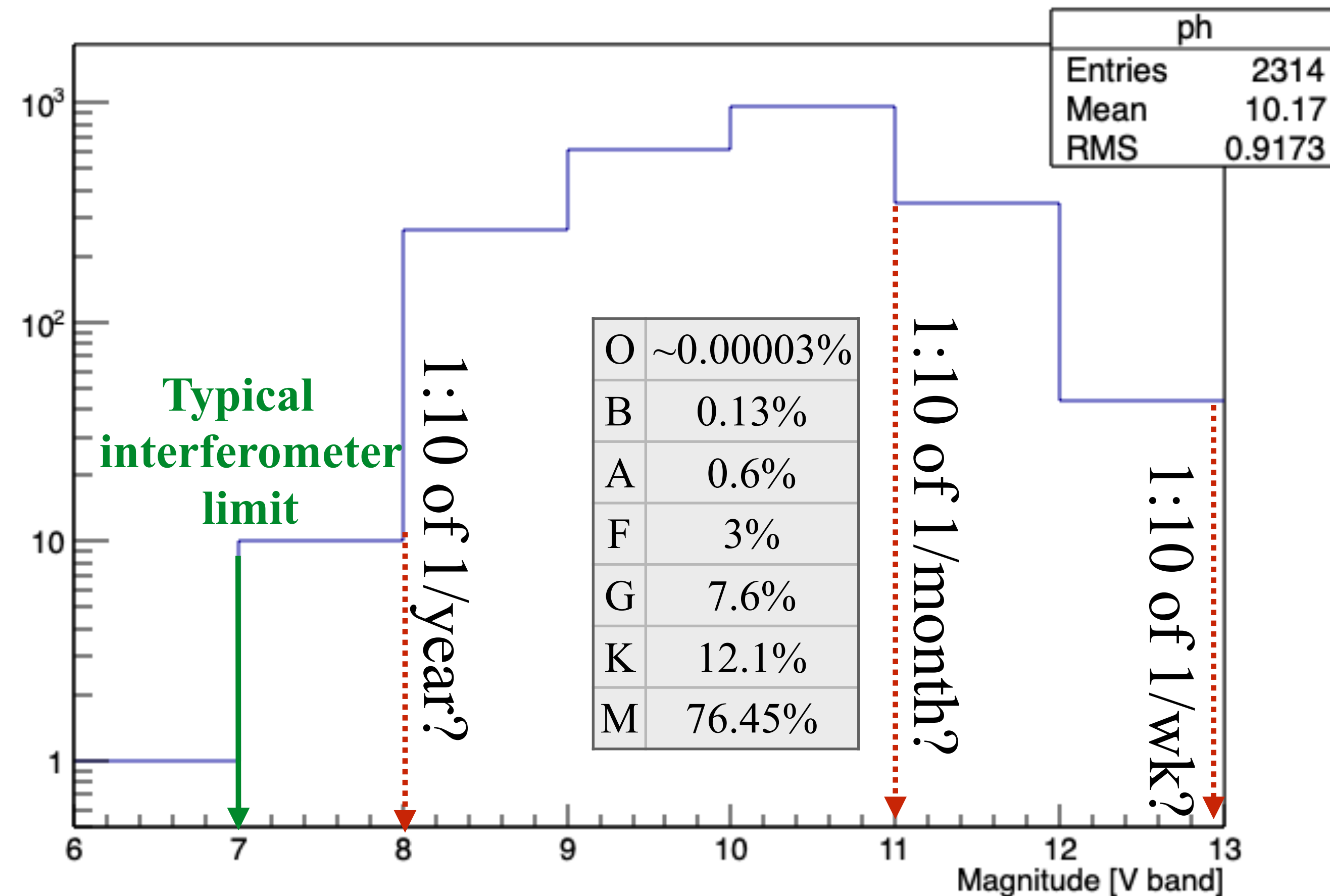
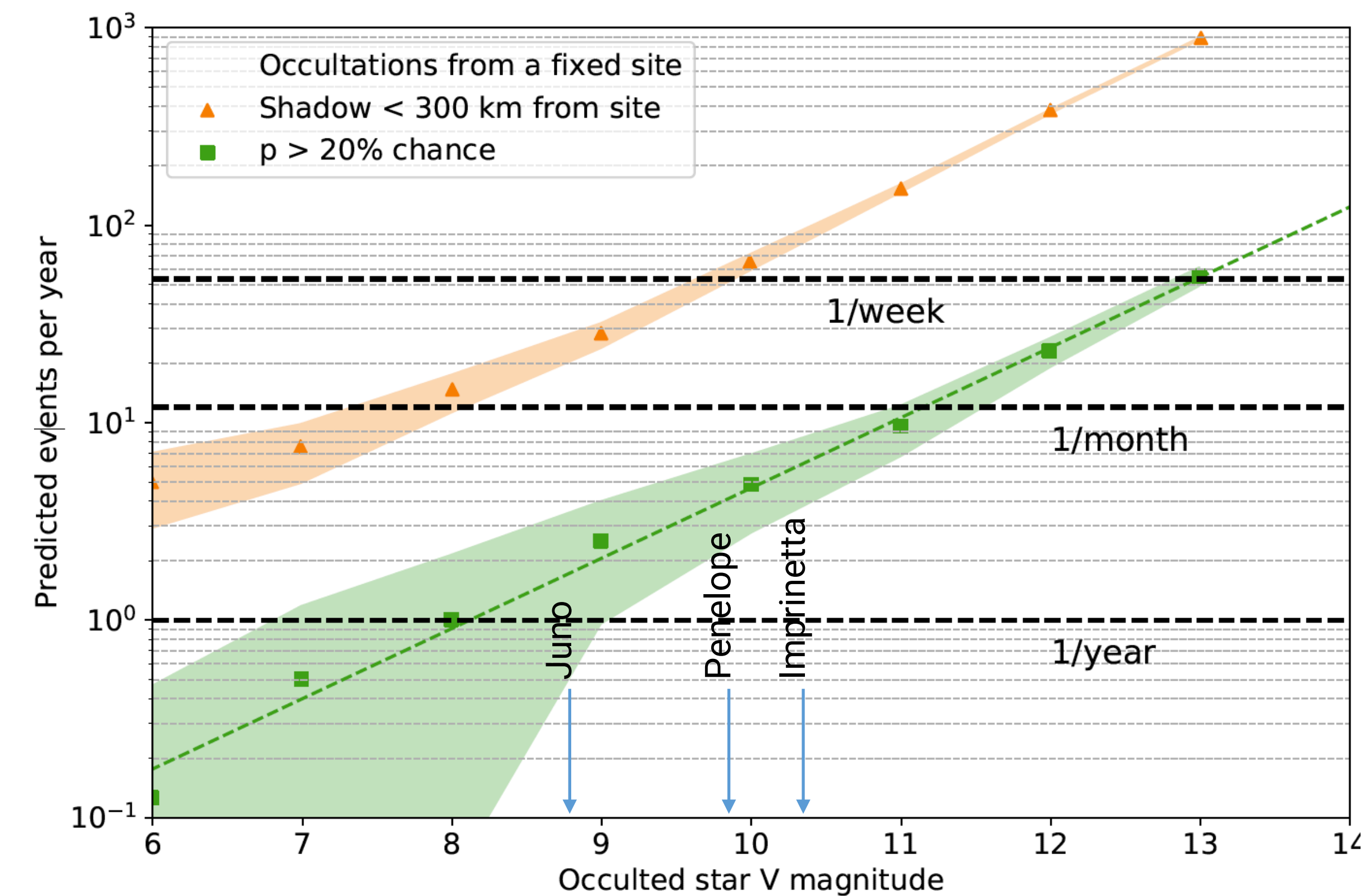


# Why are we interested in small, faint stars?

$$\text{Transit Depth} = \left( \frac{R_p}{R_*} \right)^2$$

There's a particular interest in K star radii, since there is growing evidence of a discrepancy between models and reality at the ~5% level

K stars

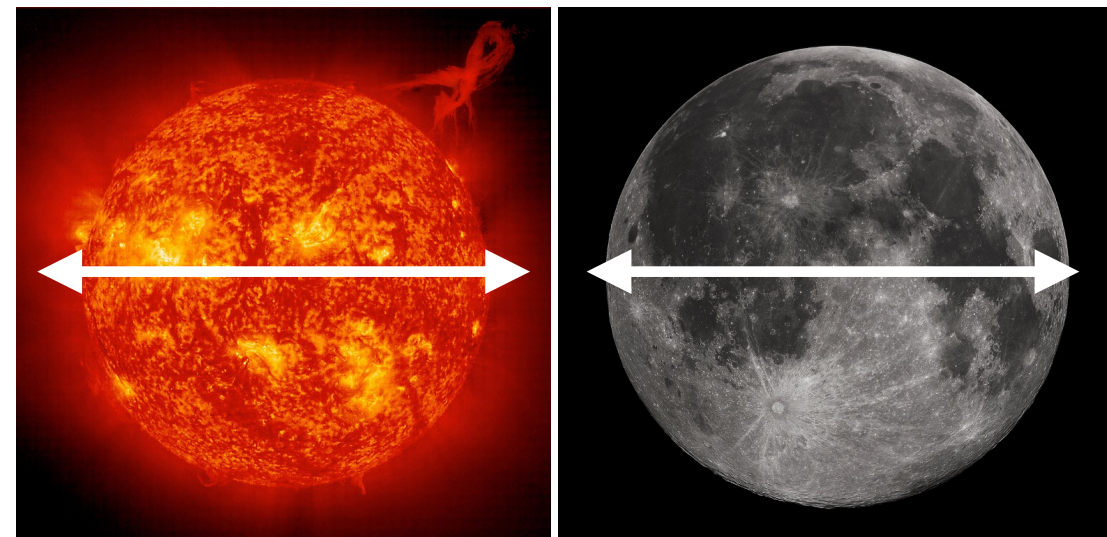




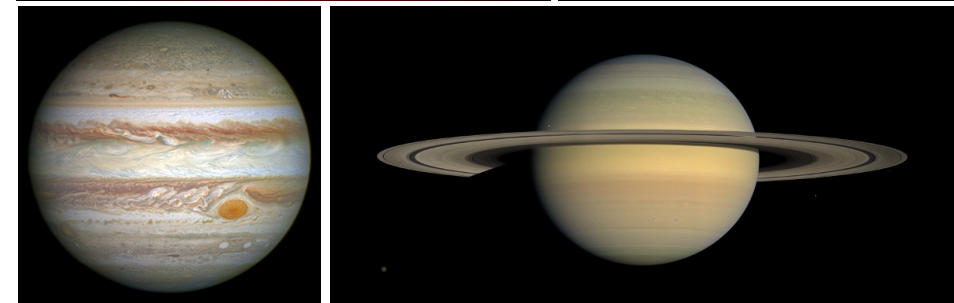
# Intensity Interferometry



# The motivation for sub-milliarcsecond astronomy



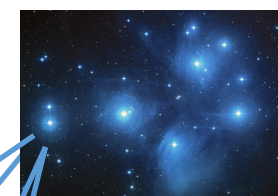
Sun, Moon  
~30arcmin



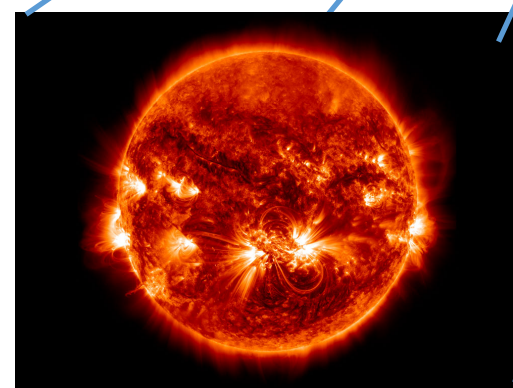
Local planets  
~30arcsec



Largest stars  
~30mas



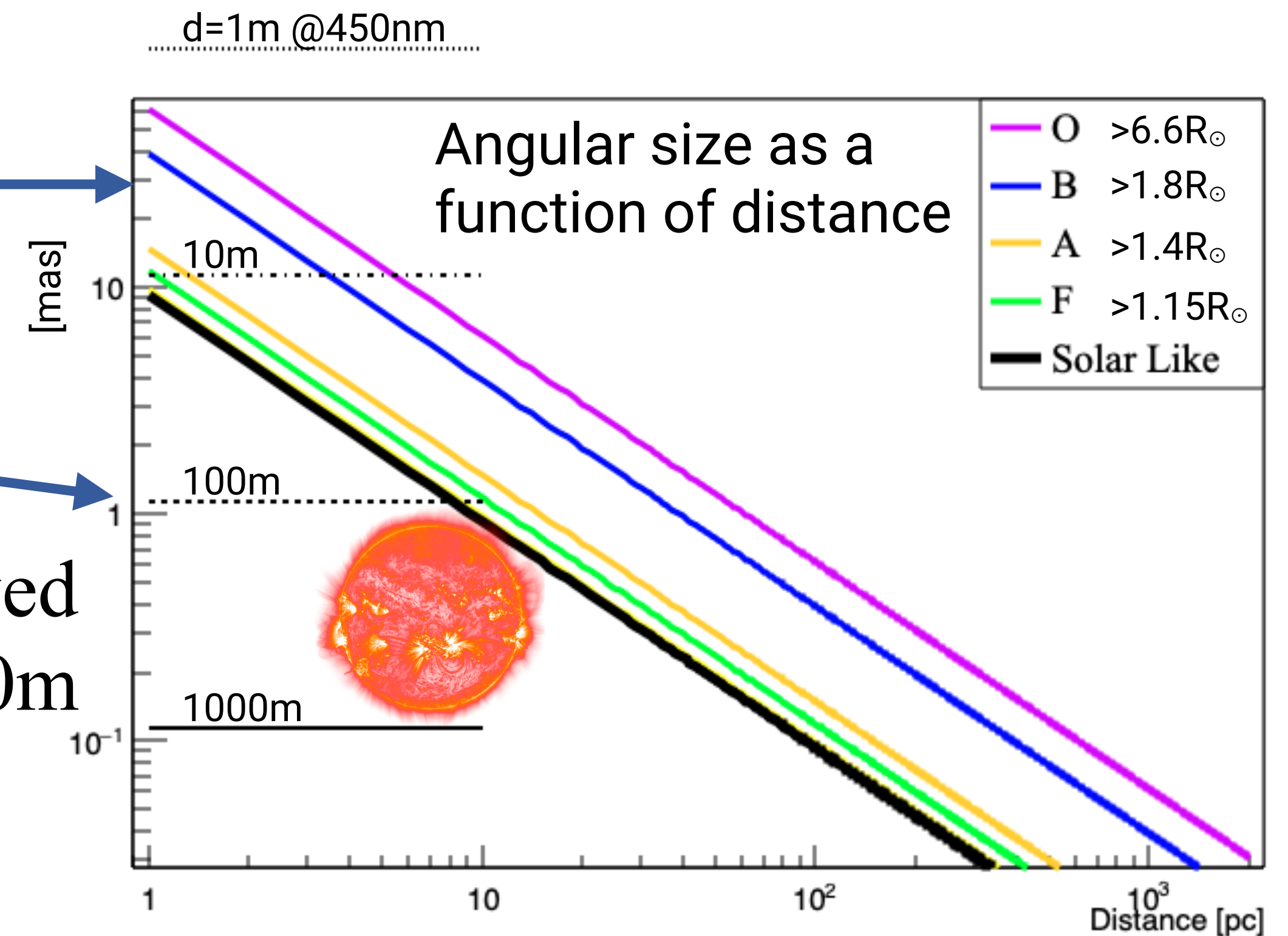
Typical bright stars  
~1mas



Many stars only become resolved surfaces for baselines 100-1000m

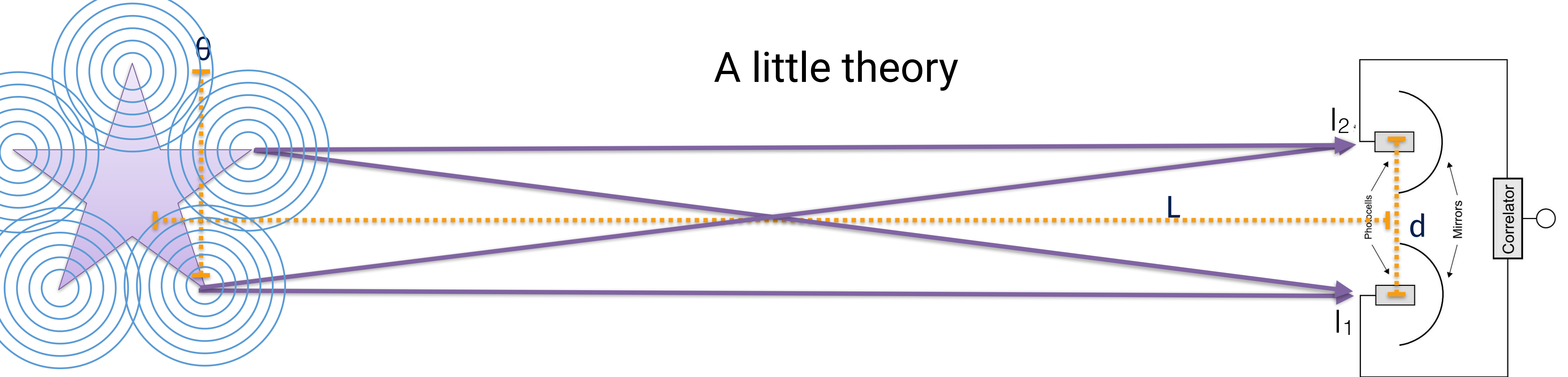
$$\theta \sim \lambda/d$$

*Remember the interferometer is "blind" to any scale that does not have a baseline measurement*





## A little theory



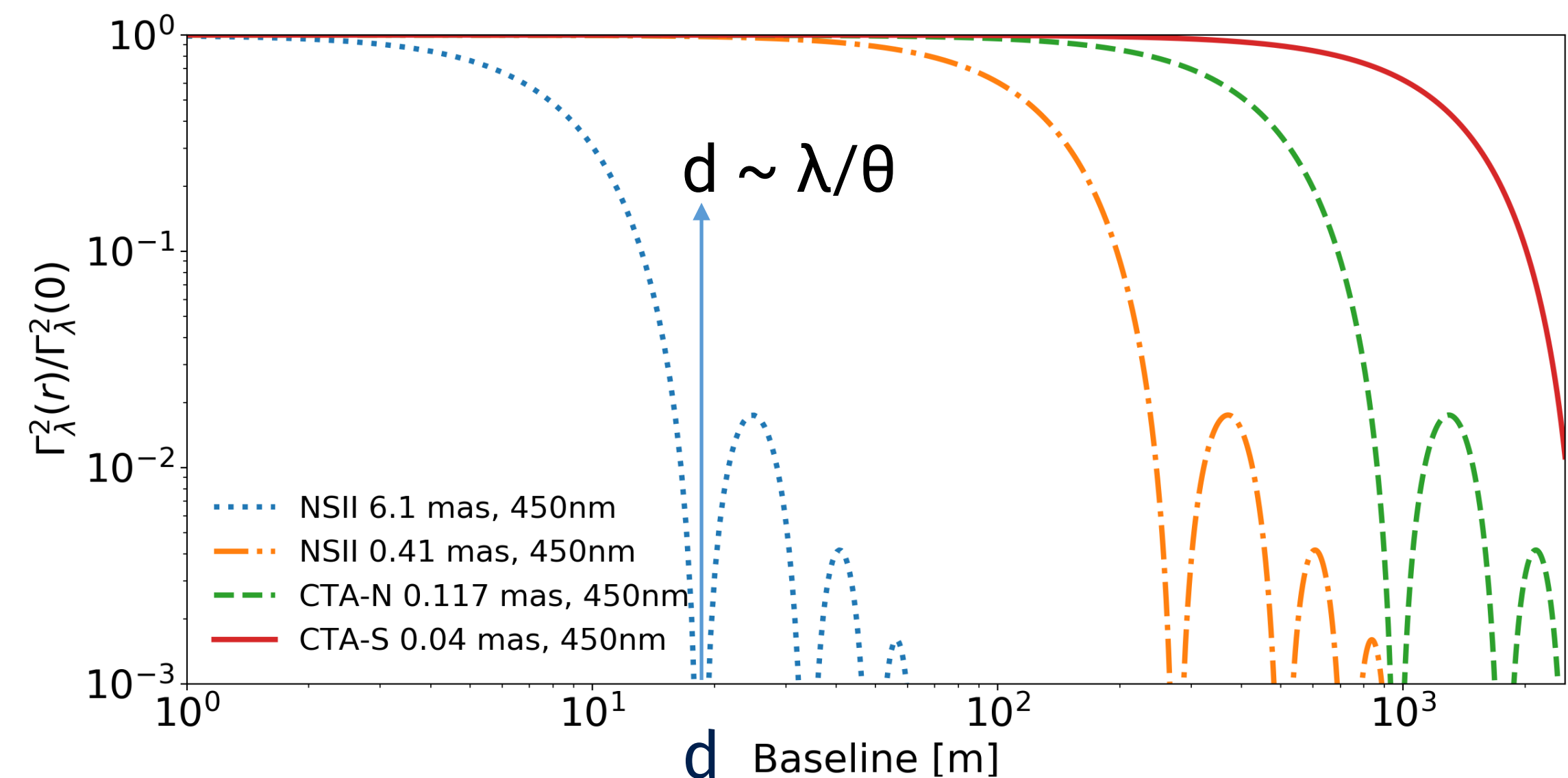
An extended body of angular diameter  $\theta$  consisting of many incoherently emitting sources produces a speckled pattern at the observer of typical size  $\lambda/\theta$

A pair of observers separated by a distance  $\ll \lambda/\theta$  are in the same speckle and  $\therefore$  see the same intensity fluctuations.

Observers separated by  $\gg \lambda/\theta$  are likely to be in different speckles and see fluctuations with less or no correlation.

Measuring the scale at which the signals become de-correlated gives a measure of the angular size of the emission region.


$$\langle I_1(t)I_2(t) \rangle = \langle I_1(t) \rangle \langle I_2(t) \rangle (1 + |\Gamma_{12}(d)|^2)$$

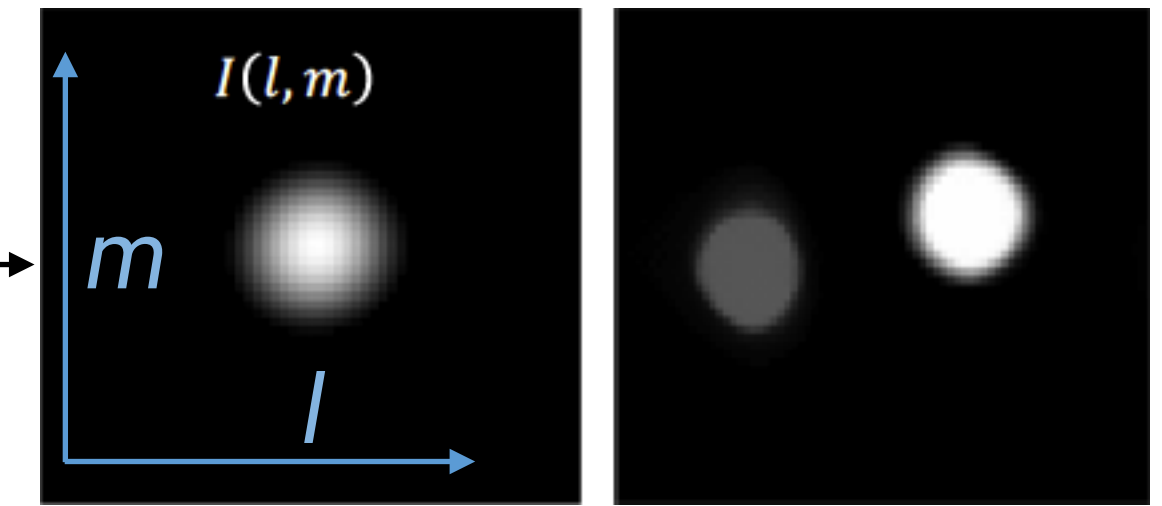




## Second order time coherence $g^{(2)}$ & Fourier image plane

Van Cittert-Zernike Theorem  $g^{(1)}(u, v, 0) = \iint I(l, m) e^{-2\pi i(lu + mv)} dl dm$





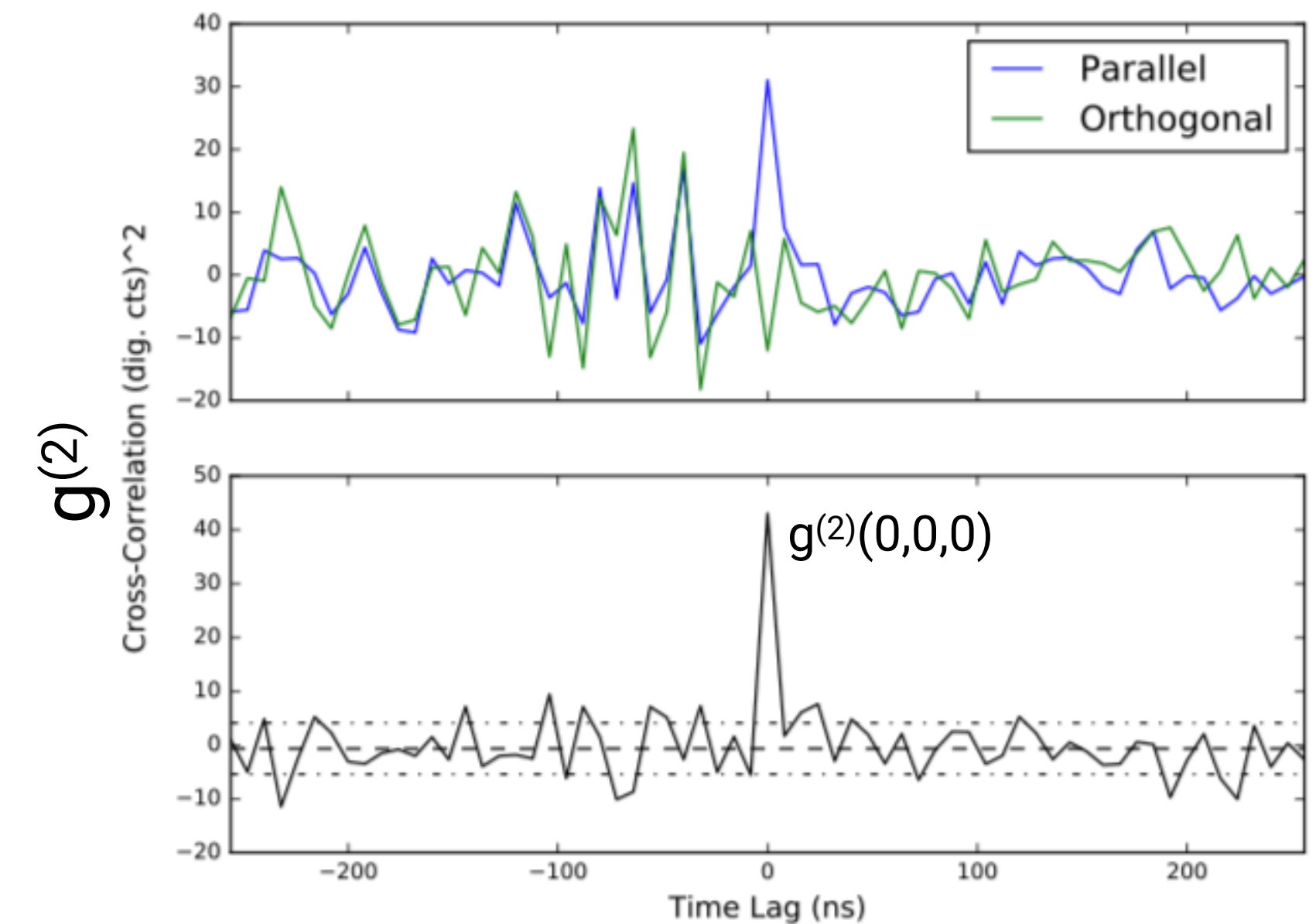
Matthews, Kieda & LeBohec *JMOp* **65**, 1336 (2018).

$$\frac{\langle I_1 I_2 \rangle}{\langle I_1 \rangle \langle I_2 \rangle} = g^{(2)}(u, v, t) = 1 + |g^{(1)}(u, v, t)|^2$$

$g^{(2)}(0,0,0) = 1 + \varepsilon \sim 1 + 10^{-4} \rightarrow$  small non-Gaussian fluctuations requires large photon statistics, i.e. **large collecting surfaces**

Intensity fluctuations lose the phase information, but this can be recovered / compensated for

- e.g. Cauchy-Riemann algorithm Nuñez et al. MNRAS (2012).
- e.g. three point intensity correlations Nuñez & Domiciano de Souza MNRAS (2015).





# Narrabri Stellar Intensity Interferometer (NSII)

- 2x 6.5m dishes on a 188m diameter circular track
  - large mirror surface, with simple optics looks like an IACT.

- Measured angular diameter of 32 stars  $-2 < m_v < 3$

Hanbury Brown, Davis & Allen *MNRAS* **167**, 121 (1974)

- Directly measured limb darkening of Sirius

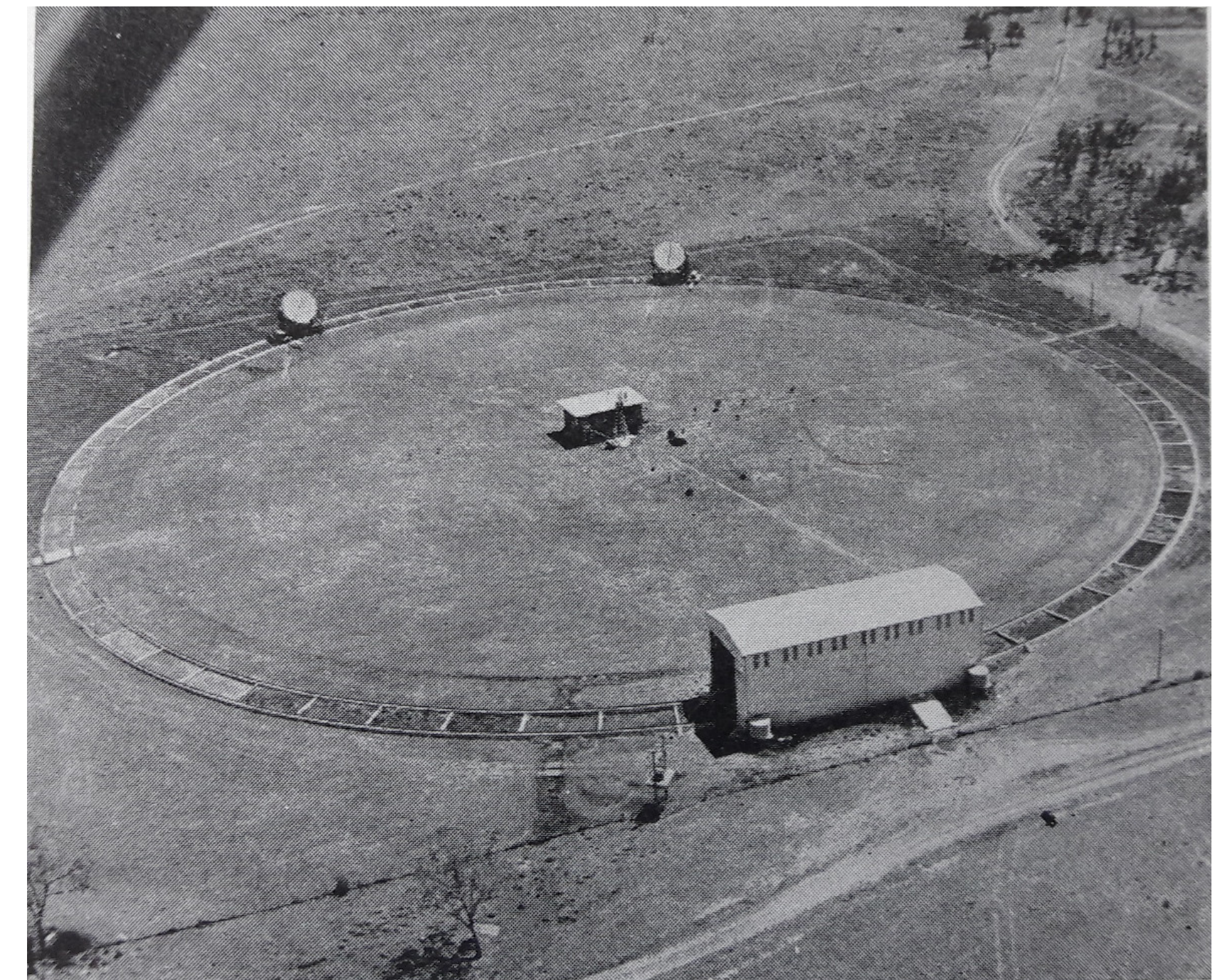
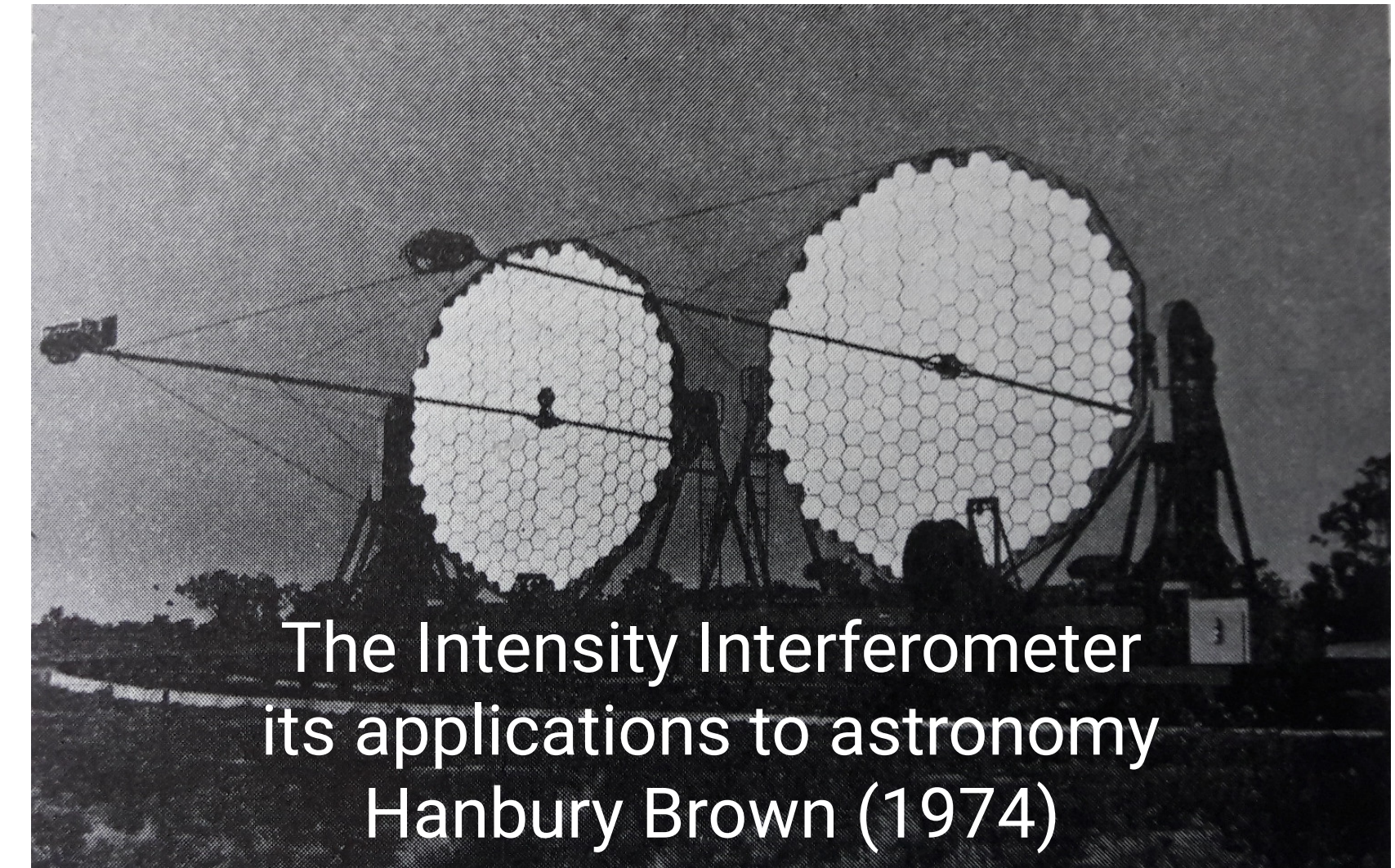
Hanbury Brown, Davis Lake & Thompson *MNRAS* **167**, 475 (1974)

- Multiple stars & spectroscopic binaries (e.g. Spica/ $\alpha$  Vir)

Herbison-Evans, Hanbury Brown, Davis & Allen *MNRAS* **151**, 161 (1971)

- Emission line regions around a star ( $\gamma$  Velorum)

Herbison-Evans, Hanbury Brown, Davis & Allen *MNRAS* **148**, 103 (1970)



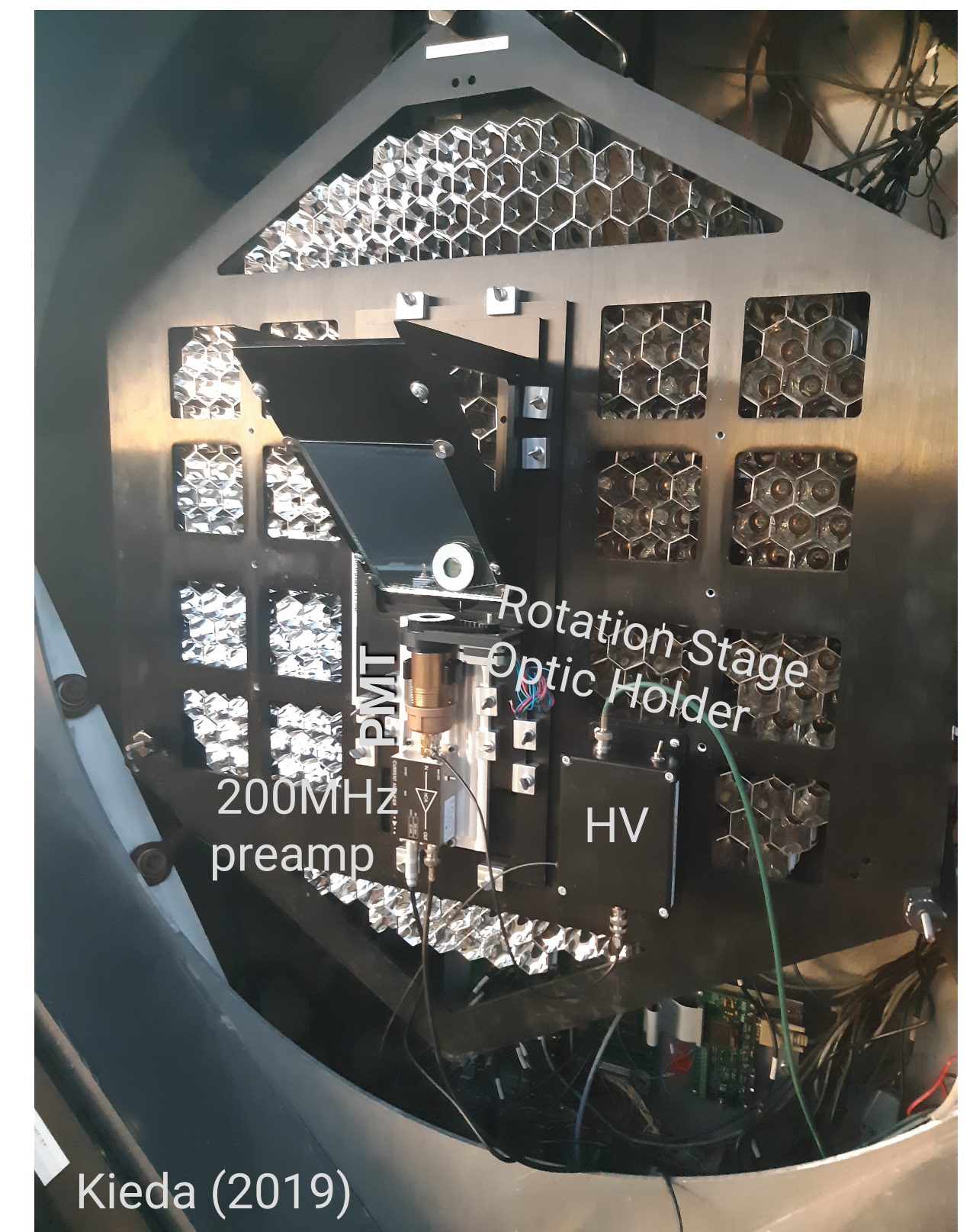


# Stellar intensity interferometry at VERITAS

See poster PS1-76 (session 1)

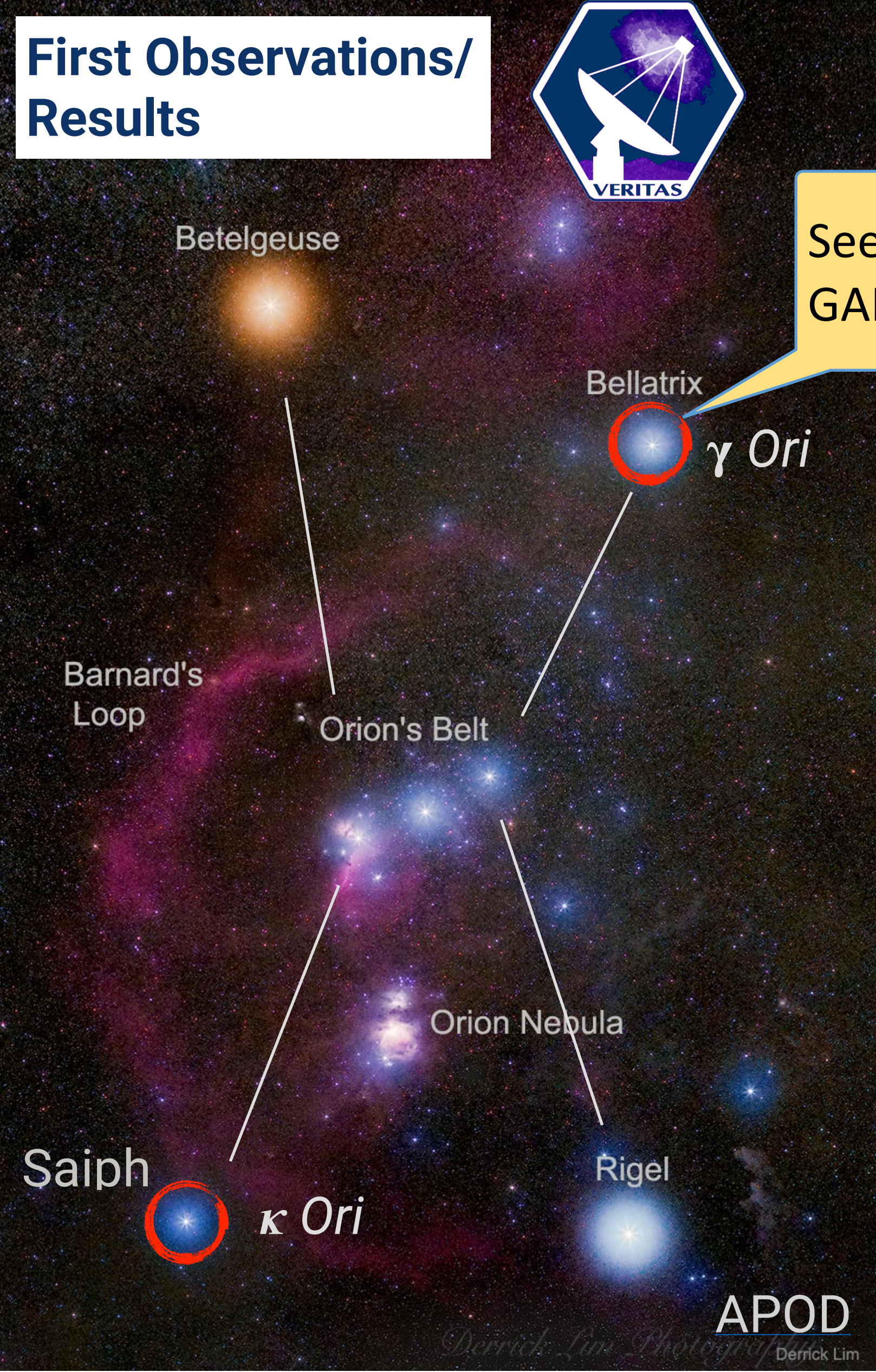


- 4x 12m diameter telescopes, arranged on rectangular grid of  $\sim 100\text{m}$
- Equipped VERITAS for SII observations (augmentation funded by an NSF-AST RAPID grant)
  - beginning October 2018 (2 telescopes)
  - 3 telescope observations began in February 2019
  - measures photon intensity at each telescope with continuous digitization directly to disk (correlation is offline)
- Goal: image  $\sim 30$  nearby stars in U/V band
  - observe  $\pm 2$  days from full moon (when gamma-ray observations not scheduled)
  - not a problem for bright ( $m < 4$ ) sources with suitable filters

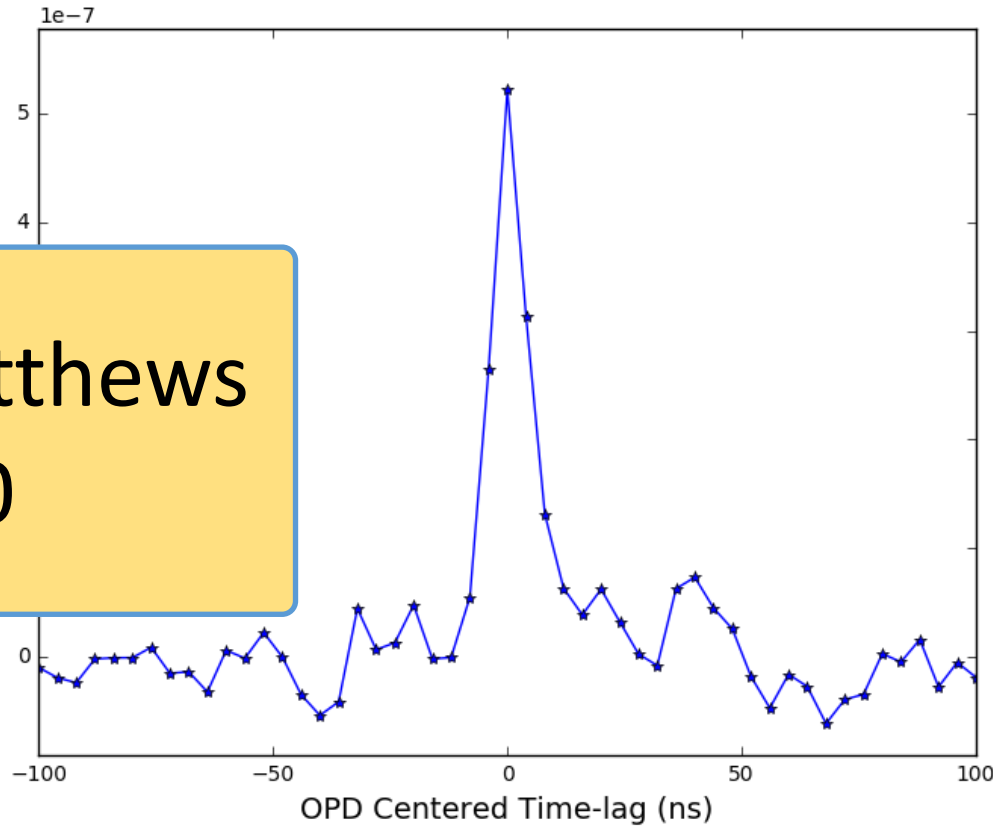




# First Observations/Results



See talk N. Matthews  
GAI3e Fr. 14:30

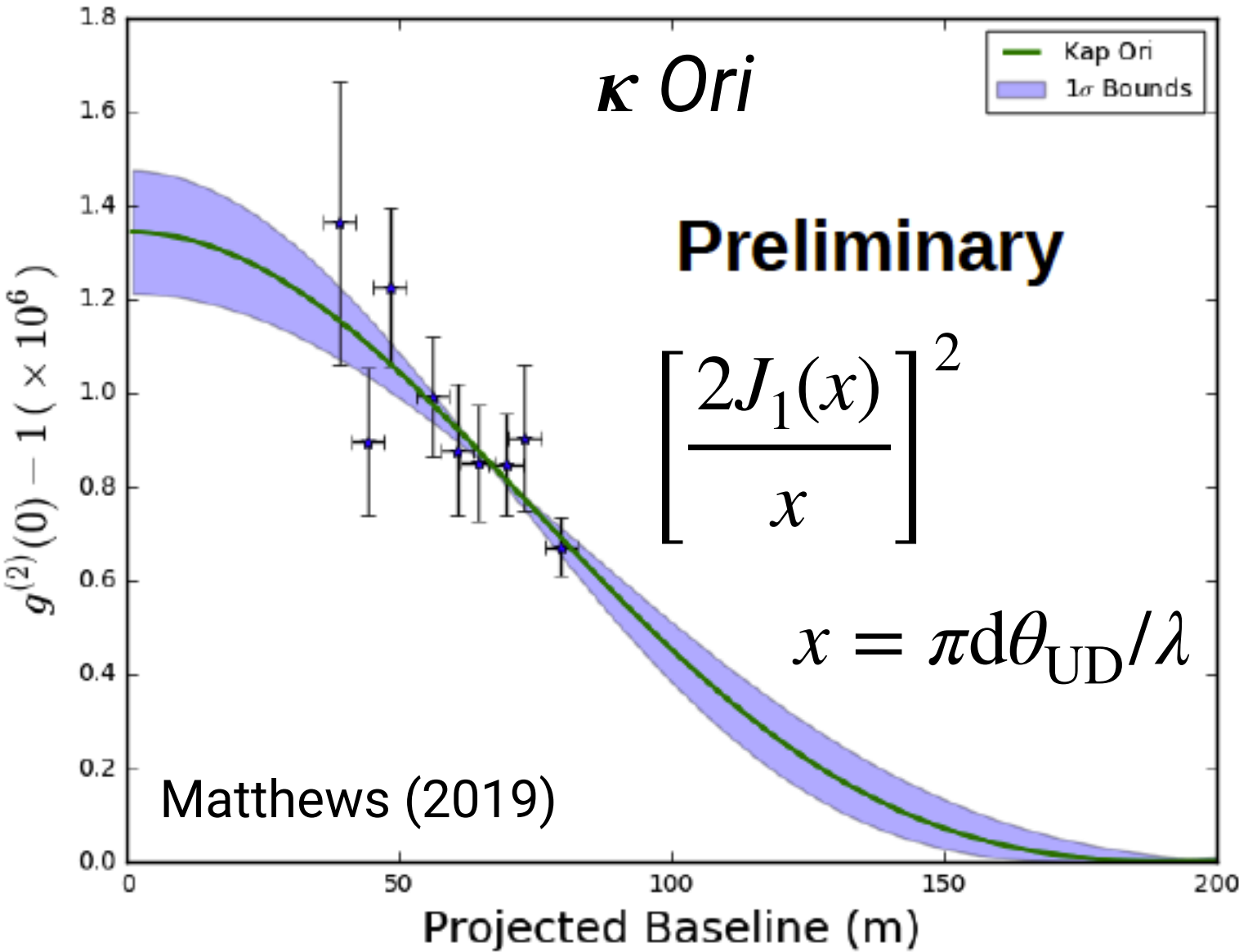
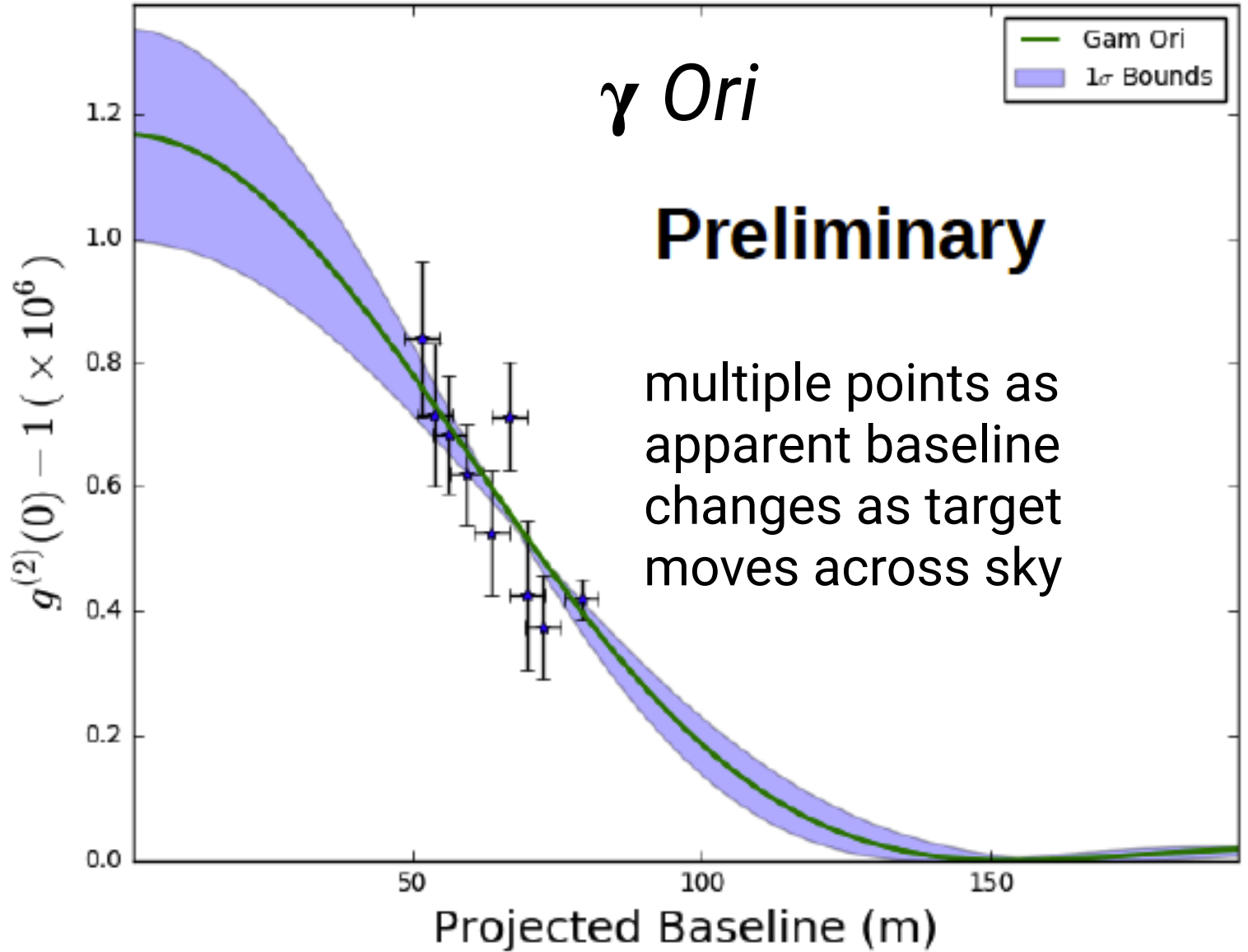


- Data taken in 20m ‘runs’
- Streamed to disk (@250MS/s)
- Correlated offline next day
  - next step, perform higher order correlations with more telescopes (phase recovery).

	$T_{\text{obs}}$ [h]	$\theta_{\text{meas}}$ [mas]	cf $\theta_{\text{UD}}$ [mas]
$\gamma$ Ori	4.74	$0.68 \pm 0.06$	$0.701 \pm 0.005$
$\kappa$ Ori	5.13	$0.48 \pm 0.06$	$0.44 \pm 0.03$

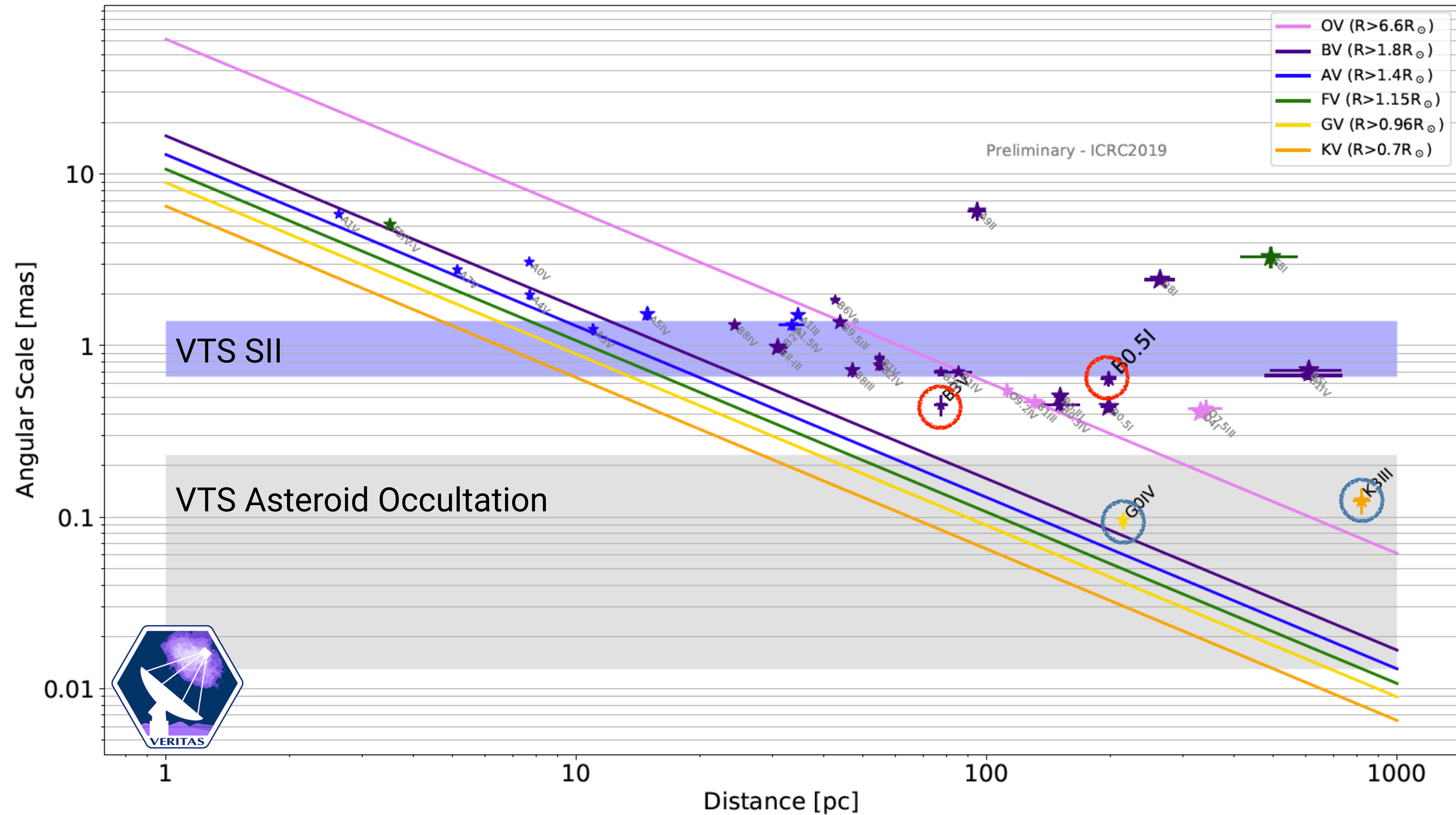
Richichi et al (2005)

## 2 telescope results



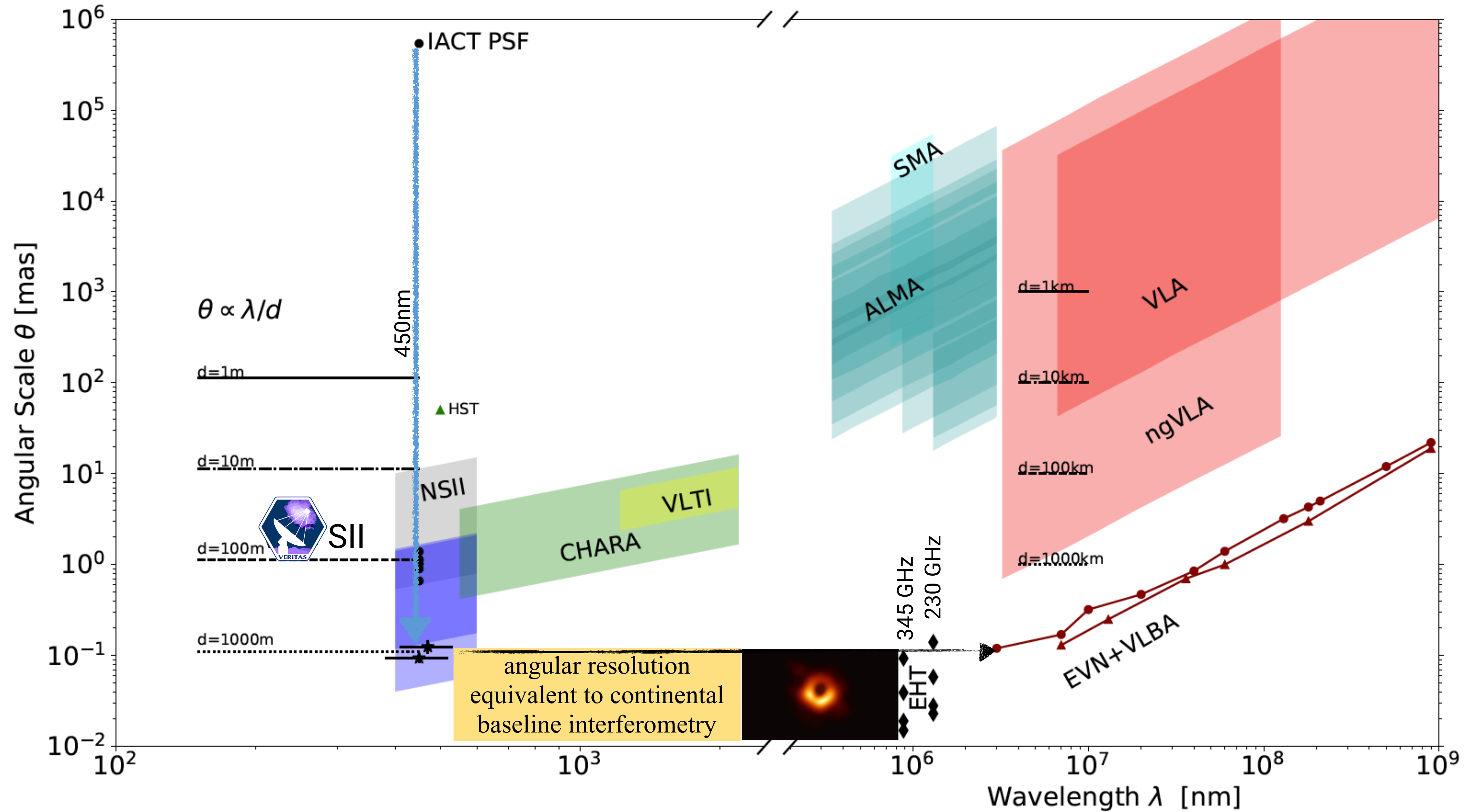


# Stellar angular diameters measured by intensity interferometry and asteroid occultations





# How does an IACT compare?





# A lot of science...

in a short space of time

- angular diameters
- limb darkening
- rapid rotators
- binary systems
- emission line regions
- star spots
- ...

see also, e.g.

Hanbury Brown (1974)

Barbieri et al *Astro2010* paper 61, arXiv:0903.0062

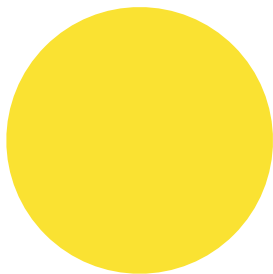
Dravins et al *NewAR* **56**, 143 (2012).

Dravins et al *APh* **43**, 331 (2013).

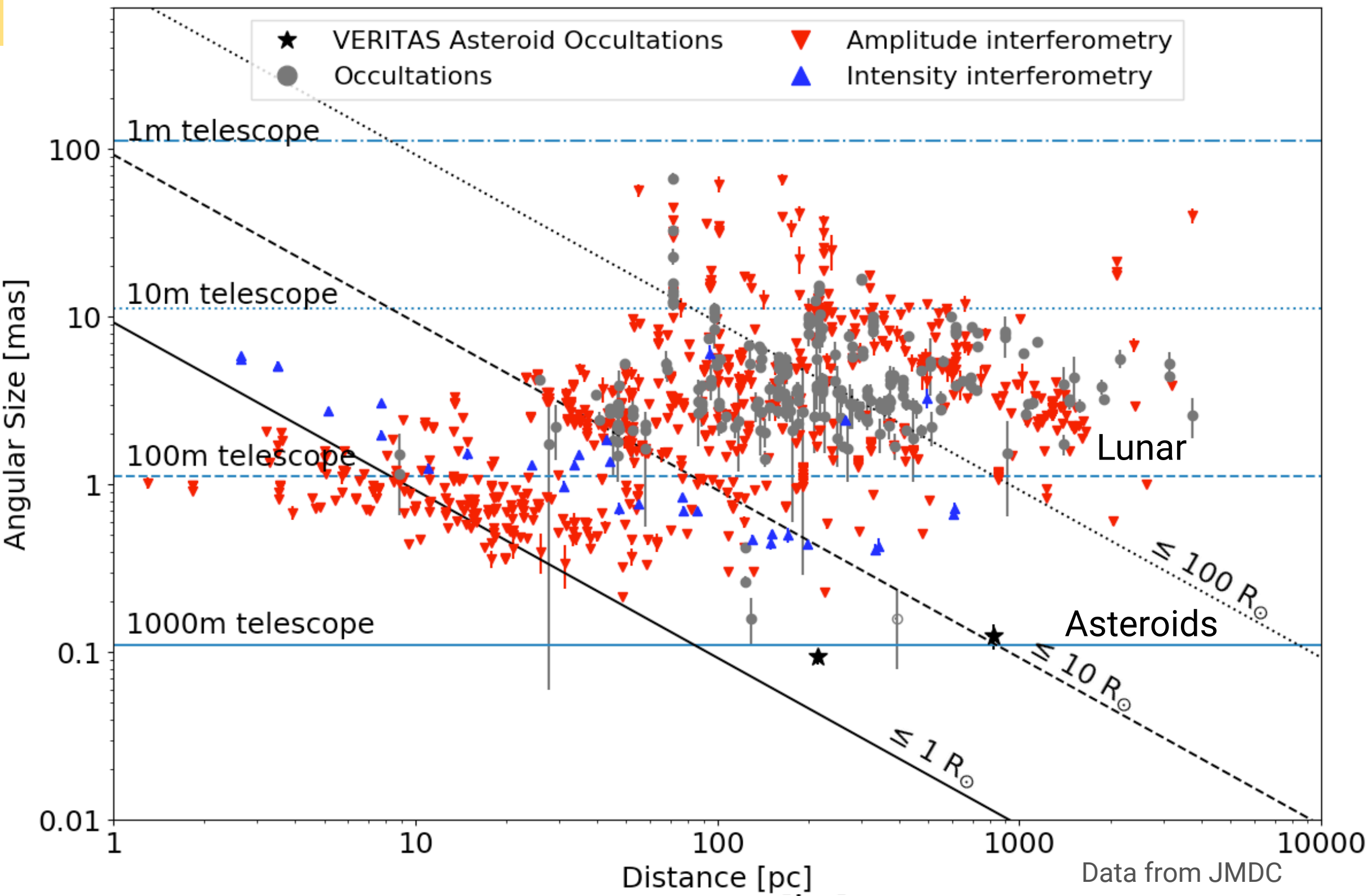
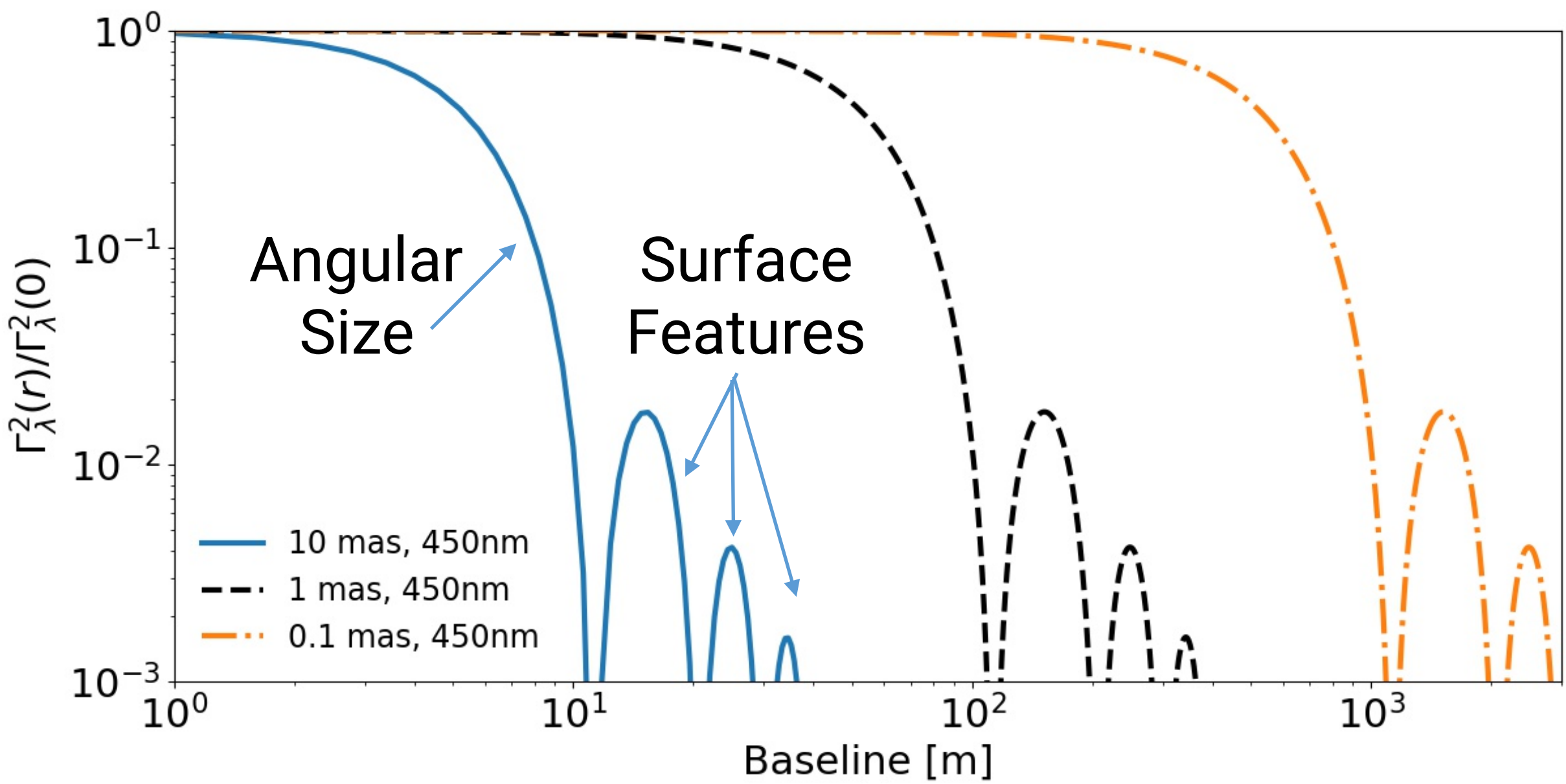
Kieda et al *Astro2020* paper ID 304 (2019).



The first dimension – angular size of stars - uniform disc



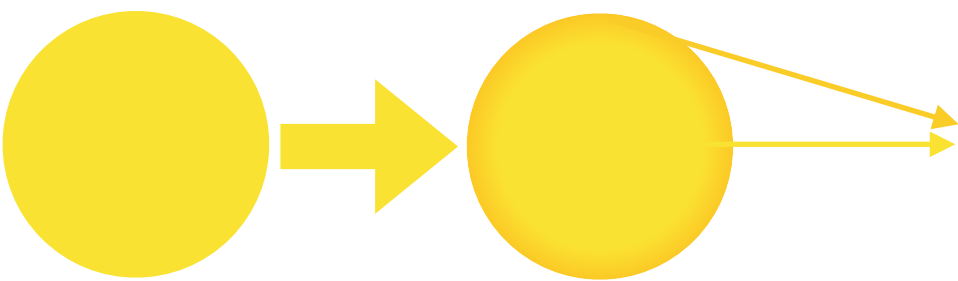
The larger the baselines, the smaller the detail we can see



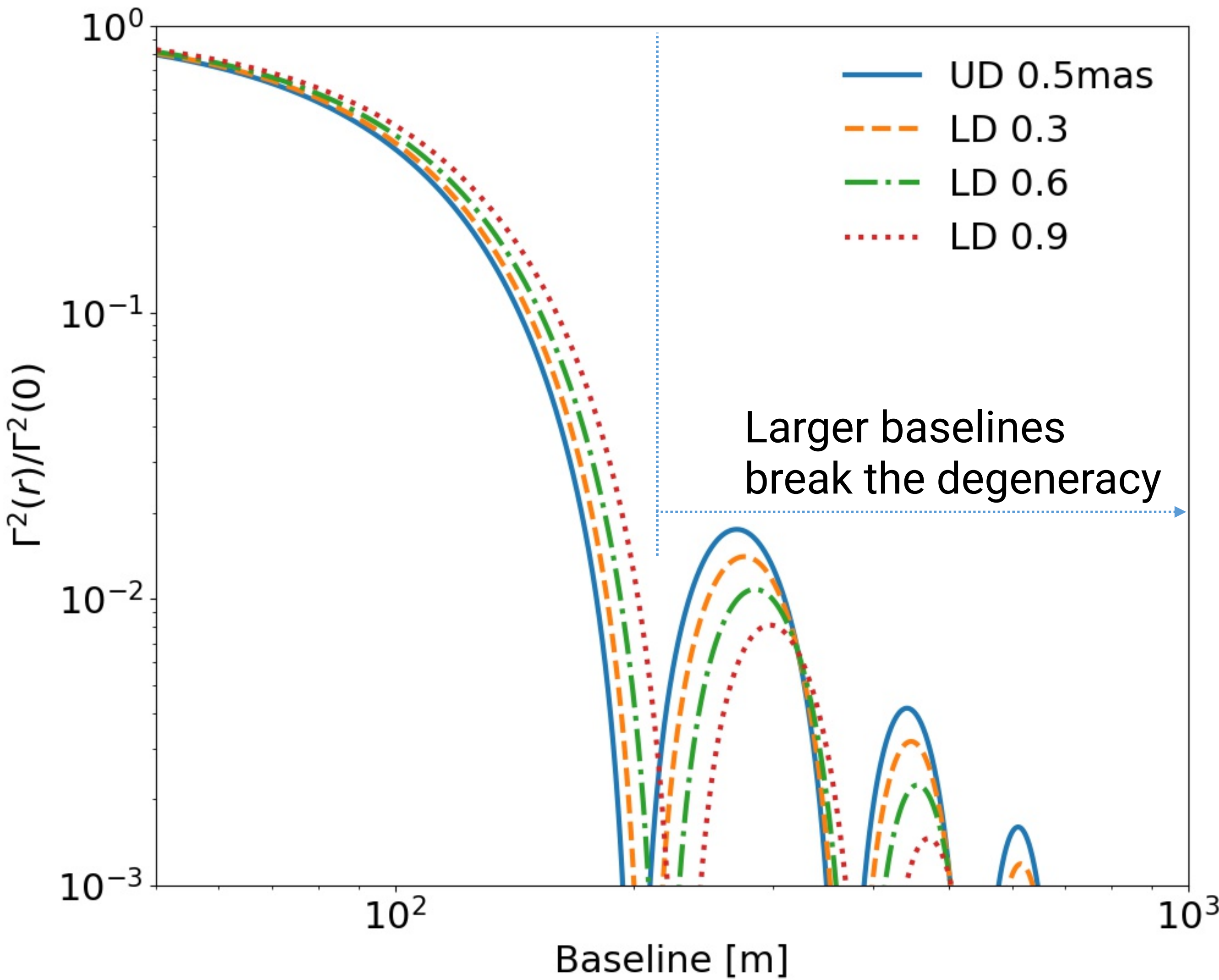
- Constrain stellar evolution models
- Also useful in determining size of transiting exo-planets



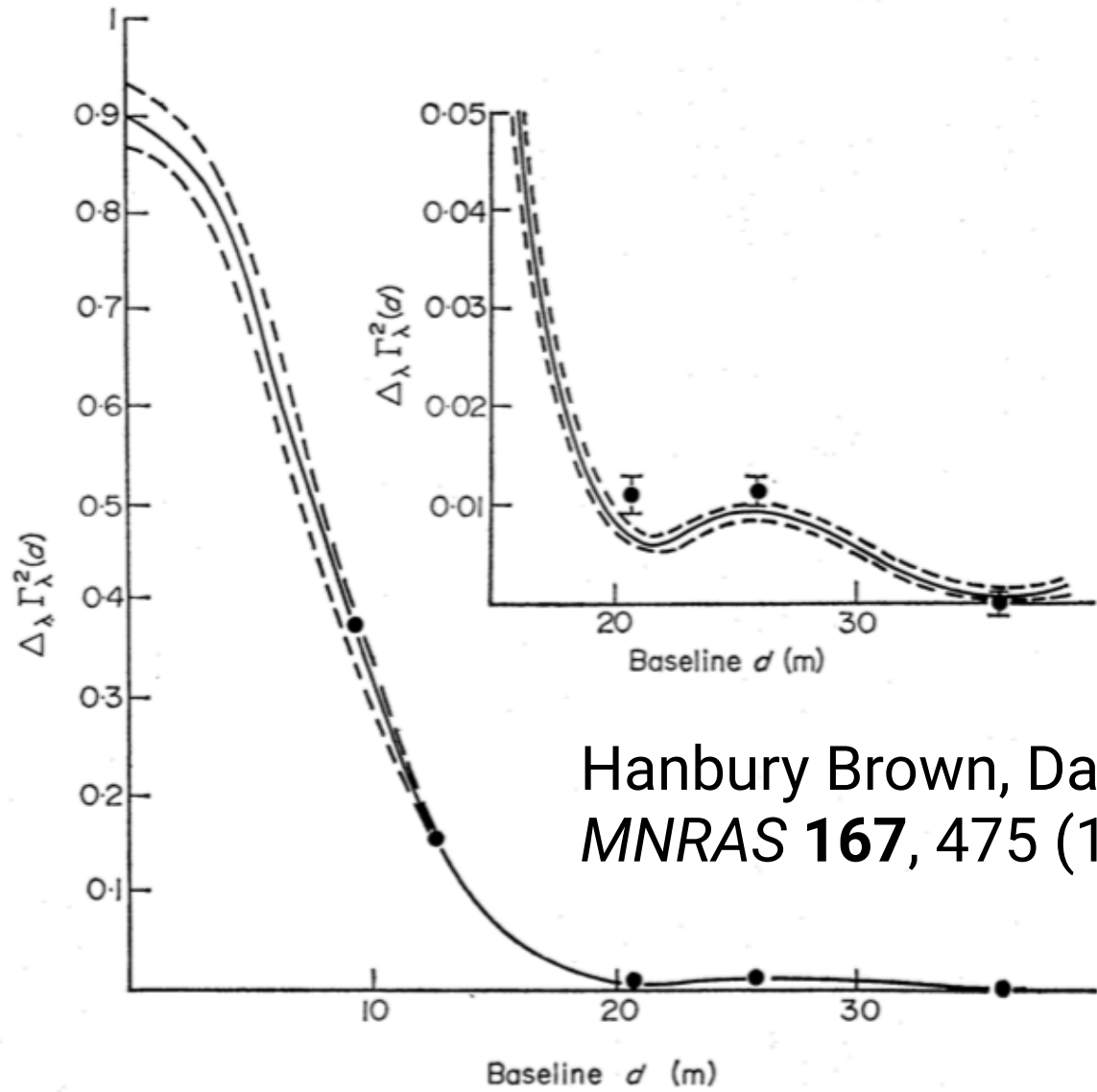
The next dimension – limb darkening



The longer the baselines,  
the more sensitive the  
observation... the more:



- **accurately** constrain stellar evolution models in a model independent way
- for <5% error can **accurately** determine size of transiting exo-planets



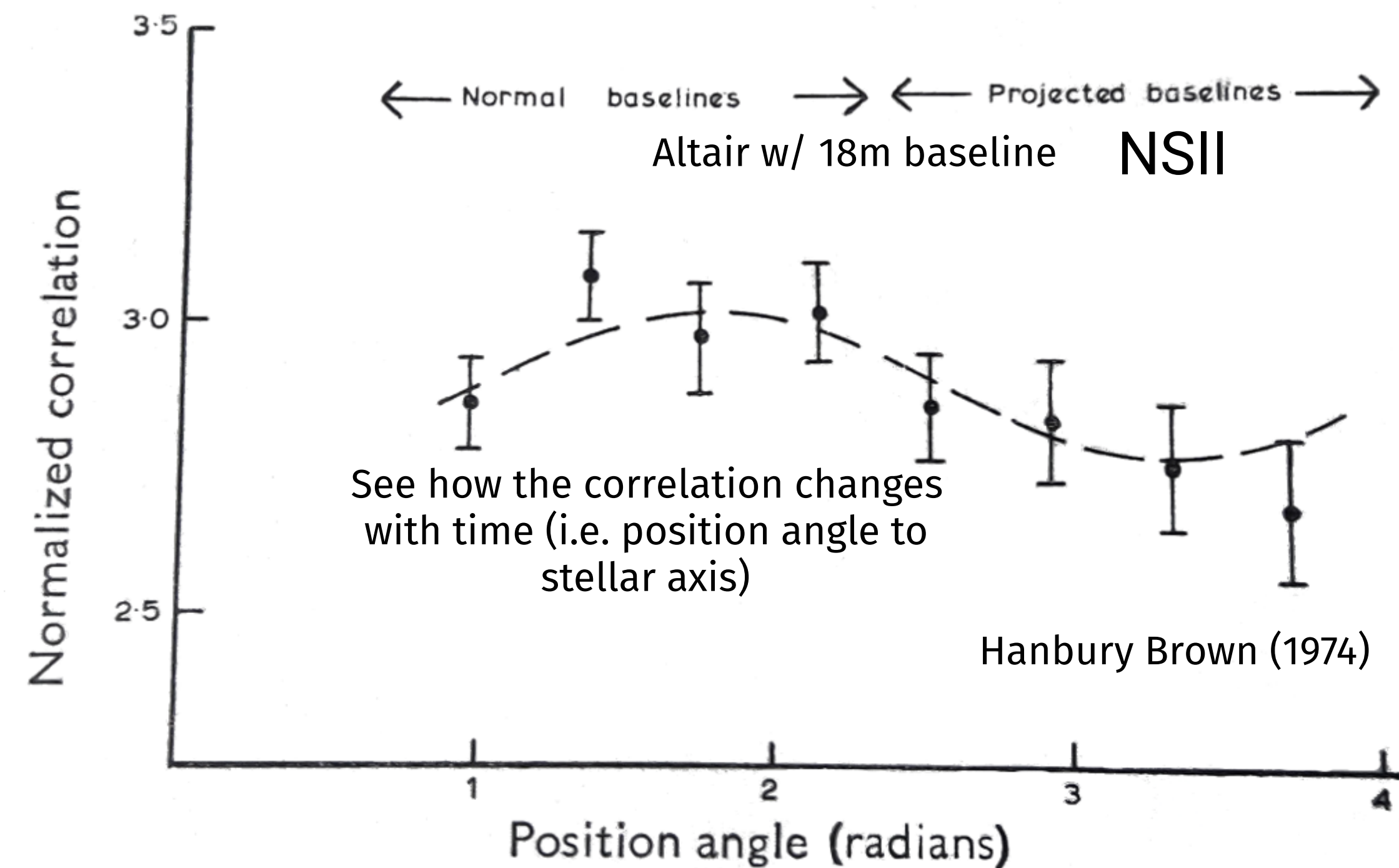
Hanbury Brown, Davis Lake & Thompson  
*MNRAS* **167**, 475 (1974)

FIG. 3. The variation of correlation  $\Delta_\lambda \Gamma_\lambda^2(d)$  with baseline  $d$  for Sirius. The points show the observed values; the full line is a theoretical curve, based on a model stellar atmosphere ( $T_e = 10\,000\text{K}$ ,  $\log g = 4$ ), with zero-baseline correlation and angular size adjusted to give the best fit to the observations. The broken lines represent the rms uncertainty in the theoretical curves.



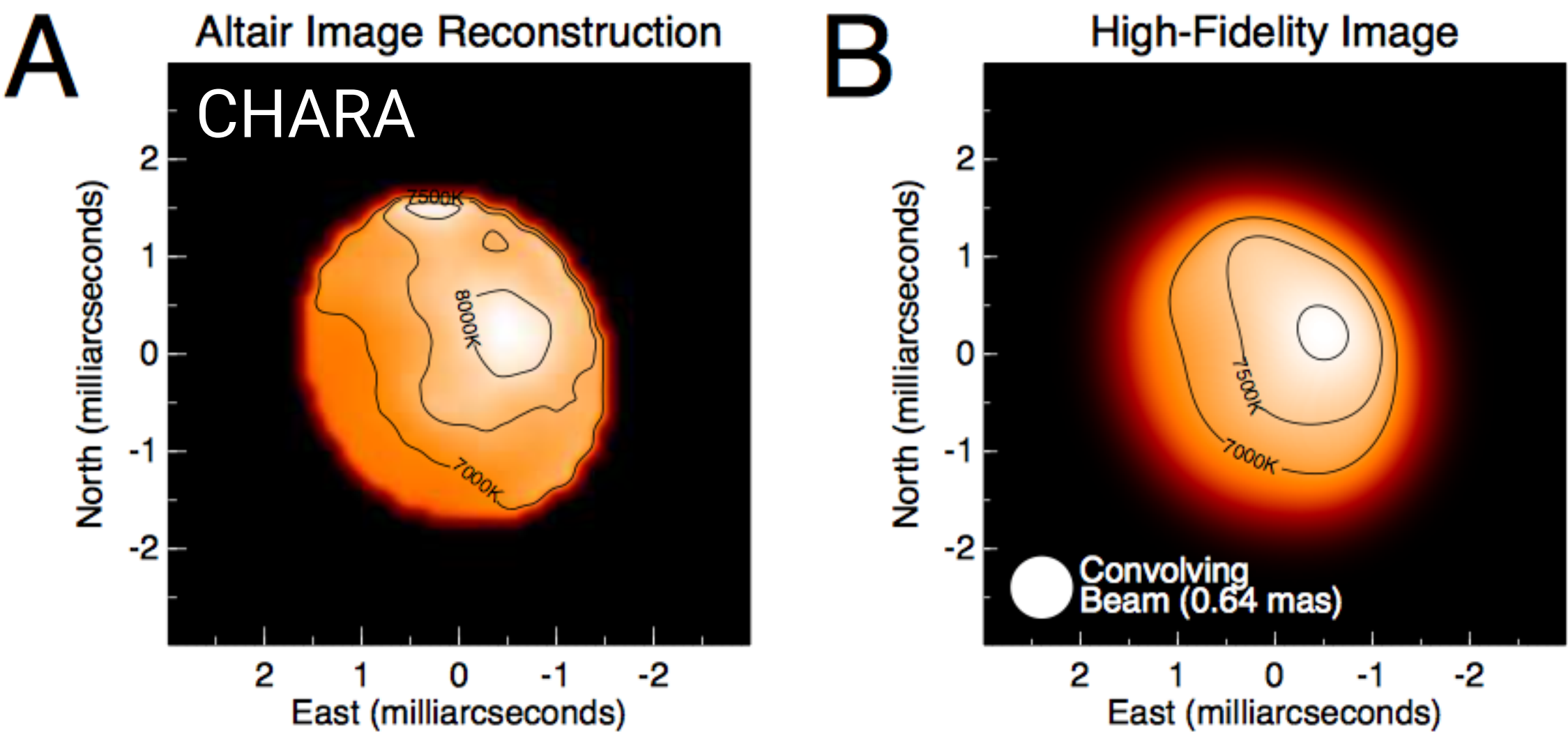
Rapidly rotating stars — distorted discs — gravitational darkening — e.g. Altair

- Be star disk formation
- winds from hot stars
- Wolf-Rayet star environments
- GRB pre-cursors
- ...



with 2 telescopes... *get an impression*

With more telescopes we provide the data to fit a model to, rather than vice versa



with 6 telescopes... **start to build a picture**

The difference between the CHARA observation and the theoretical model “shows stronger darkening along the equator, inconsistent with any von Zeipel-like gravity darkening prescription assuming uniform rotation.”

CHARA Science **317**, 5836 (2007)



# Binary systems & star spots & accretion zones ...

Remember, these are dynamic systems.

A time averaged correlation provides some information, a time sequence or series of images provides more

- So requirements are:
- ▶ Many baselines of >100m
  - ▶ Many baselines measuring simultaneously for shorter observation times

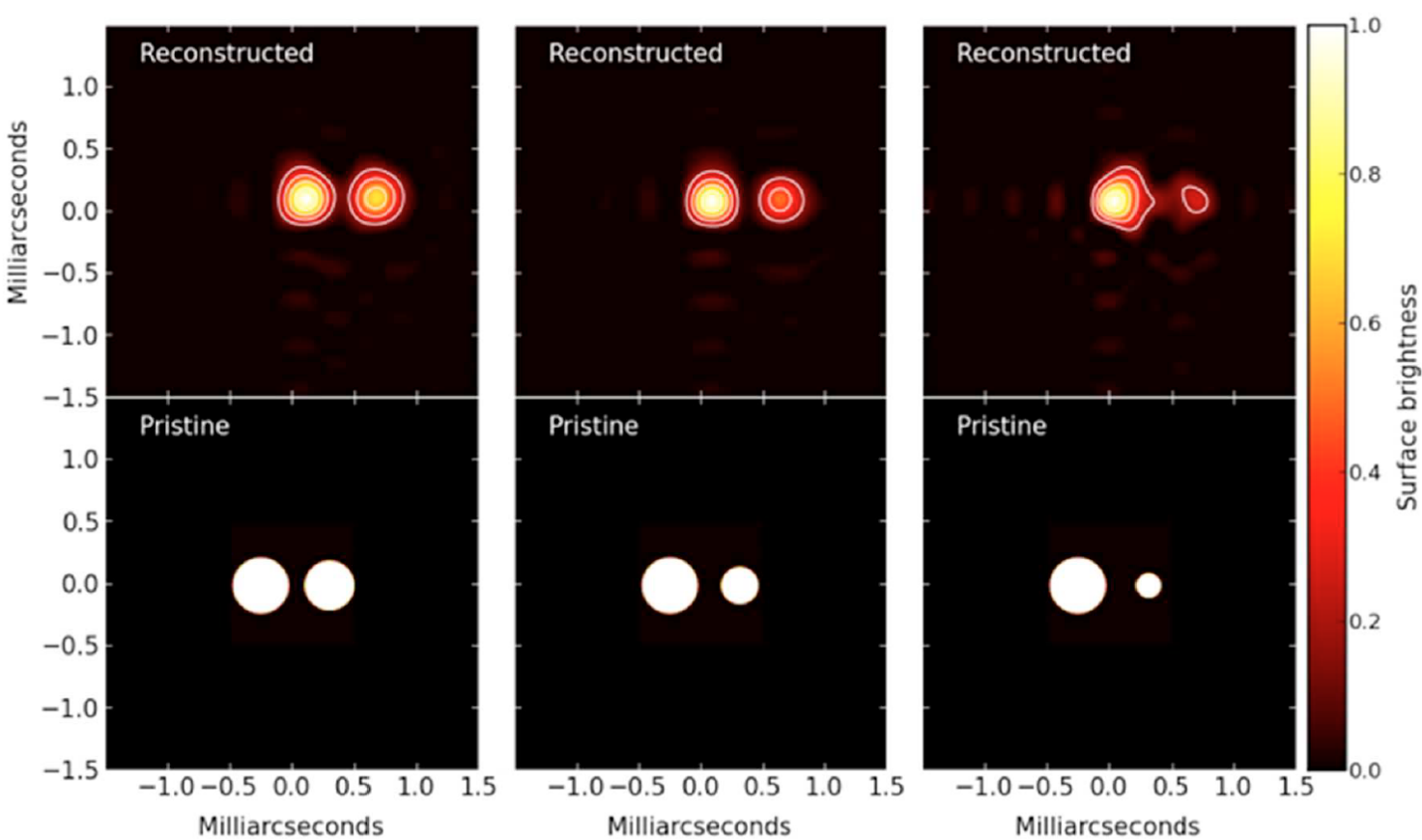
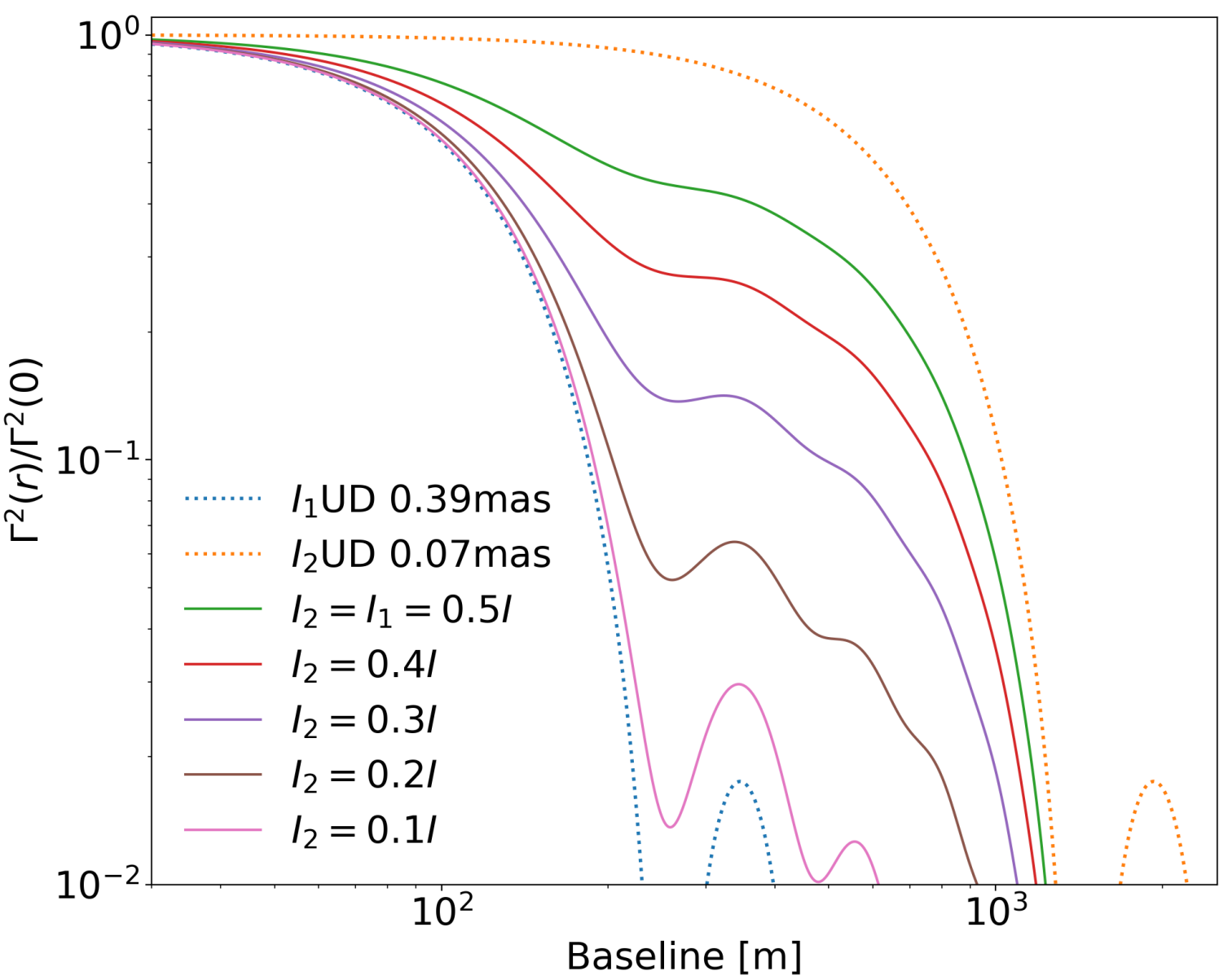
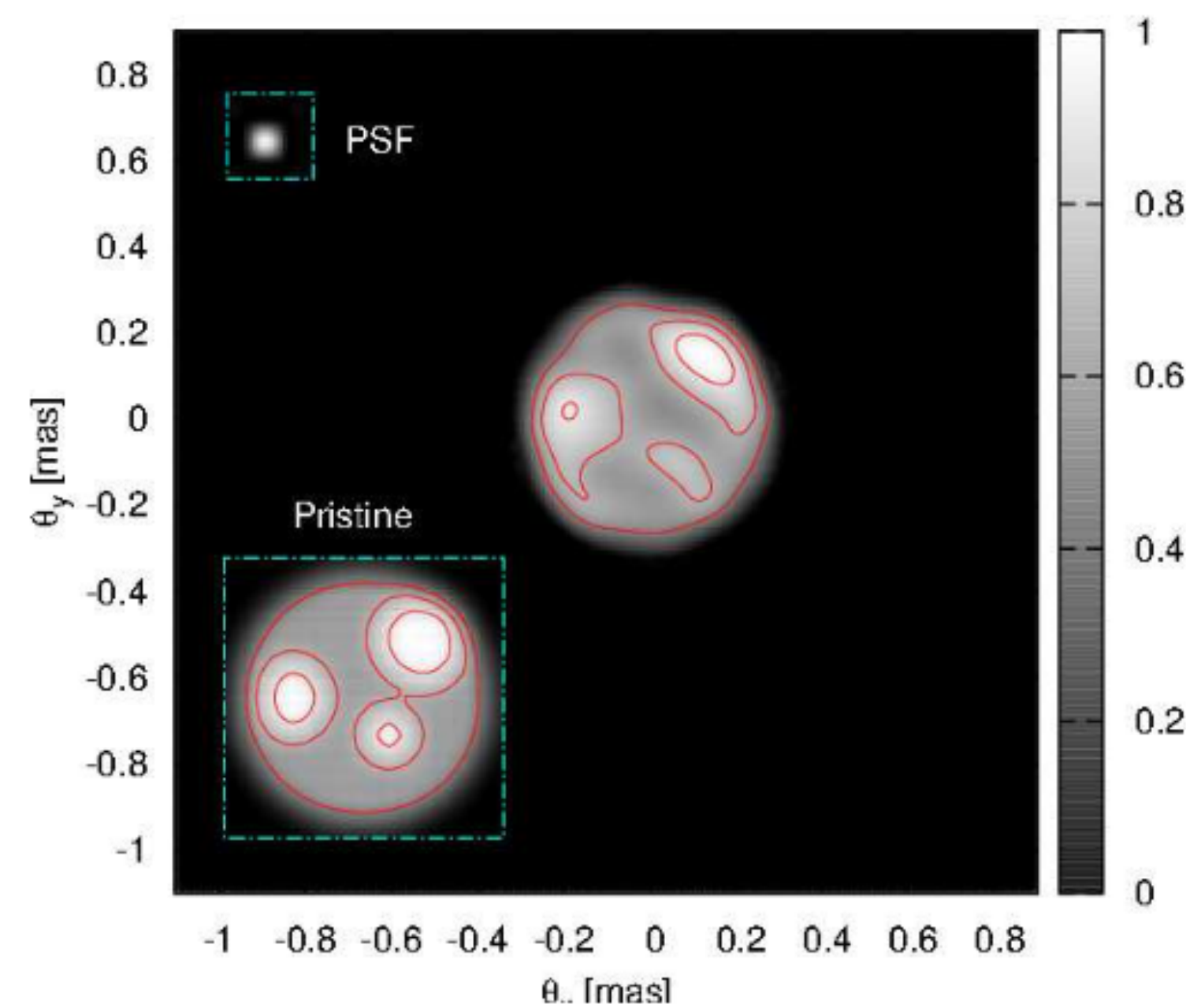


Figure 5: Reconstructed images of binary stars (with varying diameter of the secondary) from simulated CTA observations. These simulations were for the array layout B (Figure 2), for sources assumed to have visual magnitude  $m_V=3$ , and effective temperature  $T_{eff} = 7000\text{K}$ . The assumed pristine images are shown below while the corresponding  $(u, v)$ -plane coverage is in Figure 6.

*Aph* **43**, 331 (2013).

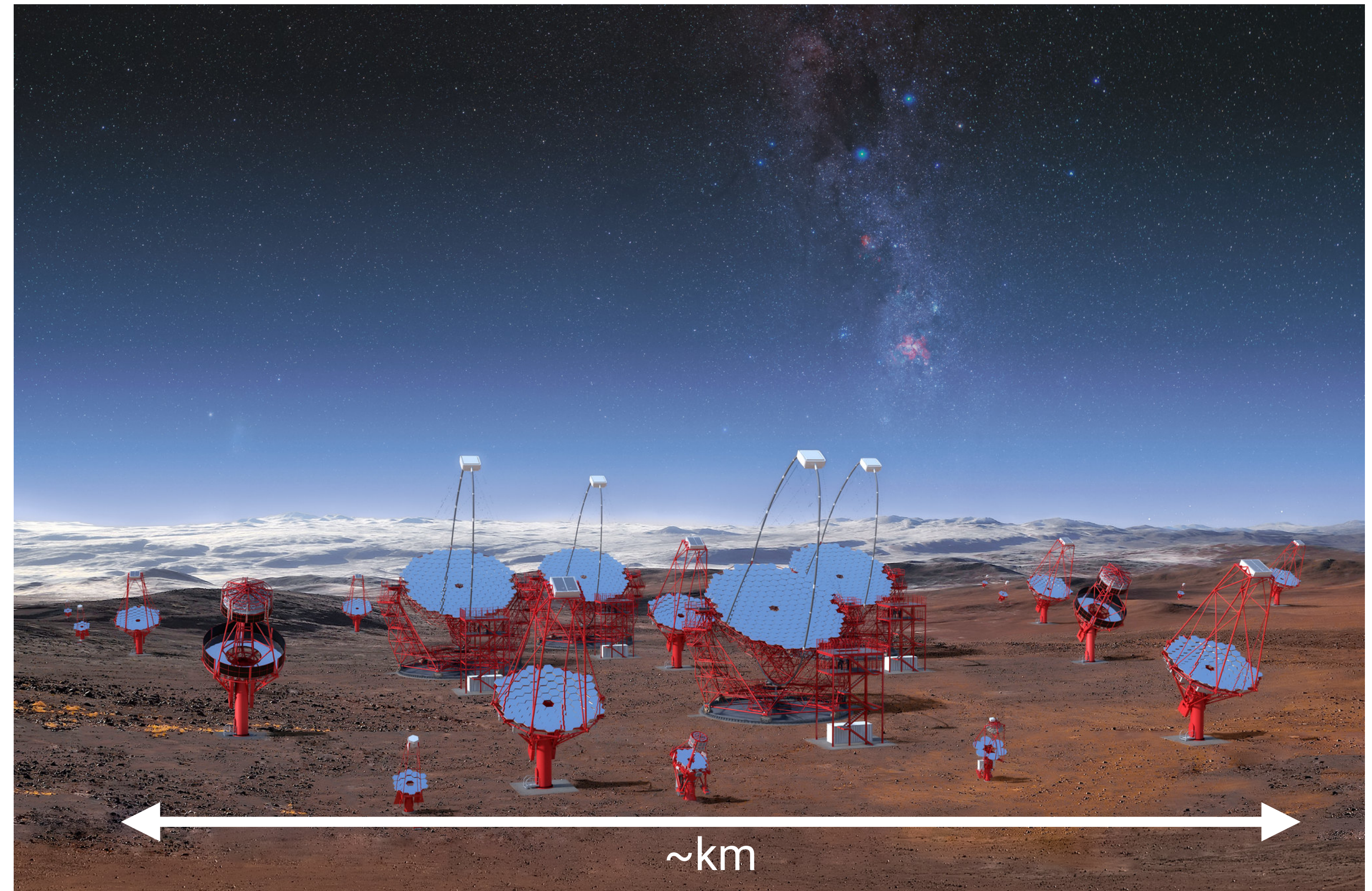


# A big future...

$$N_{pairs} = \frac{N_{tel}(N_{tel} - 1)}{2}$$

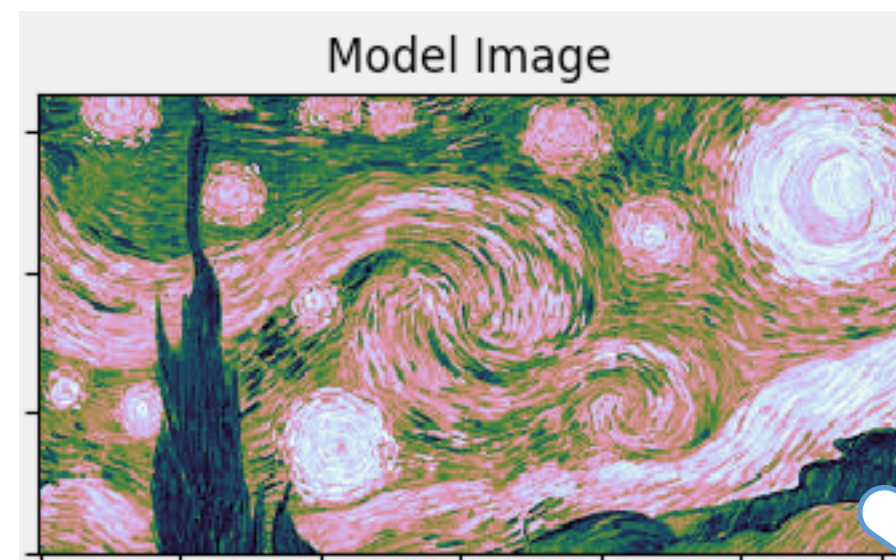
# telescopes	2	5	15	25	50	100
# baselines	1	10	105	300	1225	4950

With so many available baselines  
**model independent** imaging  
becomes a realistic possibility



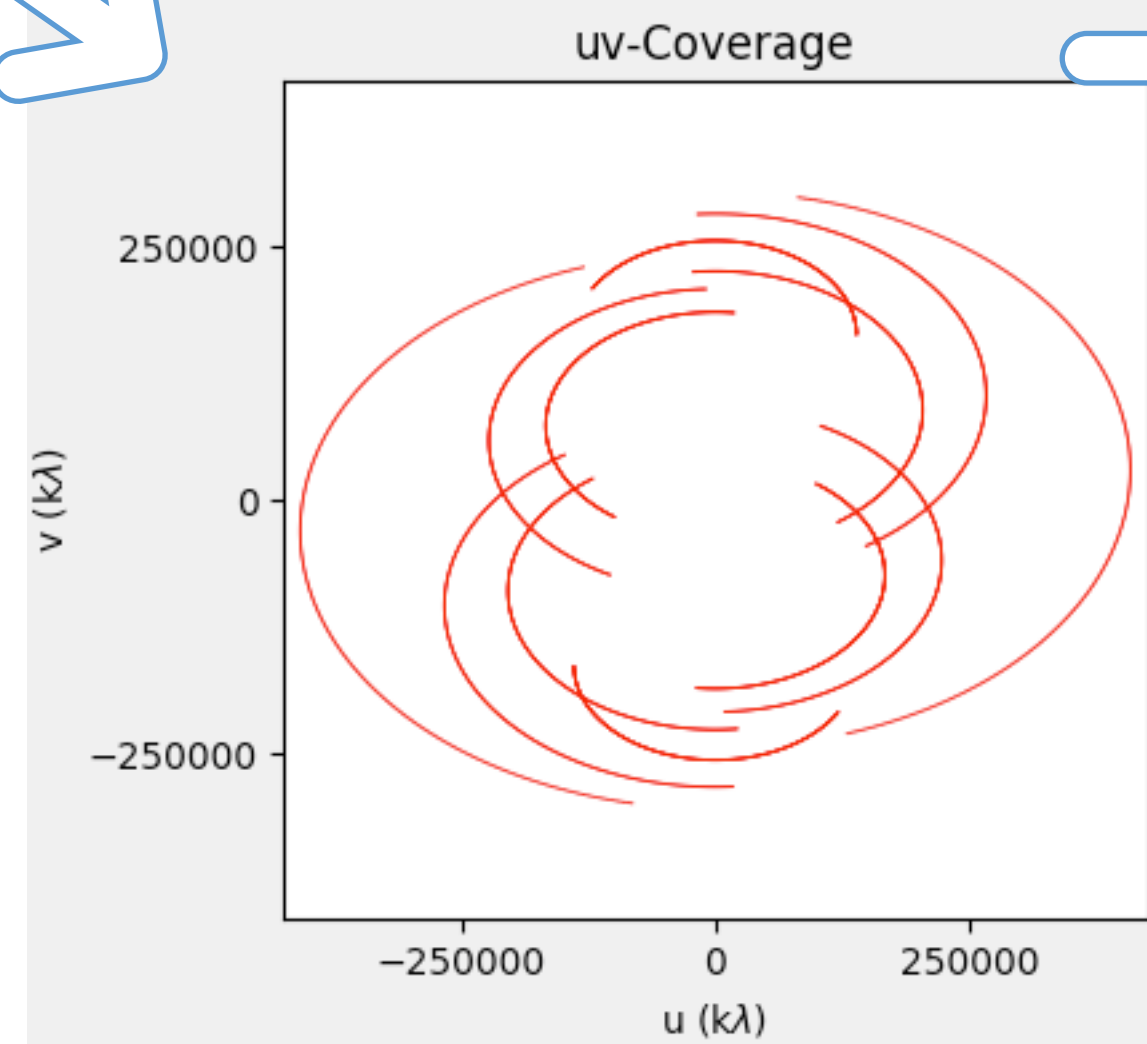
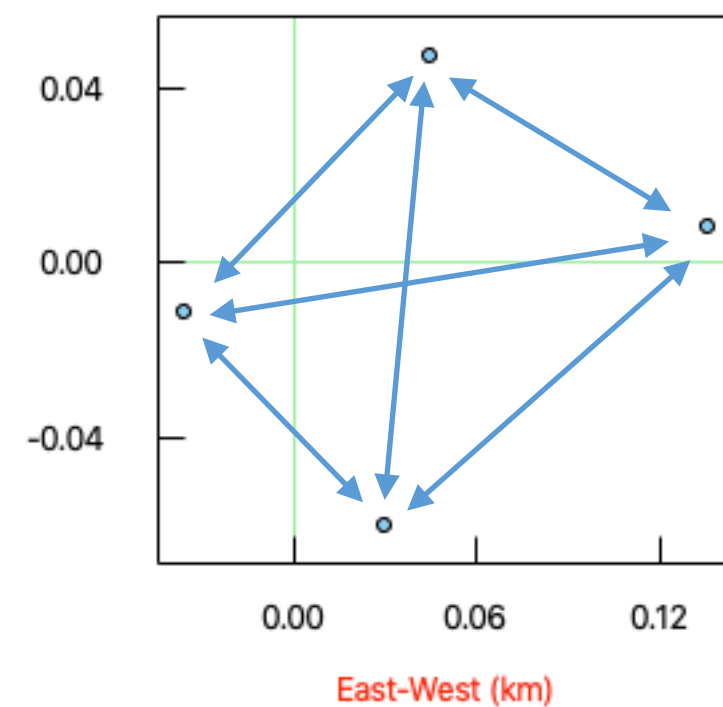


# More than one-dimension: imaging with optical aperture synthesis

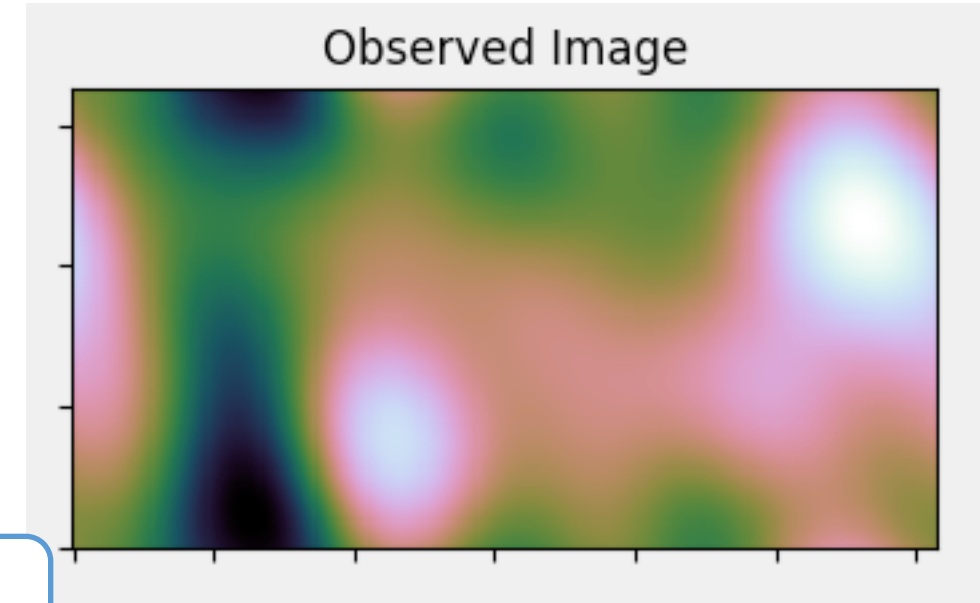
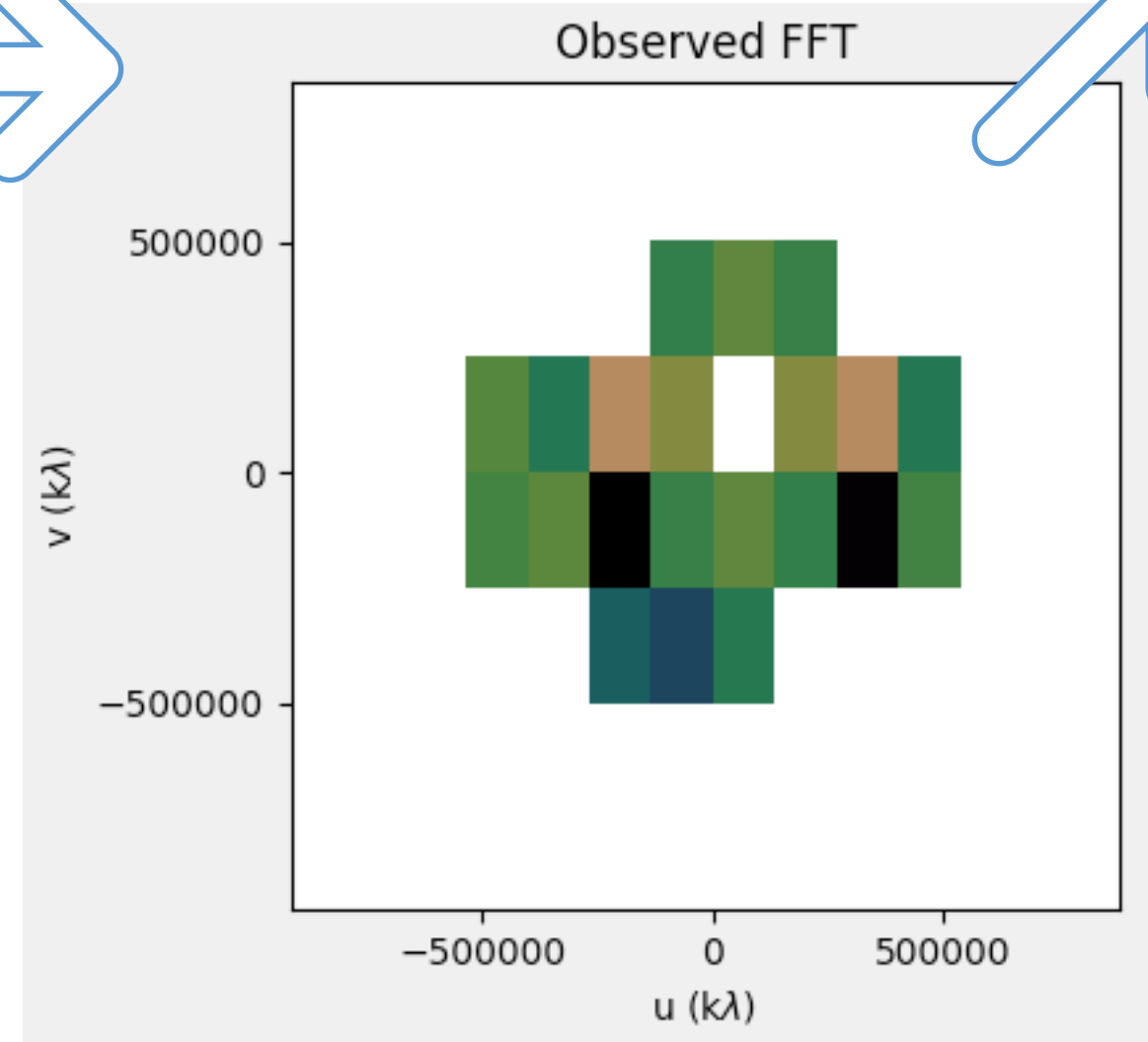


Source tracks through the sky increasing number of available baselines.

Take a few telescopes



Sampling more of the Fourier spatial distribution of the observed target brightness.



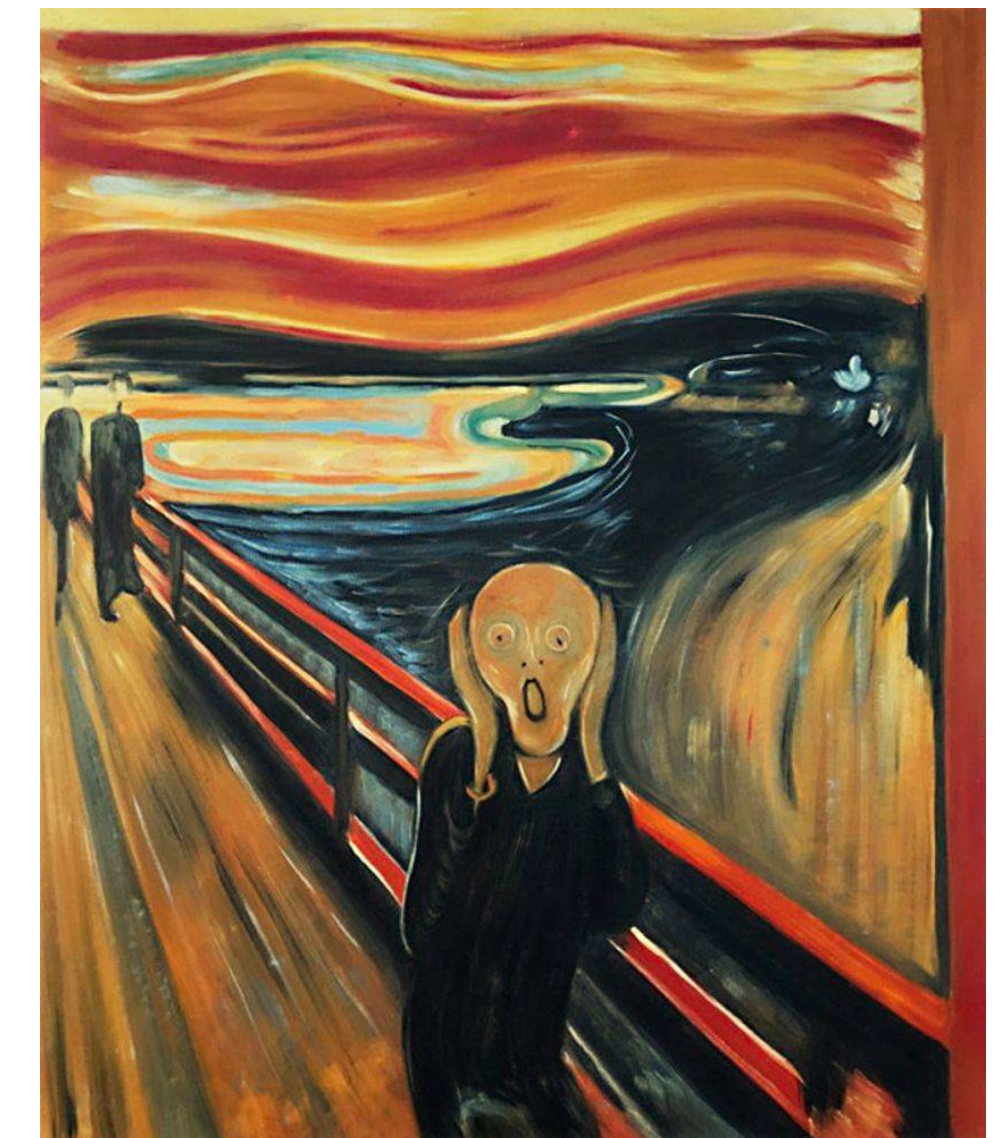
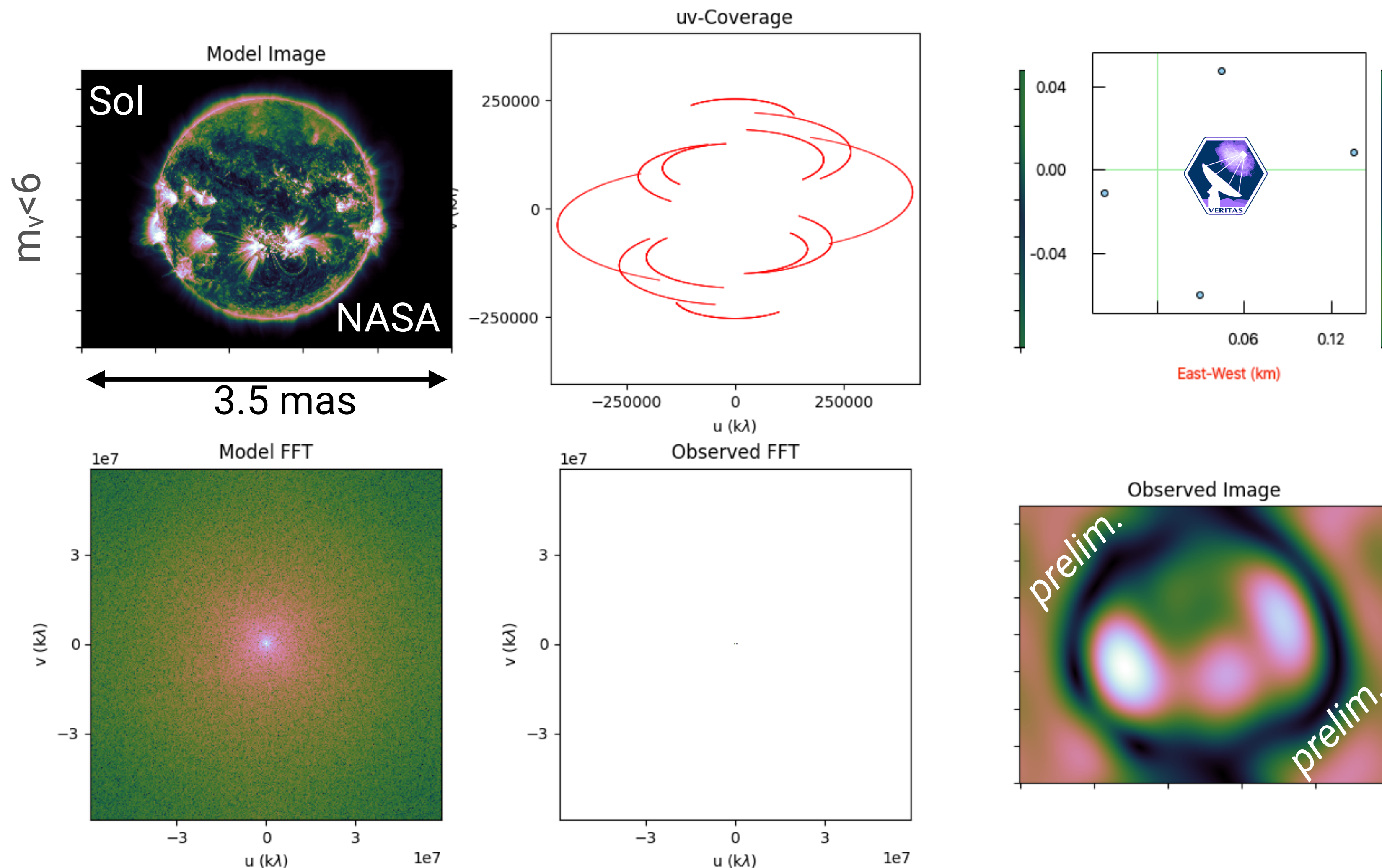
But, it measures the square of the visibility, so phase information is lost. However, there are ways to recover this.

- e.g. Cauchy-Riemann algorithm Nuñez et al. MNRAS (2012).
- e.g. three point intensity correlations Nuñez & Domiciano de Souza MNRAS (2015).



The VERITAS spacing is okay for large structure, but not for fine details

8h observation with VERITAS for a  $<10\text{mas}$  giant “solar-like” star at  $20^\circ$  declination



To do:

- *estimate noise*
- *phase recovery*
- **Get more telescopes**

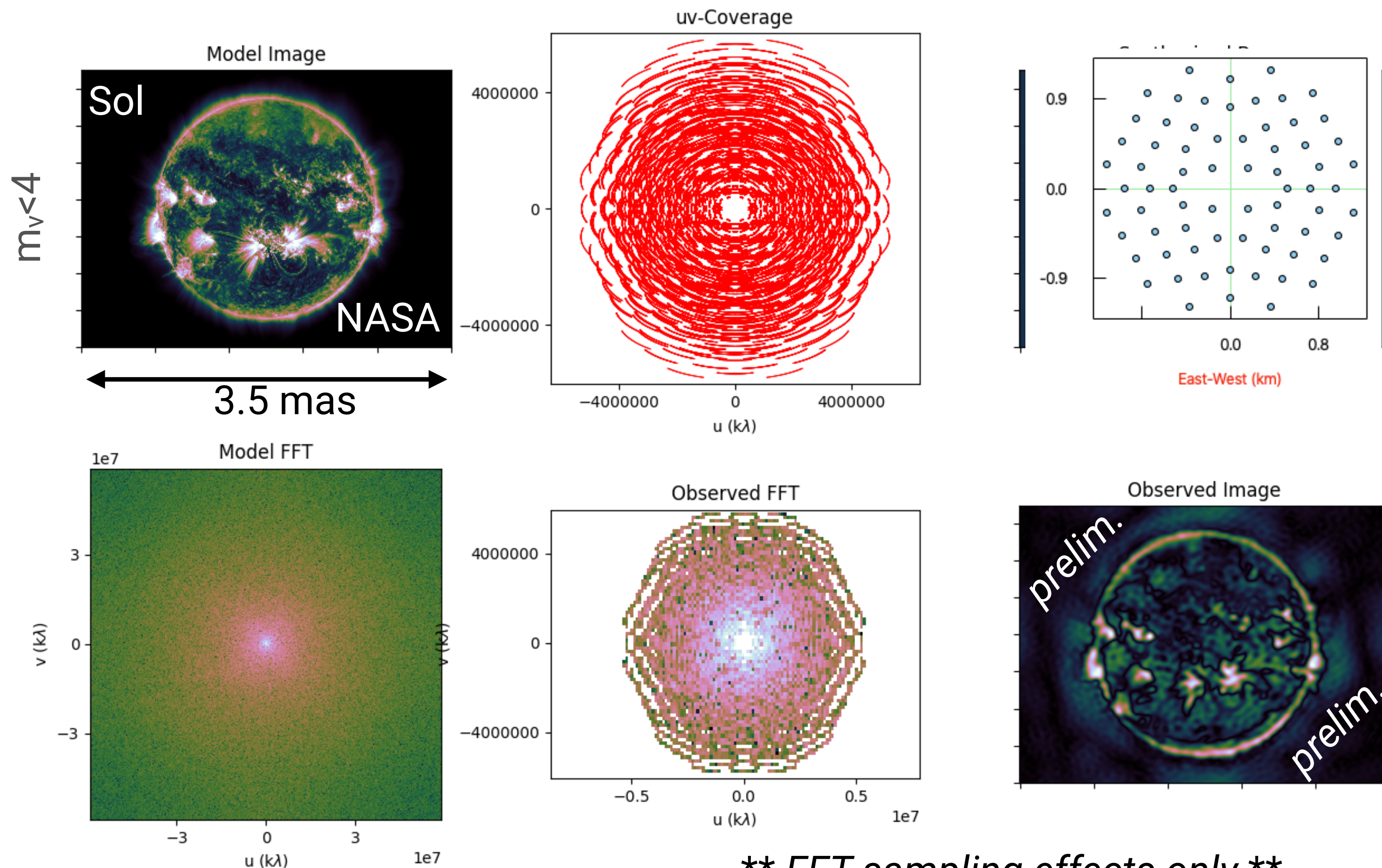
Simulation adapted from the friendlyVRI  
<https://crpurcell.github.io/friendlyVRI/>

**\*\* FFT sampling effects only \*\***



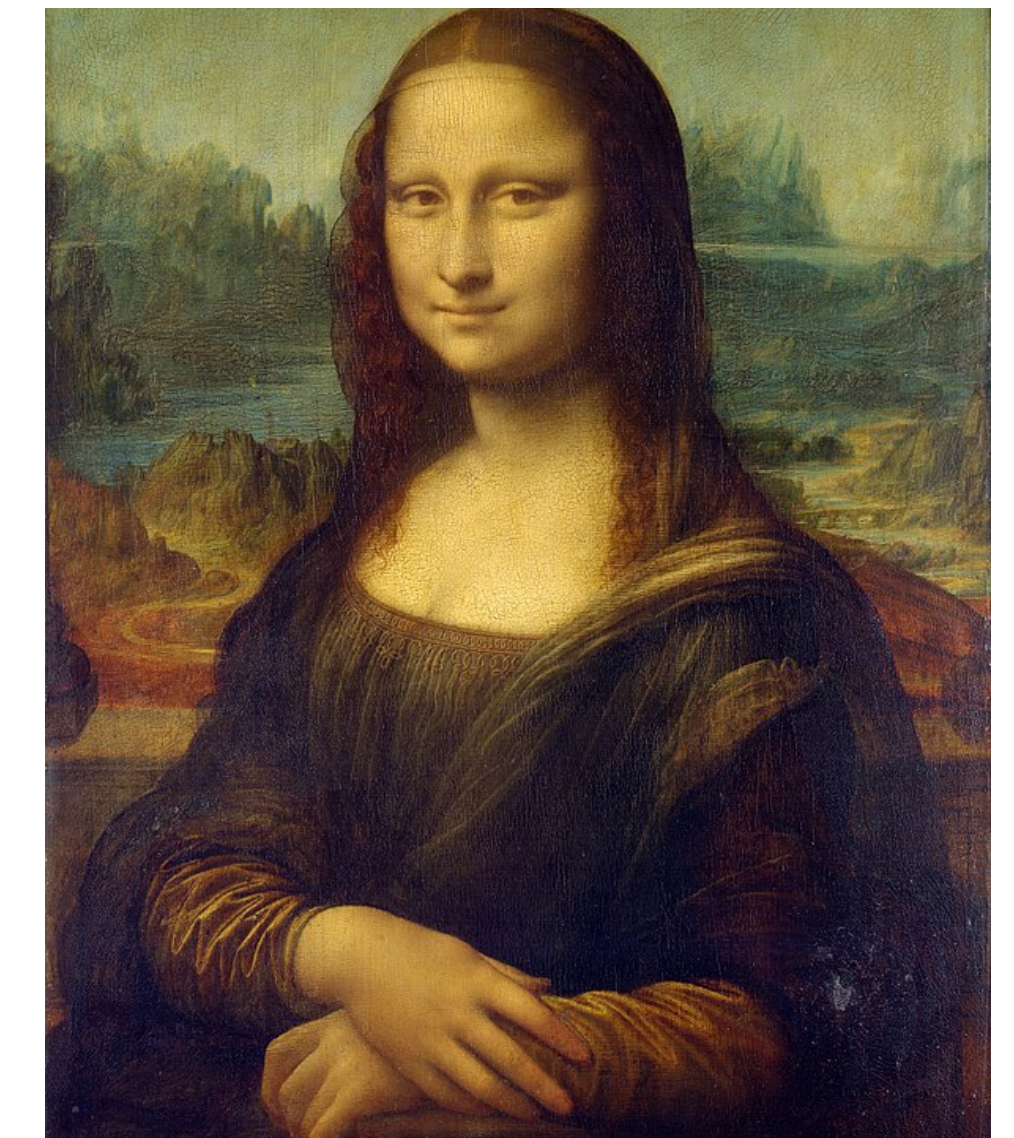
The VERITAS spacing is okay for large structure, but not for fine details

2h observation with CTA-S SSTs for a  $<10\text{mas}$  giant “solar-like” star at  $-20^\circ$  declination



to do:

- estimate noise
- phase recovery methods
  - e.g. Cauchy-Riemann algorithm Nuñez et al. MNRAS (2012).
  - e.g. three point intensity correlations Nuñez & Domiciano de Souza MNRAS (2015).



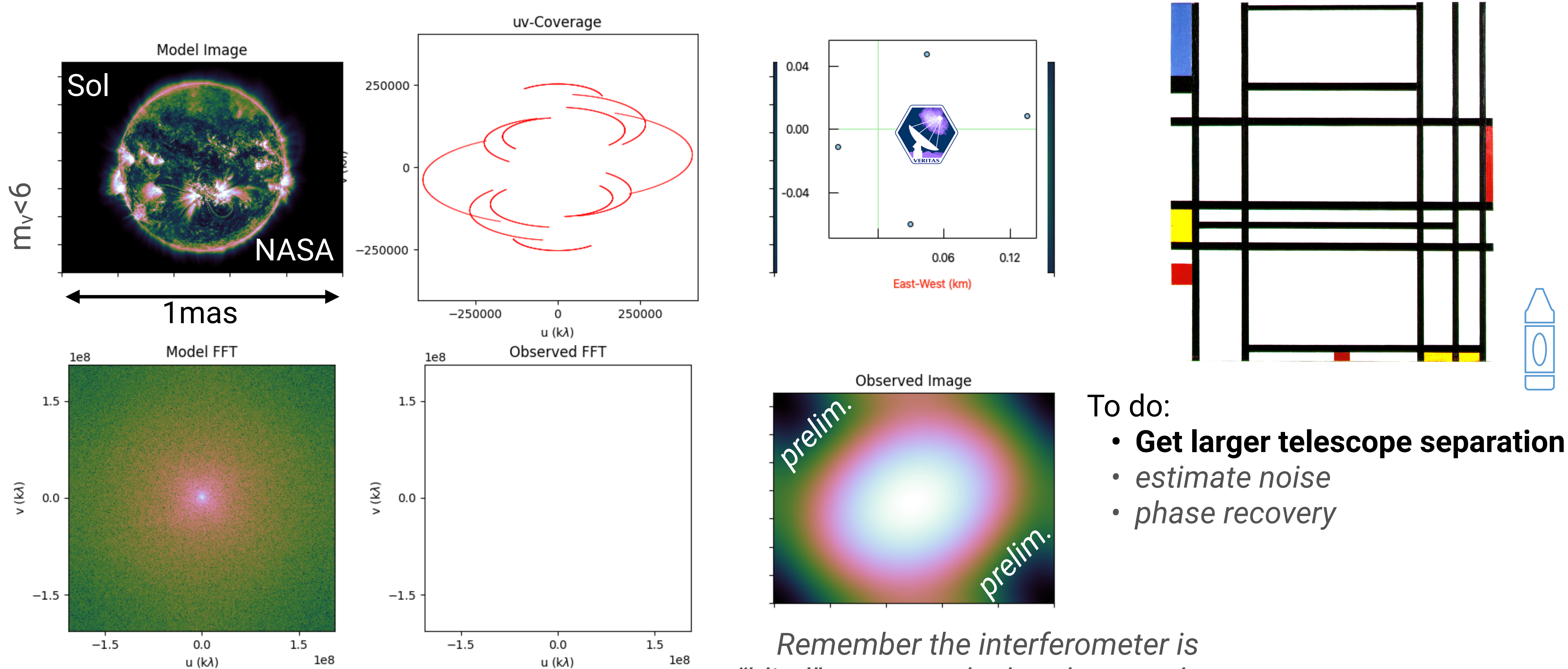
Simulation adapted from the friendlyVRI

<https://crpurcell.github.io/friendlyVRI/>

**\*\* FFT sampling effects only \*\***



8h observation with VERITAS for a  $<1\text{mas}$  “solar-like” star at  $20^\circ$  declination



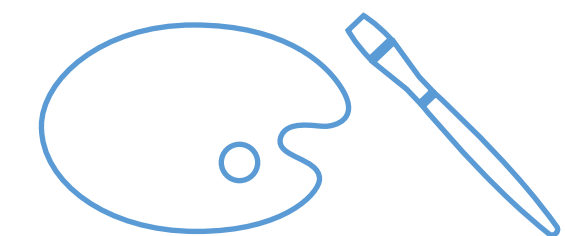
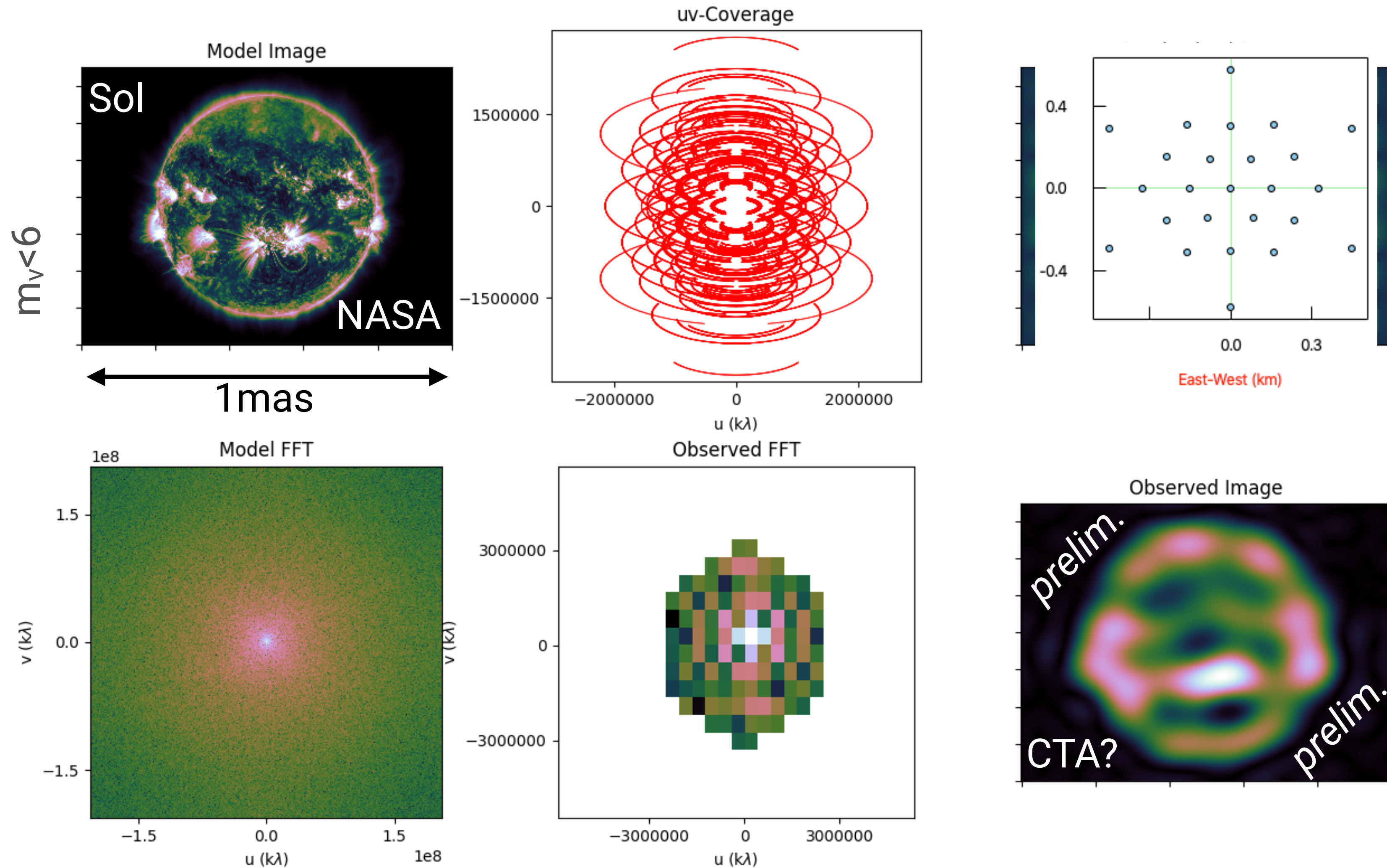
- To do:
- **Get larger telescope separation**
  - *estimate noise*
  - *phase recovery*

*Remember the interferometer is “blind” to any scale that does not have a baseline measurement*

Simulation adapted from the friendlyVRI  
<https://crpurcell.github.io/friendlyVRI/>



# 8h observation with CTA-S MSTs for a <1mas “solar-like” star at -20° declination



To do:

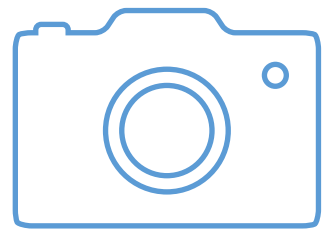
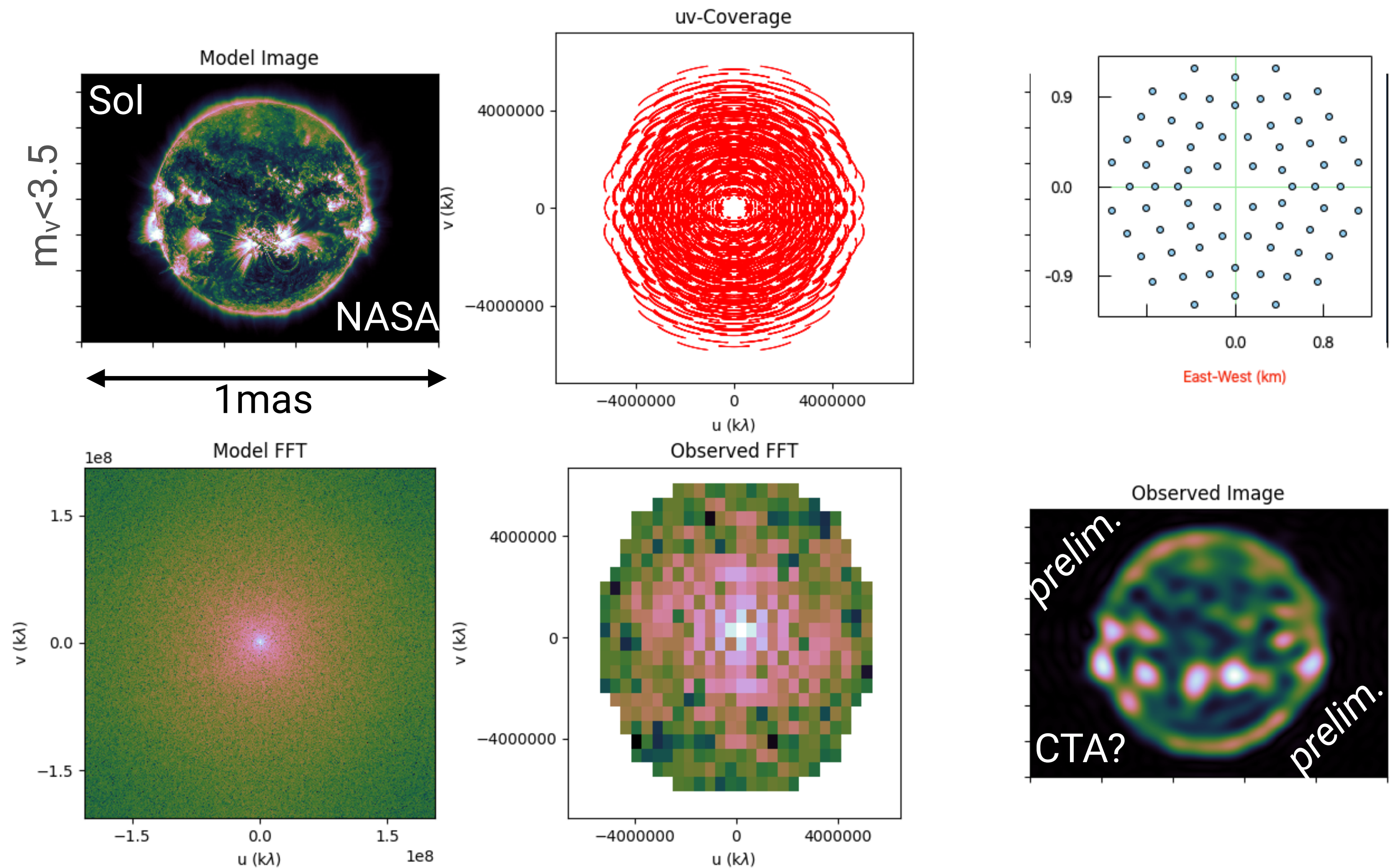
- estimate noise
- phase recovery methods

Simulation adapted from the friendlyVRI  
<https://crpurcell.github.io/friendlyVRI/>

**\*\* FFT sampling effects only \*\***



2h observation with CTA-S SSTs for a  $<1\text{mas}$  “solar-like” star at  $-20^\circ$  declination



To do:

- estimate noise
- phase recovery methods
- **Count the star spots**

Simulation adapted from the friendlyVRI  
<https://crpurcell.github.io/friendlyVRI/>

**\*\* FFT sampling effects only \*\***



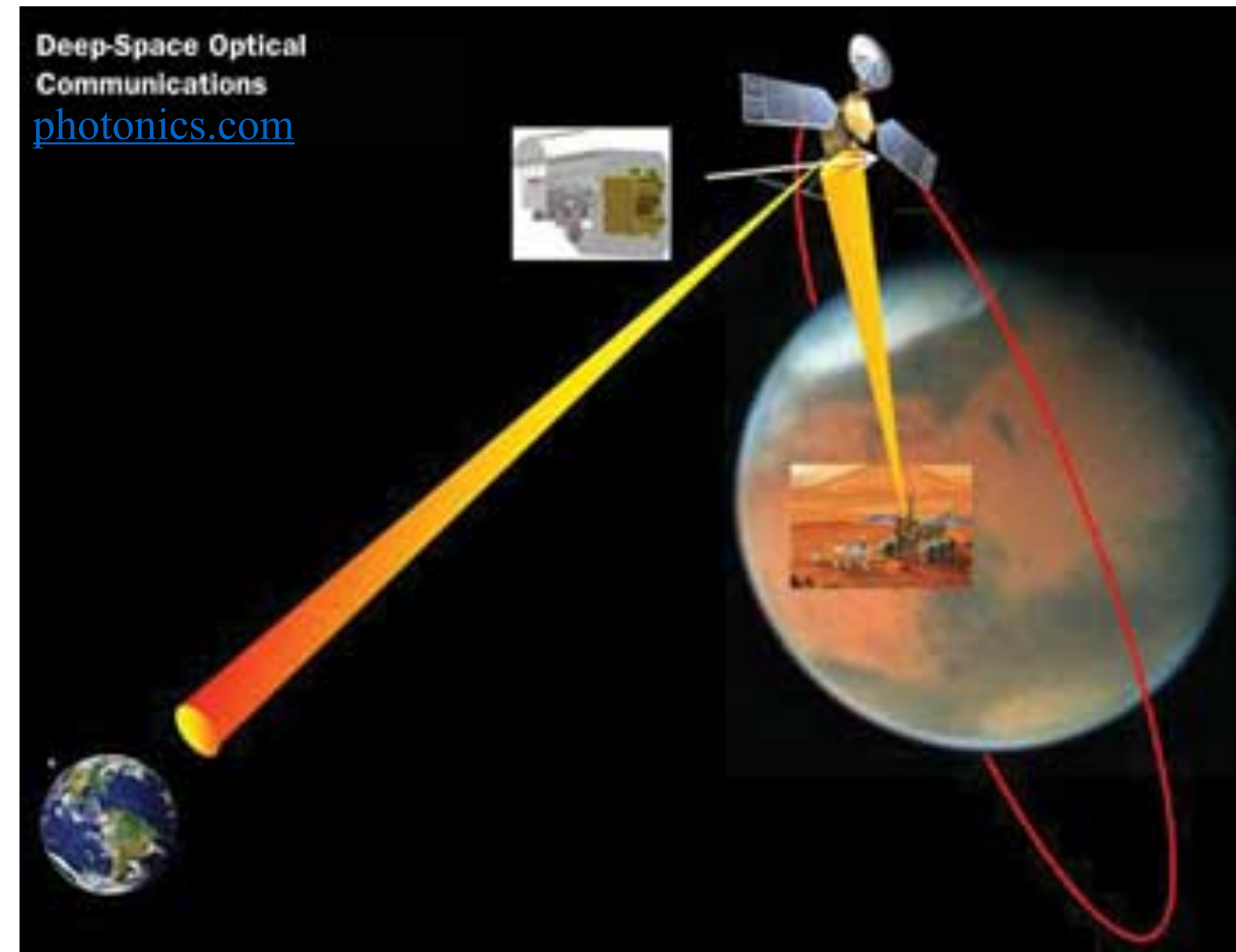
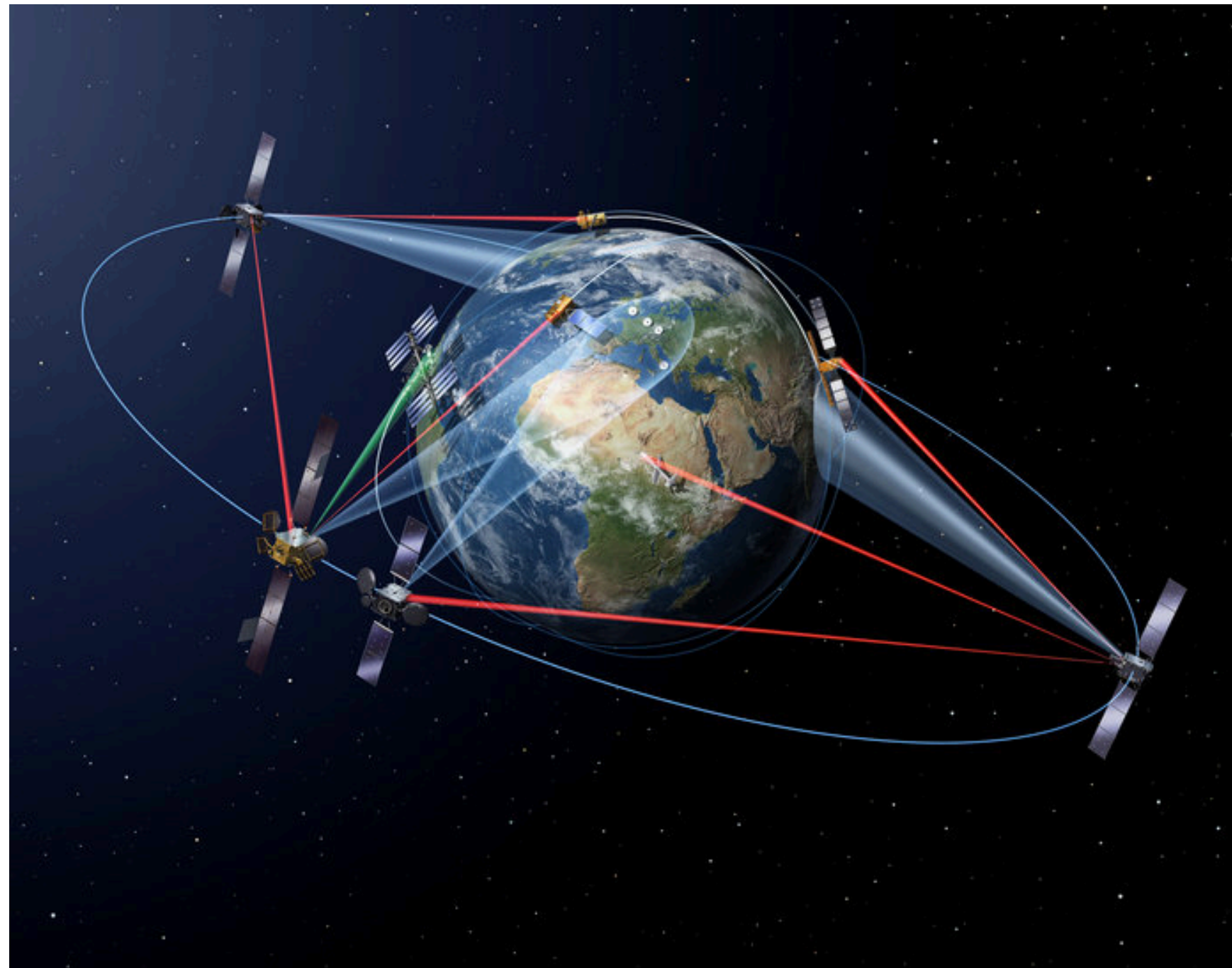
# Anything else?

See talk J. Holder  
GAI11h We. 18:15

- Optical counterparts to FRBs?
- Fast transients?
- Free space optical communications?
- ... ?



# Free Space Optical Communication



aka OSETI



# WHY OPTICAL RATHER THAN RADIO?

Idea first floated by R.N. Schwartz & C.H. Townes

‘Interstellar and Interplanetary Communication by Optical Masers’ *Nature* **190**, 205 (1961).

- **It is easier to deal with noise**

- radio waves contend with interference from radio antennas, radio stations, the receiver itself adds noise (thus can require cooling), ...
- for optical the only significant source of terrestrial interference is lightning & Cherenkov radiation

- **Pulsed lasers can easily outshine the host star**

- no known natural sources would have photons within a few ns of each other
  - ➔ could easily be 1000x brighter in the receiving telescope

- **Much easier to form a narrow beam of light**

- a radio transmitter 100 ly distant & projecting omni-directionally would require 5800 trillion watts to be detectable ~ 7000x the electricity-generating capacity of the USA!
- width of beam  $\propto$  wavelength of beam / diameter of the antenna used
  - ➔  $\lambda_{\text{optical}} \ll \lambda_{\text{radio}}$

M. Ross *IEEE Spectrum* **7**, 32 (2006).

**Just need a suitable optical light bucket as a receiver...**



# How do Cherenkov telescopes compare?

## The Additional IACT Advantages

The large field of view of the cameras helps to

- remove background signals
- monitor multiple stars simultaneously

**3.5° camera can monitor ~45-150 stars ( $V < 12$ ) in a single pointing**

	Detector	$\lambda$ [nm]	Sensitivity [ph m <sup>-2</sup> ]
<b>VERITAS<sup>1</sup>, 12m</b>	3pmt / <5ns	300-600	<b>1</b>
STACEE <sup>2</sup> , heliostats	pmt ~12ns	300-600	10
Planetary Society <sup>3</sup> , 1.8m	pmt / ~5ns	300-800	60
Harvard Oak Ridge <sup>4</sup> , 1.5m	2 apd / 5ns	450-650	100
Lick Obs <sup>5</sup> , 1m	2 apd / <1ns	950-1650	40
Princeton <sup>6</sup> , 0.9m	2 apd / 5ns	450-650	80
Leuschner Obs <sup>7</sup> , 0.8m	3 pmt / 5ns	300-700	41
METI / Boquete Obs <sup>8</sup> , 0.5m	1pmt / 25ns	350-600	67

<sup>1</sup> Abeysekara et al. (2016)

<sup>2</sup> Hanna et al. (2009)

<sup>3</sup> Mead (2013)

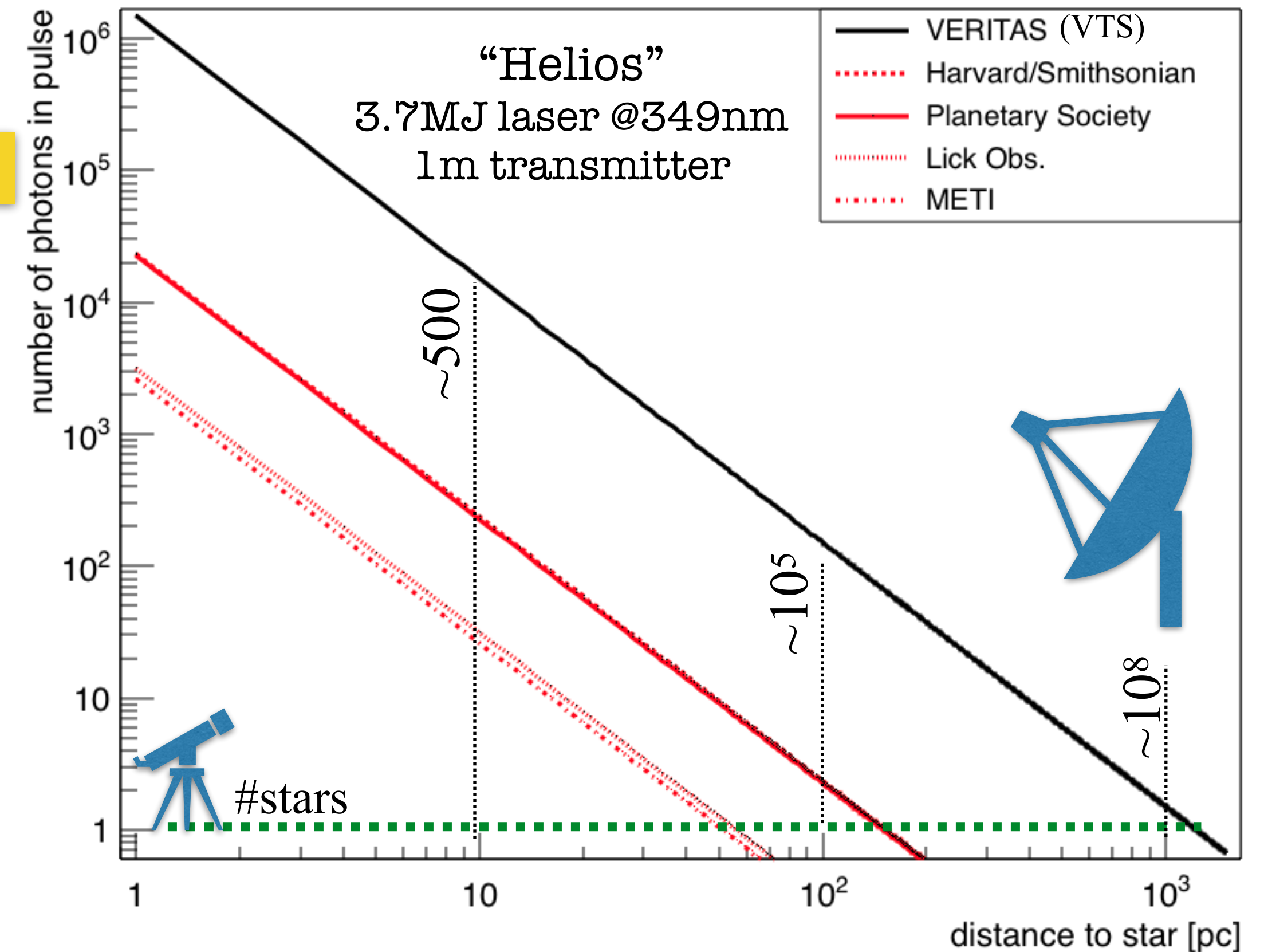
<sup>4</sup> Howard et al. (2004)

<sup>5</sup> Maire et al. (2014)

<sup>6</sup> Howard et al. (2004)

<sup>7</sup> Korpela et al. (2011)

<sup>8</sup> Schuetz et al. (2016)





# Summary

- IACTs are (not)surprisingly good optical telescopes when it comes to photometry
  - large mirror surface means low scintillation and shot noise
  - low noise makes for good high time resolution photometry
  - angular resolutions *equivalent to VLBI* are possible
- Sub-mas angular scale resolution with IACTs has been achieved
  - through measurement of diffraction pattern in asteroid occultations of stars
  - and as an offline optical intensity interferometer
    - can be scaled to arbitrary number of telescopes
    - simple to add new telescopes with commercial fibre optics



Backup



Recap

Enhanced Current Monitor (ECM)  
**DATAQ INSTRUMENTS**  
**DI-710-ELS**

16 channel ethernet data logger and data acquisition system

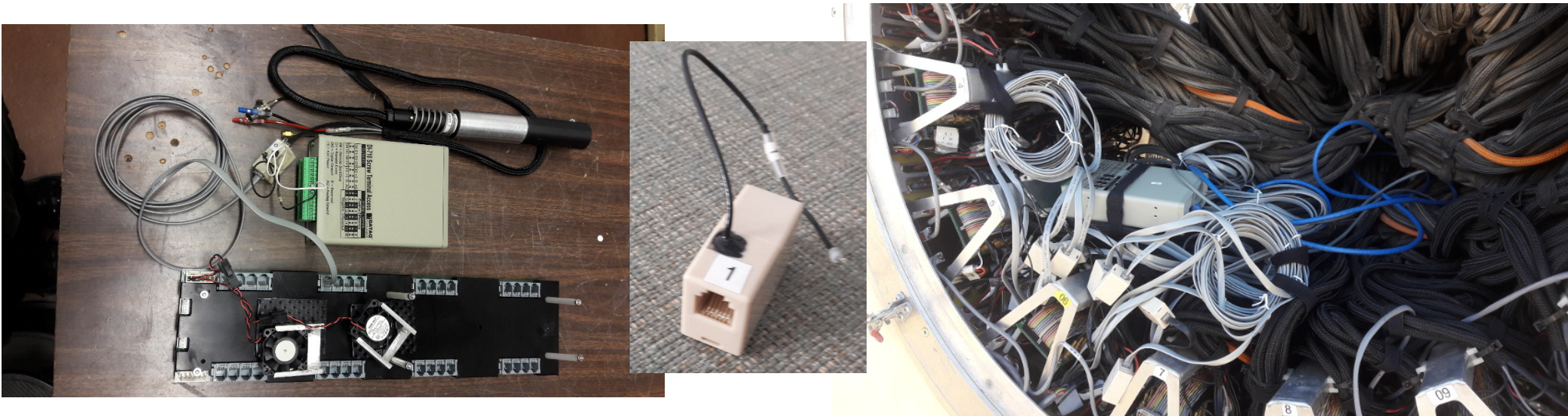
- **DC powered** — using same camera supply as flashers
- **Ethernet readout** or SD card
- **16 single ended**, 8 differential analogue inputs
- 14-bit ADC
  - $\pm 0.012\%$  of full scale measurement range
- Measurement range of  $\pm 10\text{mV}$  to  $\pm 10\text{V}$  (in 4 gain stages)
- Record up to 4,800Hz when connected to PC
  - For asteroid/FRB sampling at 2,400 Hz
  - For transiting exoplanet measurements sampling at 10Hz

16 channel obs =  $4,800/16 = 300 \text{ Hz/channel}$   
2 channel obs =  $4,800/2 = 2,400 \text{ Hz/channel}$



gain	range	resolution	limit
1	$\pm 10\text{V}$	$\pm 1.22\text{mV}$	$\sim 13\text{th mag?}$
2	$\pm 1\text{V}$	$\pm 122\mu\text{V}$	$\sim 11\text{th mag}$
3	$\pm 100\text{mV}$	$\pm 12.2\mu\text{V}$	
4	$\pm 10\text{mV}$	$\pm 1.22\mu\text{V}$	

The advantage is the  
VERITAS cabling scheme  
made this plug & play





$$(S/N)_{\text{RMS}} = A \cdot \alpha \cdot n \cdot |\gamma_{12}(d)|^2 \cdot \sqrt{\Delta f \cdot T/2}$$

mirror area      photon detection efficiency      correlation      electronics bandwidth      observation time

photons/m<sup>2</sup>/s/Hz

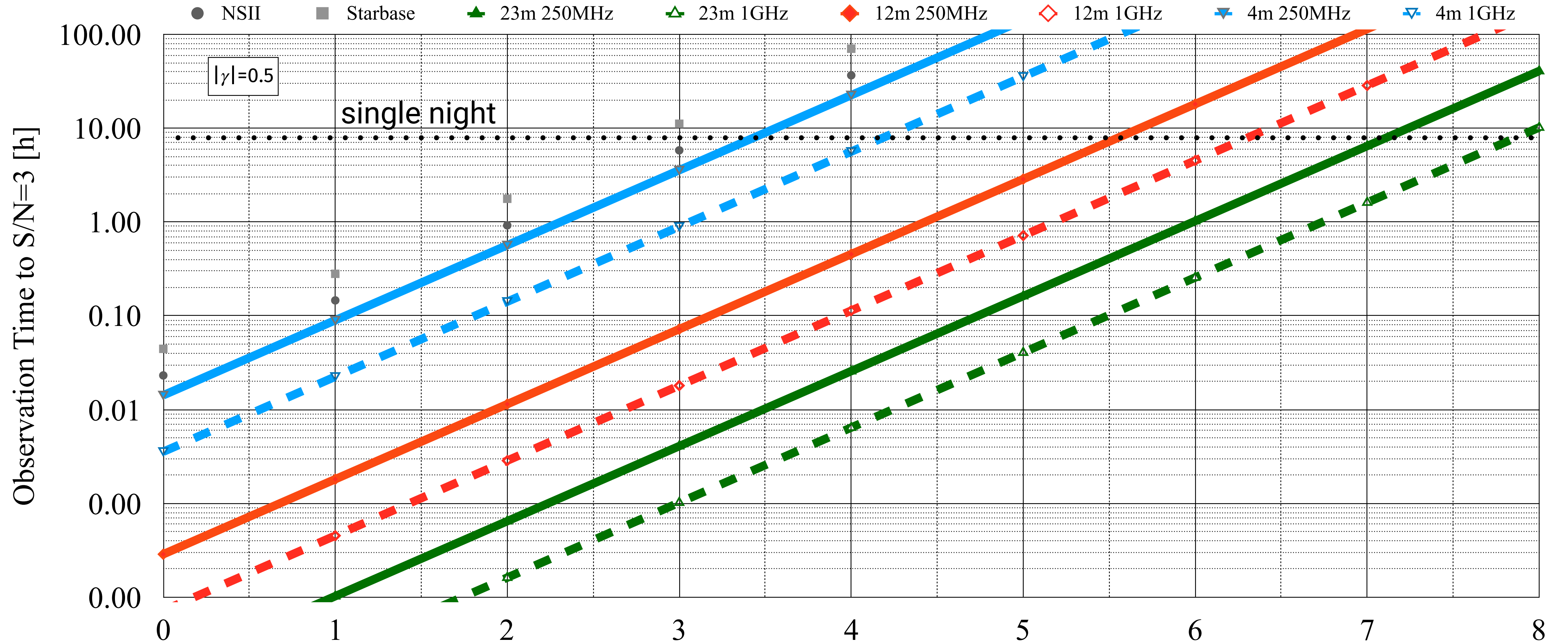
α = 0.35  
cf NSII

Dish [m]	250 MHz	1 GHz
4	~0.5	~1
12	~5	~10
23	~20	~40

LeBohec & Holder *ApJ* **649**, 399 (2006)  
 $|\gamma_{12}|^2=0.5$  at 5σ to 14% accuracy in 5h for  $m_\nu=6.7$   
(3% for  $m_\nu=5$ )



# Sensitivity



magnitude



Table 2: Candidate sources from The Bright Star Catalogue: 35 stars brighter than  $m_V=2$  or hotter than  $T_{\text{eff}}=25,000$  K. Those whose angular diameters were measured already with the NSII [28] are marked with an asterisk (\*).

Name	HR	$\theta$ [mas]	$V_{\text{rot}}$ [km s <sup>-1</sup> ]	Spectral Type	$T_{\text{eff}}$ [K]	$m_V$	Notes
Achernar, $\alpha$ Eri	472	1.9	250	B3 Ve	15 000	0.46	High $V_{\text{rot}}$ , *
Rigel, $\beta$ Ori	1713	2.4	30	B8 Iab	9 800	0.12	Emission-line star, *
$\lambda$ Lep	1756		70	B0.5 IV	28 000	4.29	
Bellatrix, $\gamma$ Ori	1790	0.7	60	B2 III	21 300	1.64	Variable, *
Elnath, $\beta$ Tau							
= $\gamma$ Aur [sic]	1791	1.5	70	B7 III	13 500	1.65	Binary system
$\nu$ Ori	1855		20	B0 V	28 000	4.62	Variable
HD 36960	1887		40	B0.5 V	26 000	4.78	Binary system
Alnilam, $\epsilon$ Ori	1903	0.7	90	B0 Iab	18 000	1.7	Emission-line star, *
$\mu$ Col	1996		150	O9.5 V	33 000	5.17	
$\beta$ CMa	2294	0.5	35	B1 II-III	23 000	1.98	$\beta$ Cep-type variable, *
Alhena, $\gamma$ Gem	2421	1.4	30	A0 IV	9 100	1.93	*
S Mon	2456		60	O7 Ve	26 000	4.66	Pre-main-sequence
Sirius, $\alpha$ CMa	2491	5.9	10	A1 V	9 100	-1.46	*
EZ CMa	2583			WN4	33 000	6.91	Highly variable W-R star
Adara, $\epsilon$ CMa	2618	0.8	40	B2 Iab	20 000	1.5	Binary, *
Naos, $\zeta$ Pup	3165	0.4	210	O5 Ia	28 000	2.25	BY Dra variable, *
$\gamma^2$ Vel	3207	0.4		WC8	50 000	1.78	Wolf-Rayet binary, *
				O7.5	35 000		
$\beta$ Car	3685	1.5	130	A2 IV	9 100	1.68	*
Regulus, $\alpha$ Leo	3982	1.4	330	B7 V	12 000	1.35	High $V_{\text{rot}}$ , *
$\eta$ Car	4210	5.0		peculiar	36 000	6.21	Extreme object, variable
Acrux, $\alpha^1$ Cru	4730		120	B0.5 IV	24 000	1.33	Close binary to $\alpha^2$ Cru
Acrux, $\alpha^2$ Cru	4731		200	B1 V	28 000	1.73	Close binary to $\alpha^1$ Cru
$\beta$ Cru	4853	0.7	40	B0.5 IV	23 000	1.25	$\beta$ Cep-type variable, *
$\epsilon$ UMa	4905		40	A0 p	9 500	1.77	$\alpha^2$ CVn-type variable
Spica, $\alpha$ Vir	5056	0.9	160	B1 III-IV	23 000	0.98	$\beta$ Cep-type variable
Alkaid, $\eta$ UMa	5191	< 2	200	B3 V	18 000	1.86	Variable
$\beta$ Cen	5267	0.9	140	B1 III	23 000	0.61	$\beta$ Cep-type variable
$\tau$ Sco	6165		25	B0.2 V	26 000	2.82	
$\lambda$ Sco	6527		160	B2 IV+	21 000	1.63	$\beta$ Cep-type variable
Kaus Australis, $\epsilon$ Sgr	6879	1.4	140	B9.5 III	9 800	1.85	Binary, *
Vega, $\alpha$ Lyr	7001	3.2	15	A0 V	9 100	0.03	*
Peacock, $\alpha$ Pav	7790	0.8	40	B2 IV	19 000	1.94	Spectroscopic binary, *
Deneb, $\alpha$ Cyg	7924	2.2	20	A2 Iae	9 300	1.25	Variable
$\alpha$ Gru	8425	1.0	230	B6 V	13 000	1.74	*
Fomalhaut, $\alpha$ PsA	8728	2	100	A4 V	9 300	1.16	With imaged exoplanet, *

Dravins et al *NewAR* **56**, 143 (2012).  
Dravins et al *APh* **43**, 331 (2013).

Table 5. Main-sequence stars, according to their spectral type (top) and apparent magnitude (bottom), observable from Kitt Peak.

Spectral type	Number of fully resolved stars	Overlap with CHARA	Number of partially resolved stars
M	230	230	0
K	729	726	0
G	424	282	0
F	431	118	52
A	364	77	348
B	205	44	328
O	4	0	6
Total	2387	1450	734
Apparent magnitude	Number of fully resolved stars	Number of partially resolved stars	Approximate integration time <sup>a</sup>
$\leq 1$	7	0	$\ll 1$ h
1 to 2	18	0	$\ll 1$ h
2 to 3	76	0	$\ll 1$ h
3 to 4	199	5	0.2 h
4 to 5	667	52	1.24 h
5 to 6	1420	677	8 h
Total	2387	734	

Note. <sup>a</sup>In order to obtain angular size measurement with a precision of  $\sim 10$  per cent.

SPIIFy  
Pilyavsky et al. *MNRAS* **467**, 3048 (2017)

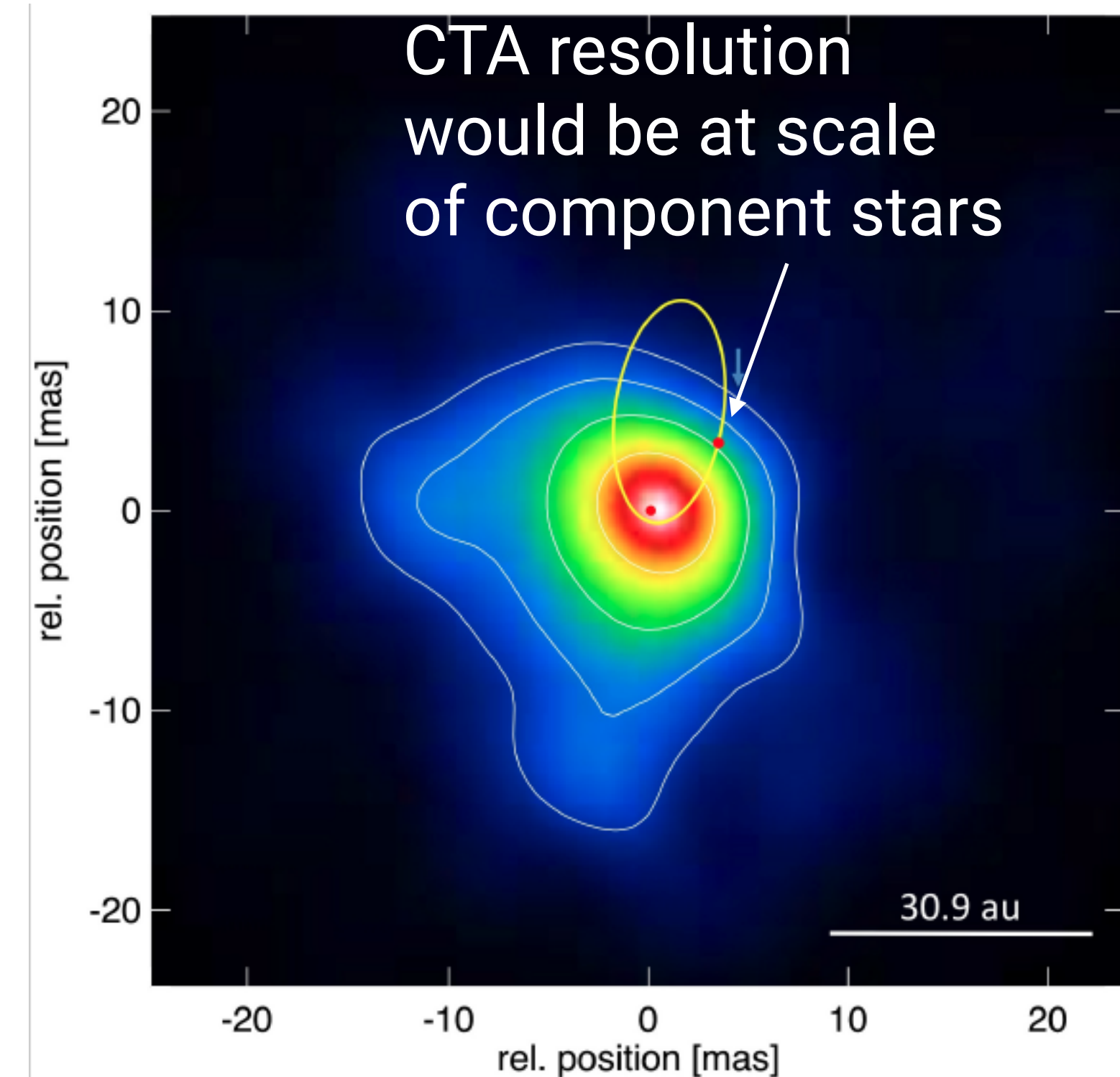


Remember these are never before achieved angular resolutions in the optical – we know that there are interesting things happening at these angular scales, but we can only predict some of what that might be...

$\eta$  Carinae:  
massive star, colliding wind binary,  
core collapse supernova / GRB  
progenitor

*NB, If signal/noise is independent of spectral bandpass. Same resolution can be achieved in spectral lines not just continuum. Different wavelengths probe different optical depths*

*-> 3D imaging?*



Weigelt et al. 'VLT-AMBER velocity-resolved aperture synthesis imaging of  $\eta$  Carinae... Studies of the primary star wind and inner most wind-wind collision zone.'

A&A **594**, 106 (2016).



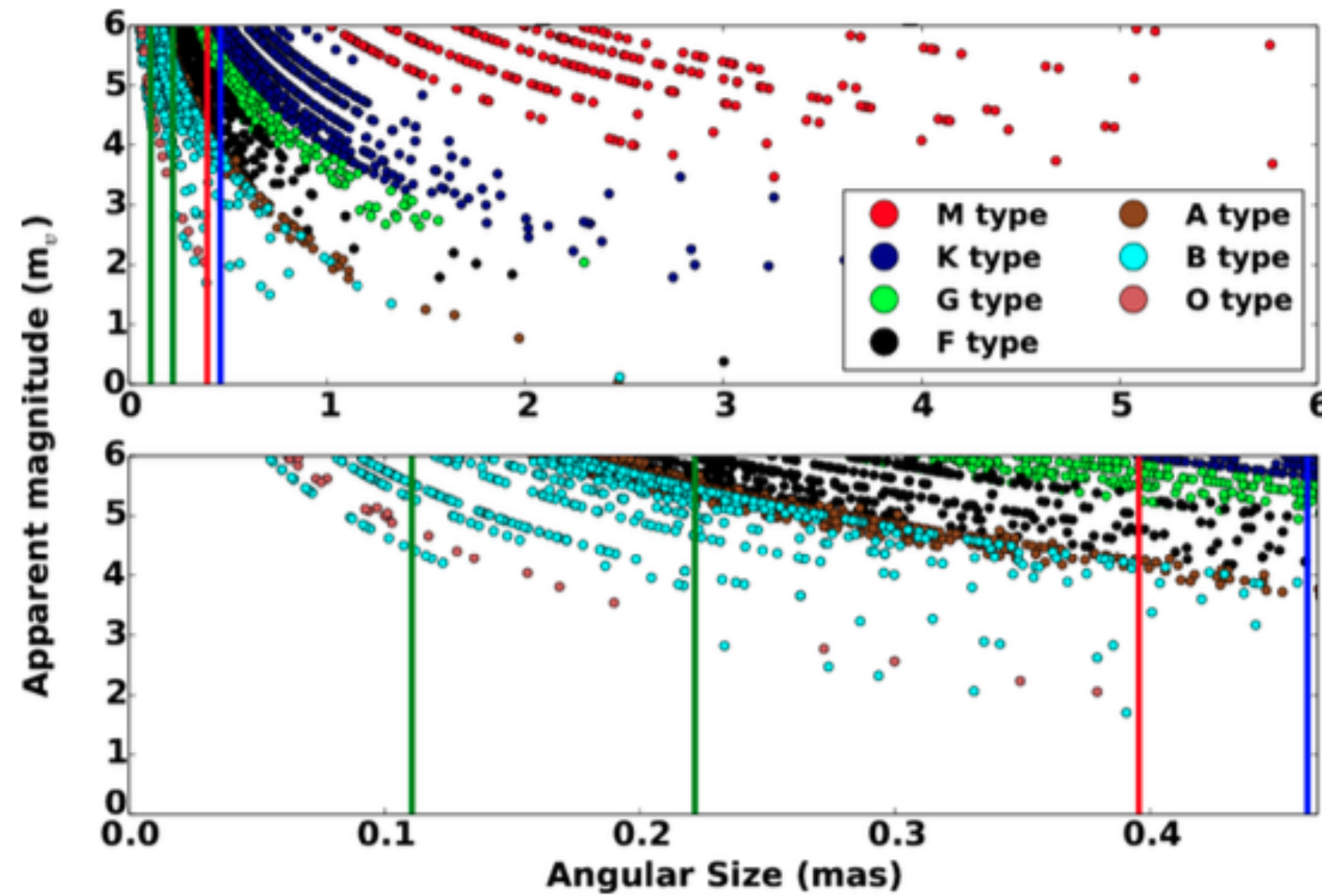
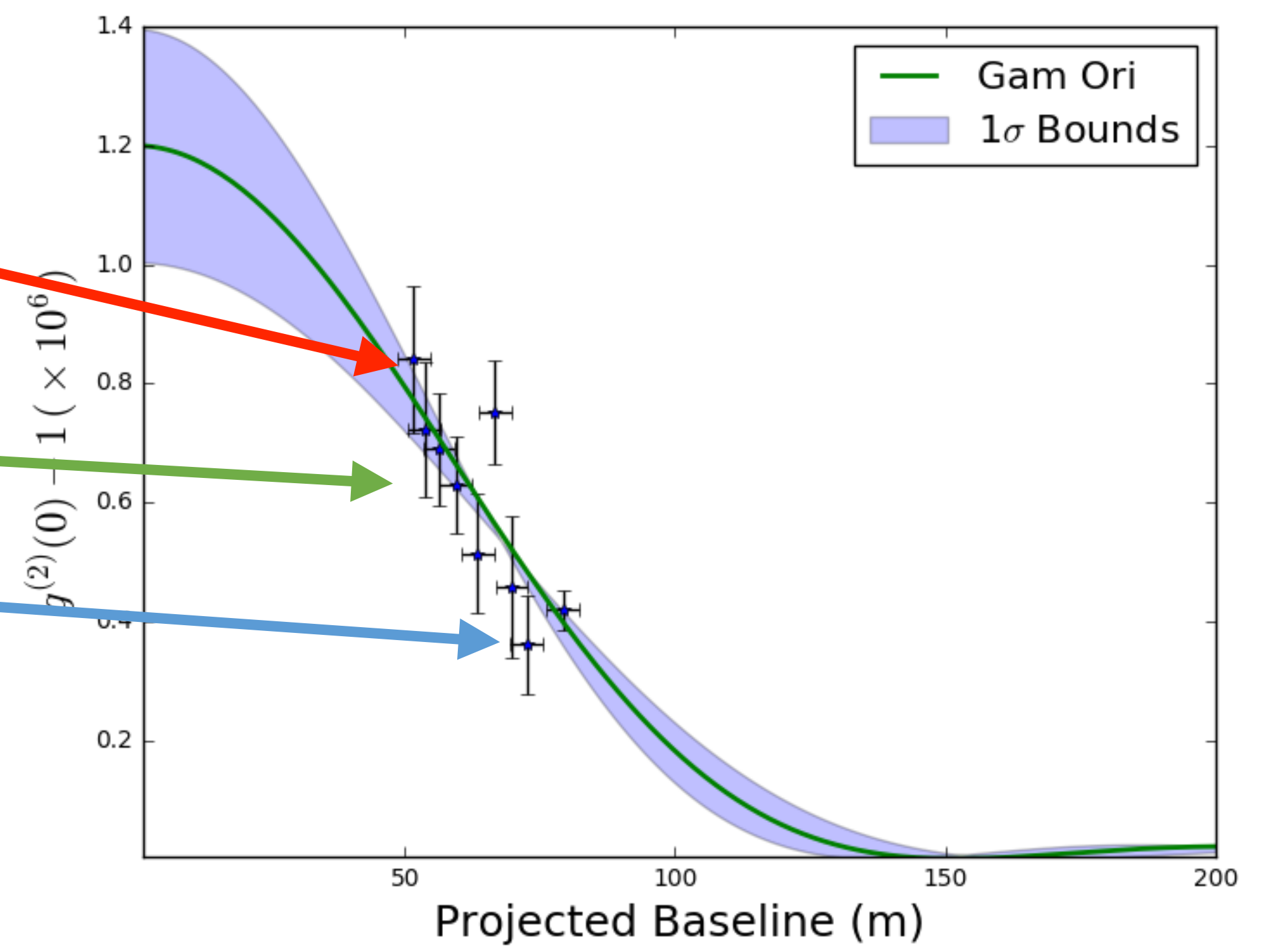
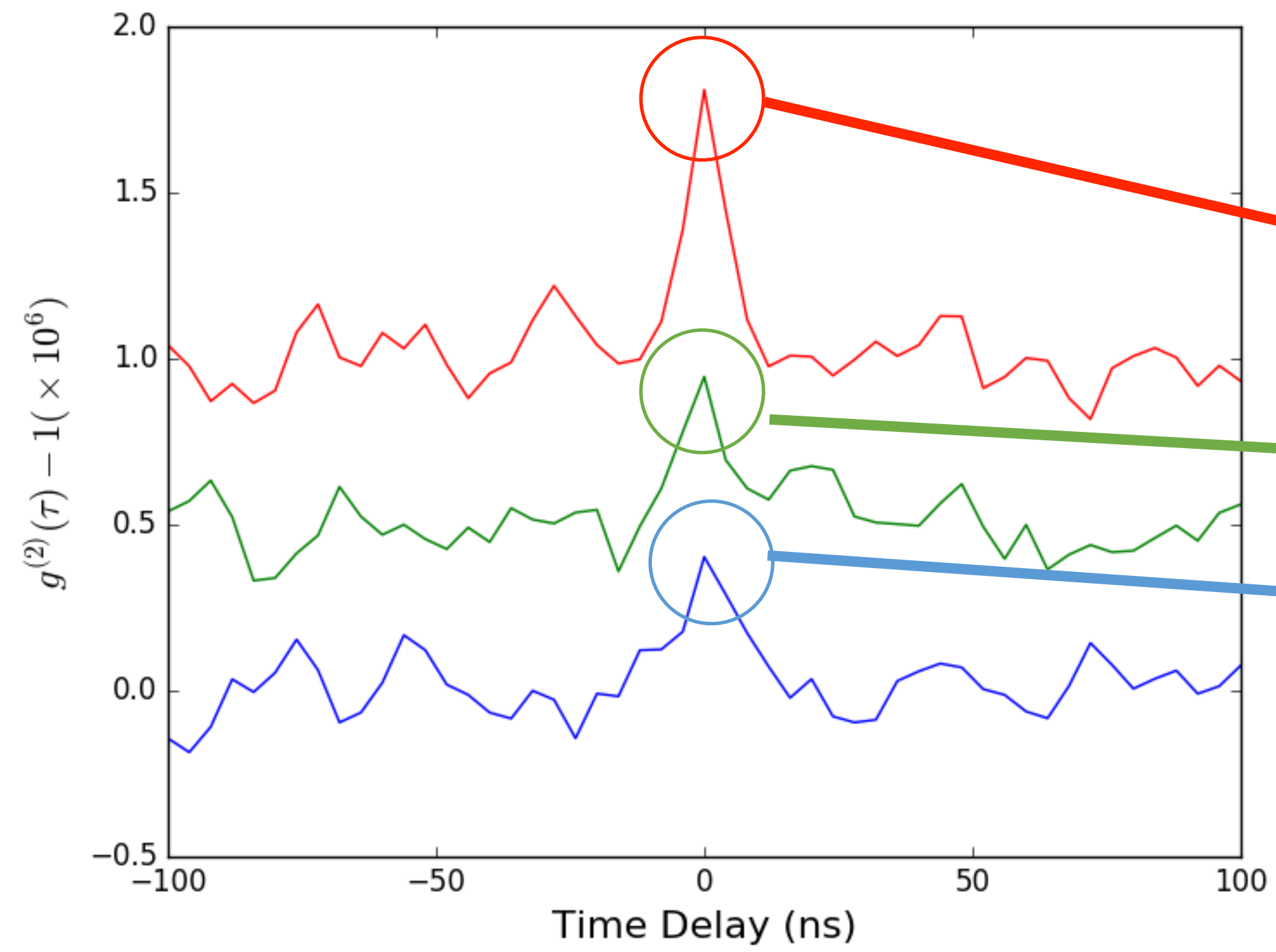


**Figure 6.** Top: stellar magnitudes from the Bright Star Catalogue plotted as a function of their approximate angular size. The colours correspond to the spectral type, given in the legend. Bottom: identical plot, with a narrower range in angular size, showing the bounds where observations from Kitt Peak can fully resolve the star ( $\sim 0.21$  milliarcsec) and bounds where stars will be partially resolved ( $\sim 0.11$  milliarcsec).

SPIIFy

Pilyavsky et al. *MNRAS* **467**, 3048 (2017)







# The Additional IACT Advantages

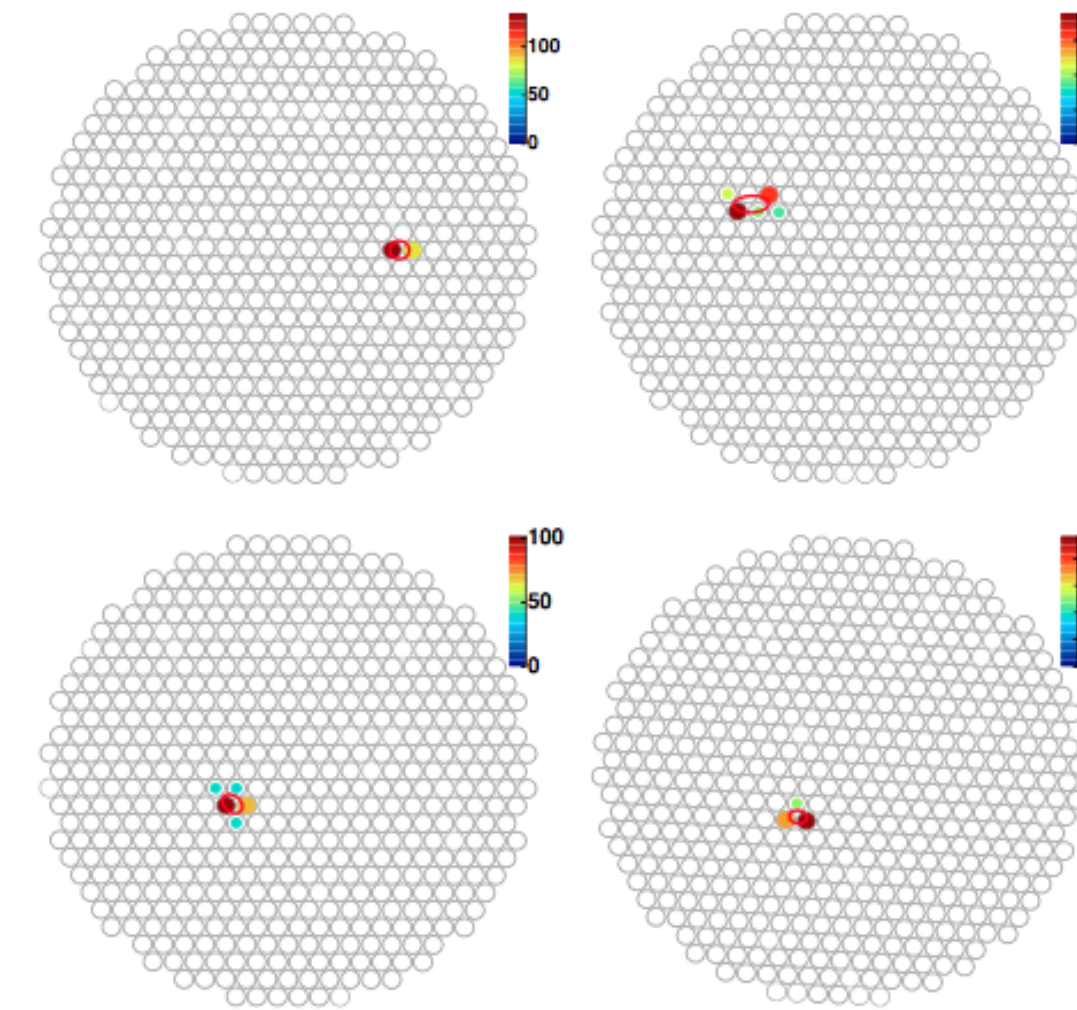
The large field of view of the cameras helps to

- remove background signals
- monitor multiple stars simultaneously

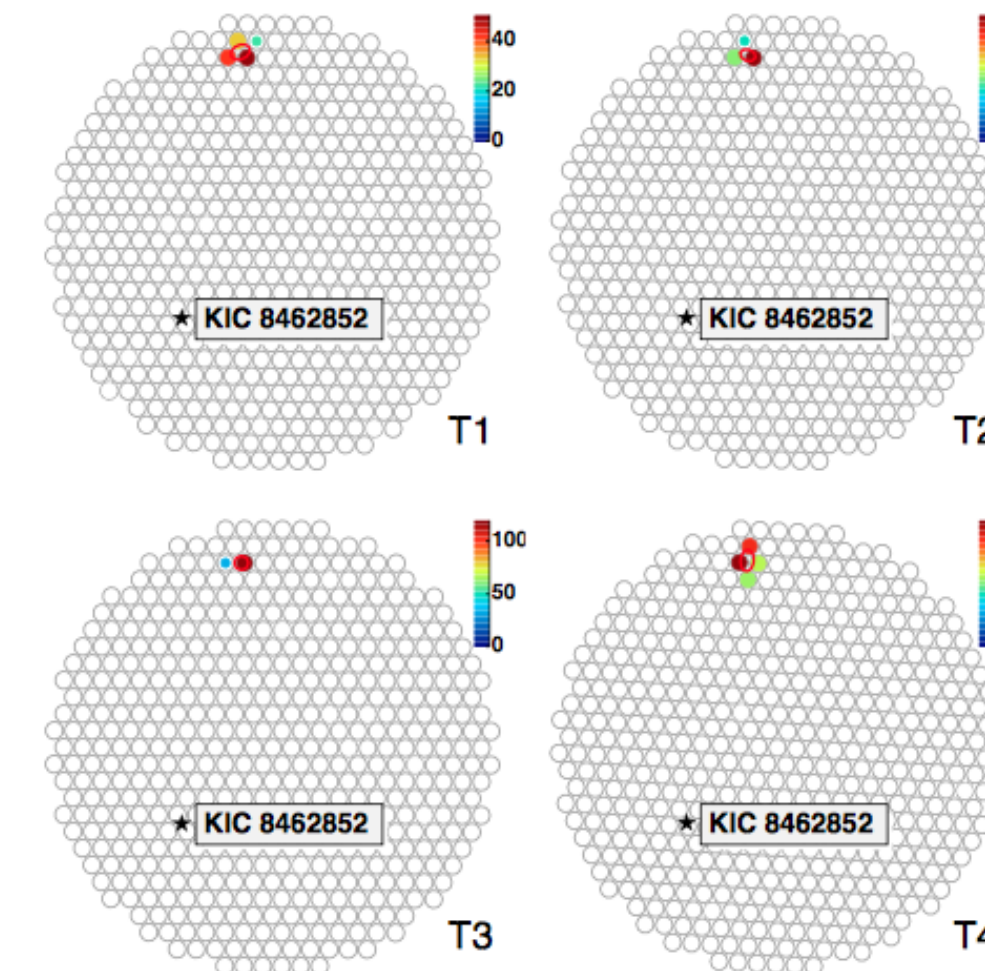
**VERITAS can monitor ~45-150 stars ( $V > 12$ ) in a single pointing**

OSETI event selection criteria

- They appear in the same place in all four telescope cameras
- They have the same intensity in each telescope
- They are point-like (c.f. optical point-spread function)



Cosmic rays show parallax due to shower max. only being a few km in altitude



Shooting stars/satellites will move through the camera

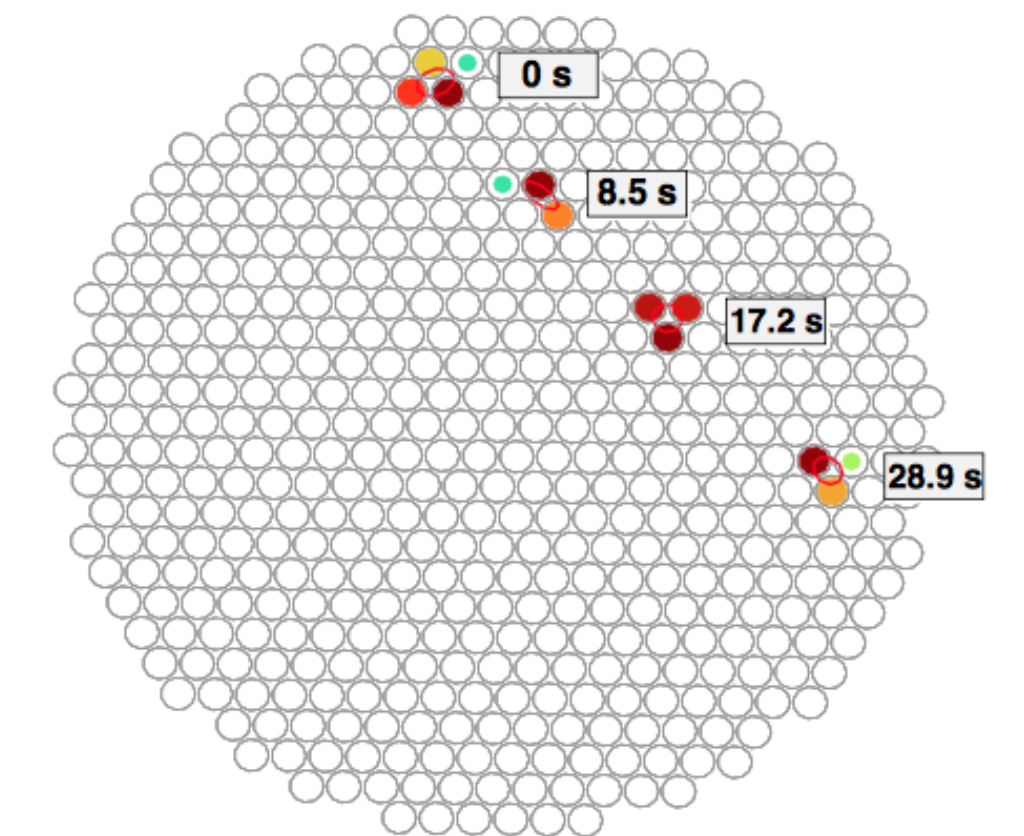


Fig. 3.— Point-like events generated by an object moving across the field-of-view of VERITAS over the course of 28.9 seconds on MJD 57283. **Left:** A single event viewed by all four telescopes. **Right:** A subset of the eight recorded events illustrating the motion of the image across the camera of a single telescope.

Abeysekara et al. *Ap.J* **818**, 33 (2016)